Allosteric Control of Beta2-adrenergic Receptor Function

by

Jacob Patrick Mahoney

A dissertation submitted in partial fulfillment
of the requirements for the degree of
Doctor of Philosophy
(Pharmacology)
in The University of Michigan
2016

Doctoral Committee:

Professor Roger K. Sunahara, University of California – San Diego, Co-Chair
Professor John J.G. Tesmer, Co-Chair
Professor John R. Traynor
Associate Professor Michael A. Holinstat
Associate Professor Georgios Skiniotis

2016

Acknowledgements

I have been fortunate to have received exceptional mentorship during my time at the University of Michigan. First and foremost, I must thank Dr. Roger Sunhara for his guidance, as well as his boundless enthusiasm and endless encouragement. Thanks also to the rest of my committee:

- Dr. John Tesmer, for providing lab space and equipment during the final year of my PhD work, and for his careful and thoughtful assessments over my whole graduate school tenure.
- Dr. John Traynor, also for providing lab space and equipment during the past year, and for many helpful discussions and advice along the way.
-Dr. Georgios Skiniotis, for encouragement and perspective.
-Dr. Michael Holinstat, for helping me keep the "big picture" in mind.

I am grateful to have worked with many great people at the University of Michigan and around the globe. Thanks to several former members of the Sunahara lab for important contributions to the work described in chapter 3, and to both current and former members for providing a truly enjoyable work environment, for many productive discussions, and for plenty of troubleshooting help. Thanks to the Tesmer and Traynor lab members for welcoming me into their labs, and especially to Dr. Kathryn Livingston for many stimulating and helpful discussions on quantitative pharmacology, receptor theory, and GPCR biology in general. Thanks also to my collaborators in the von Zastrow, Kobilka, Shoichet, and Gmeiner labs for their crucial contributions to the work described in this thesis, especially to Rachel Matt and Drs. Cheng Zhang and Yang Du (Kobilka lab) for providing purified recptors, Dr. Magdalena Korczynska (Shoichet lab) for virtual screening work, and Dr. Anne Stoessel (Gmeiner Lab) for synthetic chemistry. I must also acknowledge collaborators in the Martens, Stamou, Prive, and Lefkowitz labs for the opportunity to work together on stimulating projects not discussed here.

Table of Contents

List of Figures

CHAPTER 4

CHAPTER 5

List of Tables

List of Abbreviations

7TM	seven-transmembrane
Å	angstrom
A2a	adenosine A2a receptor
AC	adenylate cyclase
ApoAI	apolipoprotein-AI
β_1AR	beta1-adrenergic receptor
β_2AR	beta2-adrenergic receptor
B_{max}	maximum binding
cAMP	cyclic adenosine monophosphate
CI	confidence interval
CTCM	cubic ternary complex model
DHAP	dihydroalprenolol
DMEM	Dulbecco's Modified Eagle Medium
DMSO	dimethyl sulfoxide
DNA	deoxyribonucleic acid
EC_{50}	concentration producing half-maximal response
E_{max}	maximum effect/response
EPR	electron paramagnetic resonance
ERK	extracellular regulated kinase
ETCM	extended ternary complex model
FBS	fetal bovine serum
FLAG epitope	DYKDDDDK
G protein	guanine nucleotide binding protein
GDP	guanosine diphosphate
GEF	guanine nucleotide exchange factor
GFP	green fluorescent protein
GIRK	G protein-coupled inwardly rectifying potassium channel
GPCR	G protein-coupled receptor
GRK	G protein-coupled receptor kinase
GTP	guanosine-5'-triphosphate
GTPγS	guanosine-5'-O-(3-thio)triphosphate
[^{35}S]GTPγS	guanosine-5'-O-(3-[^{35}S]thio)triphosphate
H^+	hydrogen ion

HEK293	human embryonic kidney 293 cells
IC_{50}	concentration producing half-maximal inhibition
ISO	isoproterenol
K_d	dissociation constant
K_i	inhibition constant
K_{obs}	observed rate constant
K_{off}	dissociation rate constant
K_{on}	association rate constant
M2R	muscarinic acetylcholine receptor M2
MAPK	mitogen-activated protein kinase
MOPr	mu opioid receptor
MWC	Monod-Wyman-Changeux
Na^+	sodium ion
NAL	neutral allosteric ligand
NAM	negative allosteric modulator
Nb	nanobody
NLX	naloxone
NMR	nuclear magnetic resonance
PAM	positive allosteric modulator
PDB	protein data bank
PLC	phospholipase C
RGS	regulator of G protein signaling
SAM	silent allosteric modulator
SEM	standard error of the mean
TCM	ternary complex model
TM	transmembrane

Abstract

G protein-coupled receptors (GPCRs) are the largest class of transmembrane proteins and allow cells to sense their environment and respond accordingly. The transduction of an extracellular stimulus into an intracellular response relies on allosteric communication between two distant binding sites within the receptor. By binding at an extracellular site, GPCR agonists promote interaction of the receptor with a heterotrimeric G protein, thereby initiating an intracellular signaling cascade. The reciprocal interaction has also been observed for decades with many GPCRs - just as agonists promote G protein engagement, G proteins enhance agonist affinity for the receptor. Biophysical and structural studies of the β_2-adrenergic receptor (β_2AR), a prototypic GPCR, have illuminated the conformational changes within the receptor that promote agonist-mediated G protein engagement by β_2AR. Here we used G protein and a G protein-mimetic camelid antibody fragment (nanobody Nb80) to characterize the allosteric communication between the agonist- and G protein-binding sites on β_2AR. We developed a label-free assay to study the β_2AR-Nb80 interaction and used this system to demonstrate the selectivity of Nb80 for active-state β_2AR, a quality which rendered Nb80 useful to study β_2AR activation in living cells. Furthermore, we found that agonists enhance Nb80 affinity primarily by accelerating the association of Nb80 (and presumably G protein). In contrast, using several GPCRs we demonstrate that G protein or G protein-mimetic nanobodies enhance agonist affinity by constricting the agonist-binding site around the bound ligand, thereby slowing its dissociation. We identified key residues within β_2AR that form a "lid" over the agonist-binding site in the receptor's active state, which form the bottom of a potential binding site in the receptor's extracellular vestibule. Targeting this site using virtual screening, we discovered novel allosteric ligands for β_2AR. Together, these studies provide a structural mechanism to explain the allosteric communication between the binding of agonists and G protein, as well as highlight the utility of GPCR crystal structures for ligand discovery.

CHAPTER 1

Introduction

G protein-coupled receptors (GPCRs) are transmembrane proteins responsible for transducing signals in response to diverse stimuli, allowing cells to sense environmental cues and react accordingly. The GPCR superfamily consists of approximately 800 members, making it the largest family of cell-surface receptors in the human genome and the third-largest gene family overall[1]. GPCRs can be activated by molecules of diverse chemical nature: H^+ or Ca^{2+} ions, small-molecule hormones and neurotransmitters such as adrenaline or glutamate, fatty acids and phospholipids, or peptides and larger proteins like enkephalins/endorphins, chemokines, or Wnt proteins. In responding to these stimuli, GPCRs detect three of the five basic senses (sight, taste, and smell) and mediate many crucial aspects of human physiology including cardiovascular and neurological function, pain perception, metabolic processes, inflammation, organ development, and many more. Because the biological processes regulated by GPCRs are myriad, modulating GPCR signaling is an important therapeutic strategy; recent surveys of the pharmaceutical market have found that approximately 30% of available drugs target GPCRs[2]. Thus a detailed understanding of GPCR function, from the molecular to the organismal level, is critical for capitalizing on the therapeutic potential of this class of proteins.

1.1 - Cellular signaling in response to GPCR activation

Although the nature of the stimulus can vary greatly, canonical signaling by GPCRs proceeds by a shared mechanism. Activation of a GPCR promotes its association with a heterotrimeric guanine nucleotide-binding protein (G protein), which is composed of a Gα subunit and an obligate Gβγ subunit dimer. The Gα family contains 20 members divided into four families based on their signaling outputs: $G\alpha_s$ (stimulates adenylyl cyclase activity), $G\alpha_{i/o}$ (inhibits adenylyl cyclase activity), $G\alpha_q$ (stimulates phospholipase C activity), and $G\alpha_{12/13}$ (activates nucleotide exchange factors for the small G protein Rho). Likewise, the genome encodes multiple subtypes of Gβ and Gγ subunits (five and ten, respectively), and most combinations of these subunits are allowable.

In its inactive state, Gα is bound to a molecule of GDP. Interaction with an activated GPCR promotes nucleotide exchange on Gα by accelerating the release of bound GDP. The nucleotide-binding site is quickly occupied by a molecule of GTP, a reaction driven by the high intracellular concentration of GTP (~200-300 μM)[3]. The binding of GTP leads to conformational changes in Gα, promoting functional dissociation of the Gα and Gβγ subunits, and each is able to modulate the activity of specific effector proteins. Gα proteins are able to interact with partners such as adenylyl cyclase, phospholipase C, or RhoGEFs, in turn altering the activity of multiple downstream target proteins. Similarly, Gβγ subunits can serve to recruit proteins to the plasma membrane and can modulate the activity of certain ion channels, kinases, and phospholipase C isoforms to produce cellular responses.

The spatial and temporal texture of GPCR-generated signals can be controlled in several ways. The lifetime of an activated G protein is limited by the GTPase activity of the Gα subunit, which allows for hydrolysis of bound GTP and a return to the inactive GDP-bound Gαβγ

complex. For certain Gα subtypes, this process can be accelerated by the binding of Regulator of G protein Signaling (RGS) proteins. Furthermore, the activated receptor can be phosphorylated by GPCR kinases (GRKs) and subsequently be bound by the scaffolding protein arrestin, which targets the receptor to clathrin-coated pits for internalization via clathrin-mediated endocytosis. While arrestins were originally thought to simply quench GPCR signaling, a growing body of literature has lead to an appreciation of arrestins as versatile proteins able to recruit numerous binding partners (e.g. ERK, Src, phosphodiesterases). By organizing a unique set of signaling proteins, arrestins are able to initiate a second wave of cellular signaling events that are distinct from G protein-generated signals[4].

Our current understanding of GPCRs was driven by advances in DNA sequencing during the "genomic era" of the 1980s and 1990s. Prior to this, researchers had studied the GTP-dependent signaling processes downstream of the photoreceptor rhodopsin and of hormone receptors (e.g. glucagon or adrenergic receptors) somewhat independently. Upon the cloning of the β_2-adrenergic receptor, however, a team led by the Strader and Lefkowitz labs noticed that this receptor possessed the same predicted seven transmembrane helix topology as rhodopsin[5]. This finding led to the realization that the two receptors were part of a larger family of proteins that coupled to G proteins. As more receptors were cloned, the GPCR family continued to grow, until the sequencing of the human genome allowed for a complete view of the family's breadth. The human GPCR family is now divided into four main subfamilies based on their overall architecture: class A (rhodopsin-like), class B (secretin-like), class C (metabotropic glutamate-like), and class F (Frizzled family receptors)[6].

As we will see in the following sections, despite the extreme diversity in activating stimuli and even in GPCR structure itself, at its core GPCR signaling is an allosteric process that

is maintained across the superfamily. We will discuss this more in chapter 3, but first we must establish a working definition of allostery.

1.2 - Allosteric interactions in proteins

Allostery, the phenomenon of communication between spatially distinct binding sites within a protein or protein complex, allows for protein activity to be rapidly and reversibly tailored to changes in cellular environment. Thus, allosteric communication is of utmost importance in many metabolic pathways and signal transduction cascades. Studies performed in the 1950s found that the activity of several enzymes could be modified by the binding of metabolites, allowing flux through metabolic pathways to be tuned based on the needs of the cell[7–9]. Interestingly, the metabolites altered the kinetics of enzymatic reactions without competitively displacing the substrate from the enzyme's active site. Integrating these observations, Jacques Monod, Jean-Pierre Changeux, and Francois Jacob suggested that distant binding sites within a protein could influence one another, and proposed the following basic tenets of allosteric behavior in 1963[10]:

1. The allosteric protein contains at least two spatially distinct binding sites. The "active site" is defined as the site at which ligand binding results in a biological outcome (e.g. the enzymatic reaction occurs at this site). The ligand for a protein's active site is termed the substrate. In contrast, the "allosteric site" binds a ligand but no catalysis occurs at this site - the allosteric ligand is unchanged by its interaction with the protein.

2. Since the allosteric ligand has no requirement for binding at the active site or serving as a substrate, it can be quite chemically distinct from the substrate. It does not substitute for the substrate, nor does it react with the substrate.

3. Binding of an allosteric ligand alters the conformation of the protein, thereby changing the active site and in turn some kinetic parameter of the enzymatic reaction. Thus, the allosteric ligand is able to influence the protein's biological activity.

Two years later Monod and Changeux, together with Jeffries Wyman, published a general model (now referred to as the Monod-Wyman-Changeux, or MWC, model) for allosteric interactions in proteins[11]. Drawing largely from seminal studies on the cooperative binding of oxygen molecules by hemoglobin, along with the observation that most allosteric proteins known at the time were homo-oligomers, they amended their original theory slightly to include the supposition that allosteric communication results largely from changes in a protein's *quaternary* structure upon binding an allosteric ligand. Furthermore, the MWC model suggests that even in the absence of ligand, allosteric proteins exist in equilibrium between at least two discrete conformational states. The allosteric ligand binds with different affinities to these states, and thereby selectively stabilizes one state. If the states differ in their biological activity, then the shift in conformational equilibrium brought about by the binding of the allosteric ligand will manifest as a change in protein activity.

In the decades that have followed, allosteric control of protein activity has been thoroughly examined in many biological systems[12]. As mentioned above, allosteric communication has been observed in control of enzymatic function. Many multi-subunit ion channels including GABA, NMDA, and nicotinic acetylcholine receptors, also display cooperativity in ligand binding and their activity can be further modified by allosteric ligands. While the original definitions of allostery were focused on enzymatic reactions, it is easy to apply these same principles to other proteins. In this thesis we will consider how the principles of allostery are manifested in the transduction of signals by GPCRs.

1.3 - GPCRs as allosteric proteins

Applying the principles outlined by Monod, Changeux, and Jacob in 1963, it is clear that GPCR activation is an allosteric process which allows information to be transmitted across the plasma membrane. In class A GPCRs, the orthosteric binding site (the site to which the endogenous agonist binds) is generally located at the extracellular side of the transmembrane helical bundle. This site is allosterically linked to the G protein-binding site on the receptor's intracellular face, allowing binding at one site to influence the other. Indeed, orthosteric ligands of varying efficacies can influence the binding of G protein to the receptor, with agonists promoting receptor-mediated nucleotide exchange on the G protein and inverse agonists inhibiting this process. The reciprocal communication has also been observed for many decades: the affinity of an agonist for its receptor is enhanced when the receptor is bound to G protein.

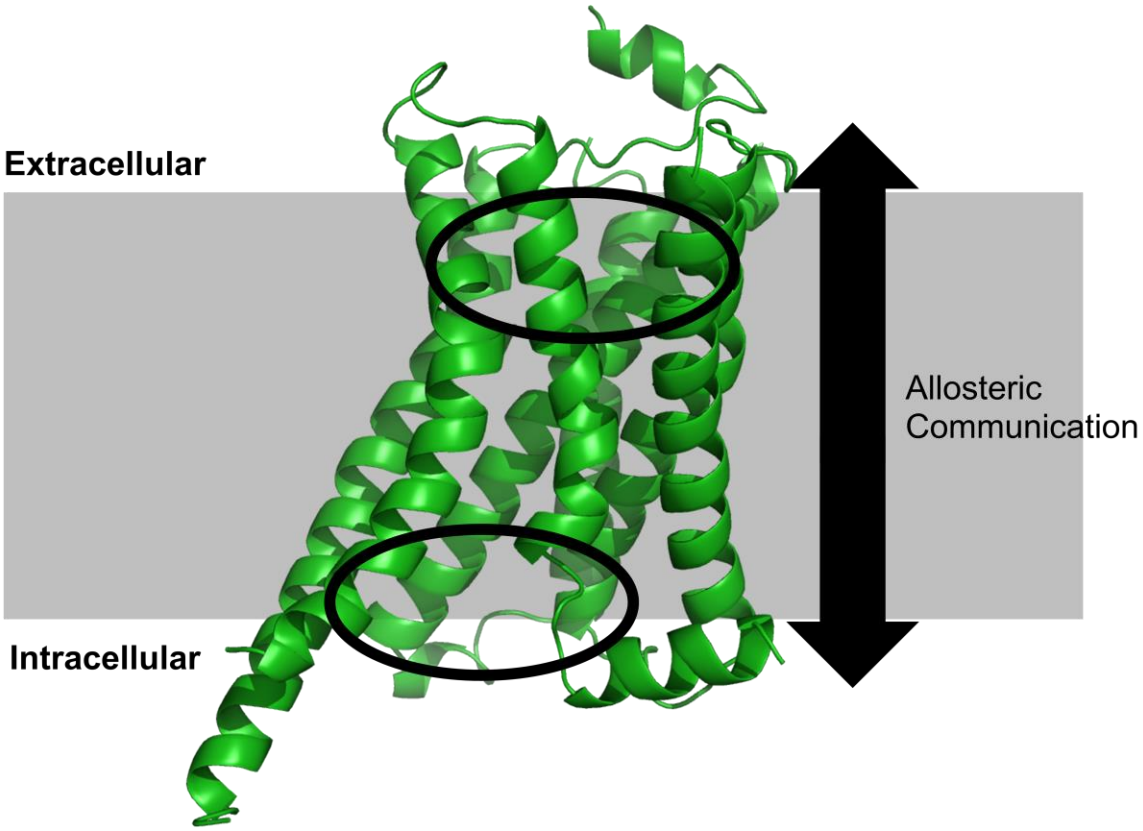

Figure 1-1. Allosteric communication is fundamental to GPCR function.
GPCRs span the plasma membrane (modeled in gray) and produce intracellular signals in response to the binding of extracellular stimuli, a process that requires allosteric communication between two distant binding sites within the receptor. For most class A GPCRs, the endogenous agonist binds at the receptor's extracellular face to stabilize conformational changes within the receptor, opening a cleft at the intracellular face to promote the receptor-G protein interaction. In turn, G protein binding enhances affinity of the bound agonist for the receptor. Circled sites indicate the epinephrine binding site at the extracellular face of β_2AR, and the G protein binding site on the cytoplasmic side of β_2AR (PDB 3sn6).

The allosteric communication within class A GPCRs represents the simplest form of allostery in GPCRs, with both binding sites localized to the receptor's seven-transmembrane (7TM) helical core. In class B receptors, the orthosteric site is formed by contributions from the receptor's 7TM helices as well as its extended N-terminus. In class C receptors, the endogenous agonist binds to extracellular "venus flytrap" domains that are separated entirely from the 7TM domain[13,14]. However, as discussed in chapter 3.6, the fundamental tenets of allosteric communication are conserved in these more complicated receptors: extracellular agonist binding enhances intracellular G protein engagement, and vice versa.

Many GPCRs also contain secondary binding sites, distinct from the orthosteric site, which can bind small molecules (or potentially other proteins). Binding of an allosteric ligand can alter the orthosteric ligand’s affinity for the receptor and/or its efficacy for a certain signaling output. Allosteric modulators are also capable of possessing efficacy in their own right due to their ability to stabilize active or inactive receptor states. Small-molecule allosteric modulators of GPCRs were first discovered for the muscarinic acetylcholine receptors, and many more examples of allosteric ligands for other class A, B, C, and F receptors have been identified[15]. Allosteric regulation of GPCR function may have therapeutic advantages over traditional orthosteric agonism/antagonism, which will be discussed further in chapter 4.

Like other allosteric proteins, GPCR function hinges on the transition between states that possess varying degrees of biological activity (i.e. the ability to interact productively with a G protein), a process that can be controlled by the binding of extracellular ligands. To fully understand the molecular basis for GPCR function, many researchers have sought to describe receptor behavior using mathematical models. These models have proven not only descriptively useful, but also serve as sources for new hypotheses about GPCR behavior.

1.4 - Evolution of thermodynamic models to describe GPCRs

Models of GPCR behavior were built on the foundations of receptor theory, which evolved gradually over the course of the 20th century. Following his studies of the cholinergic agents atropine and pilocarpine on salivary secretion, John Newport Langley first proposed the idea that these compounds were physically interacting with some cellular substance in 1878[16]. He followed this work with an examination of the effects of nicotine and curare on muscle contraction and in 1905, he suggested that the effects he observed were mediated by a "receptive substance" on the cell[17]. Langley's contemporary, Paul Ehrlich, proposed the existence of receptors for specific toxins in 1900 based on his early studies of histological stains and his later immunology work[18]. In 1907, Ehrlich extended his original hypothesis to include "chemoreceptors," or receptors able to bind drugs. Together, the work of Ehrlich and Langley laid the groundwork for receptor theory[19].

Langley's student, A.V. Hill, provided additional support for the receptor hypothesis in 1909. Hill conducted a series of experiments examining the contraction of isolated muscle in response to nicotine, the antagonism of nicotine-evoked responses by curare, and the temperature dependence of these processes[20]. Describing this relationship mathematically, Hill was able to bolster the concept that both drugs bound in a specific, reversible manner to some substance on muscle cells, and that this interaction followed the law of mass action. His work was followed in 1926 by similar studies performed by A.J. Clark[21,22]. Like Hill, Clark studied the antagonism of contractile responses and applied a rigorous mathematical analysis to his experiments. He again suggested that the effect of a drug was mediated by its binding to a receptor on the cell, and noted that the drug-receptor interaction behaved according to the Langmuir equation, an equilibrium binding equation which was originally derived in 1918 to explain the adsorption of

gases onto a metal surface (this equation was the same one derived by Hill in 1909). Clark further proposed that the response generated by a drug was directly proportional to receptor occupancy; in this simple model, unbound receptor and agonist molecules are in equilibrium with the agonist-receptor complex, which generates a response[23]. However, as the body of literature on drug-evoked responses expanded, it was quickly obvious that this correlation did not always hold true; some agonists could produce a maximal response at low receptor occupancy, while others could produce only a partial response even at full receptor occupancy. In 1954, E.J. Ariëns proposed that each agonist possessed an "intrinsic activity" which dictated the maximum response it could produce[24]. This concept addressed the issue of partial agonism, but still assumed that receptor occupancy and biological response were directly proportional (i.e. that EC_{50} and K_d values were equivalent). The theory was quickly modified by R.P. Stephenson, who in 1956 coined the term "efficacy" to describe a drug's capacity to generate a biological response upon receptor binding[25]. Stephenson's model was the first to separate receptor occupancy from biological response, and thus explained the findings that maximal responses could be achieved at low receptor occupancy (by agonists of high efficacy). However, Stephenson's definition of efficacy was composed of components from the drug and from the tissue/cell itself. These components were disentangled in 1966 by R.F. Furchgott, who mathematically revised the models of receptor activation to define the contributions of tissue sensitivity and "intrinsic efficacy," a property of the drug-receptor complex itself[26].

Receptor theory began with the idea that the drug-receptor complex generated a response and the early revisions discussed thus far focused on defining properties of the *drug* that were important in generating a cellular response. However, as more receptor types were identified and biochemical knowledge of proteins expanded, behavior of the *receptor* began to be incorporated

into models of drug action. Following their studies of the nicotinic acetylcholine receptor, a ligand-gated ion channel, del Castillo and Katz proposed a two-state model, postulating that agonists promoted transition of the receptor from a "closed" state to an "open" state[27]. Follow-up work by Karlin in 1967 applied the MWC model to explain the behavior of the system, hypothesizing that the receptor existed in equilibrium between these two states and that agonists possessed a higher affinity for the open state[28] (Fig. 1-2).

These two-state models proposed that the binding of an agonist stabilized the receptor in its active state (R*), the state responsible for producing a physiological outcome. The models satisfactorily explained drug-evoked responses in some systems, but researchers studying hormone-stimulated adenylyl cyclase soon found the need to modify receptor theory based on the peculiarities of their system. Work by Rodbell and colleagues showed that the stimulation of adenylyl cyclase by glucagon proceeded through an intermediate protein which required GTP binding for its stimulatory capabilities[29–31]; this protein was later identified as the G protein Gs by the Gilman laboratory. Importantly, Rodbell also demonstrated that the presence of guanine nucleotides was able to worsen the binding affinity of radiolabeled glucagon for its receptor[32], and studies later conducted in the Gilman, Molinoff, and Lefkowitz labs described an analogous phenomenon at adrenergic receptors. Evidence that G protein was able to affect the agonist-binding pocket of GPCRs led to the development of the first thermodynamic model specific to GPCR pharmacology, the ternary complex model[33–35] (TCM; Fig. 1-2). This model began with the assumption of the two-state models, that agonist binding to an inactive receptor induces receptor activation, but introduced G protein as a second binding partner of the agonist-receptor complex. The resulting ternary complex (agonist-receptor-G protein) represents the energetic minimum of the cycle, and the highest binding affinity of agonists is observed in this state.

As GPCR biology was explored further, the accumulating body of literature required revision of the original ternary complex model. Seminal studies on the delta opioid receptor revealed that this receptor possessed the ability to activate G proteins even in the absence of agonist[36]. This constitutive activity was able to be seen upon overexpression of other GPCRs and could also be achieved in multiple receptors by mutagenesis[37]. A new model, the extended ternary complex model (ECTM), was proposed by Costa and Lefkowitz to allow for basal transitions of a receptor into its active state. In this model, the receptor exists in an equilibrium between inactive (R) and active (R*) states even in the absence of agonist; the position of this equilibrium is thought to be receptor-dependent and can be modulated by various factors in the receptor's local environment (see chapter 5.8). The presence of an agonist represents one such factor - binding of an agonist shifts the equilibrium in favor of R*, increasing the probability of G protein engagement. The energetic minimum of this model is, once again, the A-R*-G ternary complex, in which the receptor has high affinity for agonist and G protein.

While the extended ternary complex model adequately describes the biological process of agonist-stimulated G protein recruitment to a GPCR, it is not thermodynamically complete. Thus, Kenakin and colleagues proposed the cubic ternary complex model (CTCM), a revision of the ETCM that includes a "pre-coupled" complex between inactive receptor and G protein (R_i-G)[38–40]. Pre-association of GPCRs with their cognate G proteins has been suggested in the literature, but the extent and biological relevance of this complex remains unclear[41].

Following the discovery of small-molecule allosteric ligands for GPCRs, thermodynamic models were also proposed to describe the communication of these novel binding sites with the receptors' orthosteric and G protein-binding sites[42]. As discussed above, allosteric ligands are able to alter affinity and efficacy of orthosteric ligands, and these modifying parameters are

incorporated into the allosteric TCM. In addition, this model also includes the ability of allosteric modulators to directly influence signaling outputs of the receptor, again highlighting the idea that changes in biological function are a consequence of a ligand's effect on the receptor's conformational equilibrium.

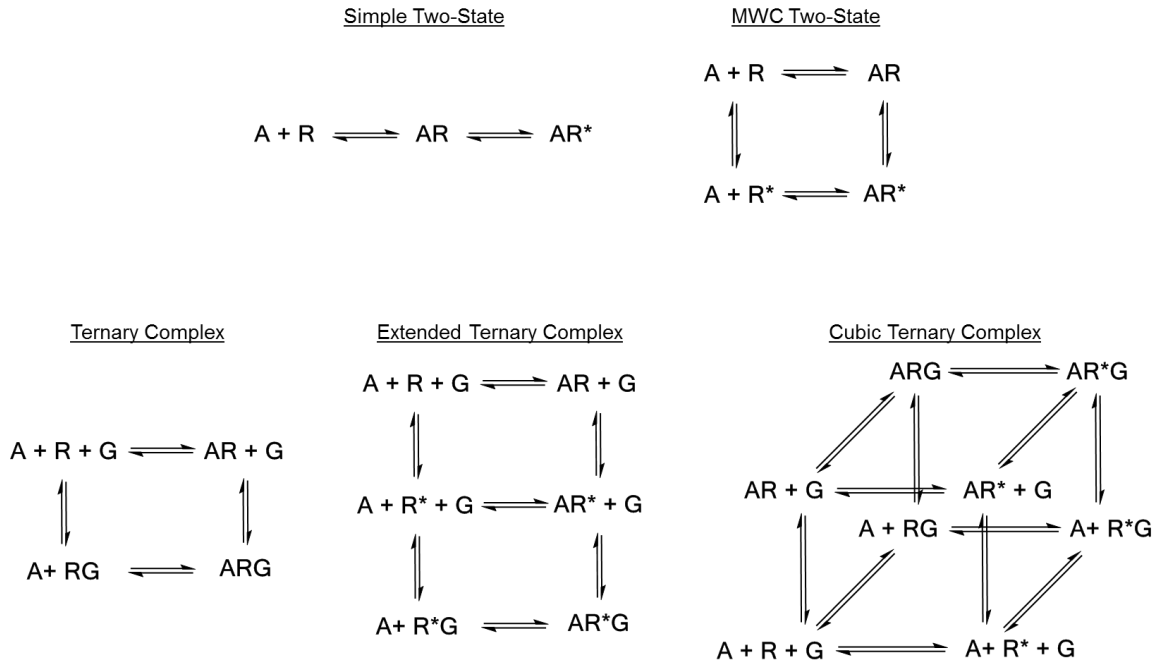

Figure 1-2. Evolution of thermodynamic models describing GPCR activation and the allosteric coupling between agonists and G protein.
Beginning with the simple two-state model, in which agonist binding induces activation of the receptor, models of receptor behavior gradually increased in complexity to explain experimental observations. Common to all models beyond the simple two-state and ternary complex models is the idea that receptors exist in an equilibrium between inactive and active conformations. The position of this equilibrium can be influenced by the binding of agonists (or inverse agonists) and, in the case of the ternary complex models, G protein. Thus, extracellular ligands are able to communicate with G proteins (and vice versa) using the receptor as a conduit.

Early definitions of allostery and receptor activation dealt with only a few conformational states: tense and relaxed in the case of hemoglobin, open and closed when considering ion channels, or active and inactive when dealing with enzymes or GPCRs. As our understanding of protein biophysics and knowledge of the breadth of GPCR signaling pathways improved, it became clear that the thought of receptors as "switches" flipping between R and R* states was overly simplistic. With protein ensemble theory permeating the GPCR field, it has become accepted that each receptor state in the TCMs represents a group of conformational states with similar biological activity[43]. Furthermore, G proteins are not the sole mediators of GPCR signals; receptors can bind multiple signaling proteins to activate diverse intracellular pathways. Consequently, more complicated thermodynamic models have been put forth by several researchers[42] to account for the conformational plasticity of GPCRs and their ability to interact with multiple transducer proteins. However, due to their cumbersome nature, these models are rarely used.

1.5 - From thermodynamics to structural models of GPCR activation

While thermodynamic models are useful representations of GPCR behavior, they are unable to provide a thorough understanding of receptor activation, namely the specific conformational changes within the receptor that accompany activation and promote signal transduction. The first high-resolution crystal structure of a GPCR, rhodopsin, was solved in 2000[44]. This model shed light on the three-dimensional organization of the GPCR 7TM bundle and displayed important contacts that had been predicted from biochemical experiments, such as the "ionic lock" anchoring TM6 and TM3 - a salt bridge between $R^{3.50}$ and $D/E^{6.30}$ which was proposed to keep the receptor in its inactive state (superscripts denote Ballesteros-Weinstein numbering[45]). Biophysical experiments performed several years earlier had identified important

conformational changes that occur during rhodopsin activation. Electron paramagnetic resonance (EPR) spectroscopy experiments suggested that upon light activation or rhodopsin, the cytoplasmic face of the receptor underwent dramatic conformational changes, with the sixth transmembrane helix (TM6) rotating and moving away from TM3. Shortly thereafter, fluorescence spectroscopy experiments showed that β_2AR operated by a similar mechanism[46,47]. The receptor was site-specifically labeled with a fluorophore at the intracellular side of TM6, and changes in fluorescence verified the movement of TM6 in β_2AR. Based on these experiments, it was hypothesized that for GPCRs which bind diffusable ligands, agonist binding stabilizes the outward movement of TM6, thereby opening a binding cleft to allow for G protein engagement by the receptor.

It took several more years to visualize TM6 movement and the GPCR-G protein interaction using x-ray crystallography. The second GPCR structure, published in 2007, was that of β_2AR bound to the inverse agonist carazolol[48]. The structures of several more antagonist- or inverse agonist-bound GPCRs followed closely behind, all displaying a similar inactive-state arrangement of the 7TM helices. The first structure of agonist-bound β_2AR was published in 2011, the structures of several other GPCRs bound to agonists have been solved by x-ray crystallography[49,50]. However, in most of these structures the position of TM6 is similar to its position in antagonist-bound GPCR structures, suggesting that these receptors are adopting an inactive conformation. A few agonist-bound GPCRs have been crystallized in "active-like" conformations which exhibit some hallmarks of activation, such as a “broken” ionic lock or a small outward movement of TM6, but the large outward movement of TM6 predicted by EPR and fluorescence spectroscopy was not observed[51,52]. This movement of TM6 was not seen until co-crystal structures with cytoplasmic binding partners were solved. The structure of activated

opsin bound to a peptide derived from the C-terminus of transducin (the Gα subunit expressed in the retina) displayed a 6 Å movement of the cytoplasmic end of TM6 away from the helical bundle[53], and a similar TM6 movement was observed in the crystal structure of the active MetaII state of rhodopsin[54]. Structures of β_2AR bound to the G protein mimic nanobody Nb80 (discussed in chapter 2) or to heterotrimeric Gs displayed much larger shifts in TM6 position (12-14 Å)[55,56]. These active-state structures also provided insights into how conformational changes at the intracellular face of rhodopsin and β_2AR are able to influence ligand binding at the orthosteric site.

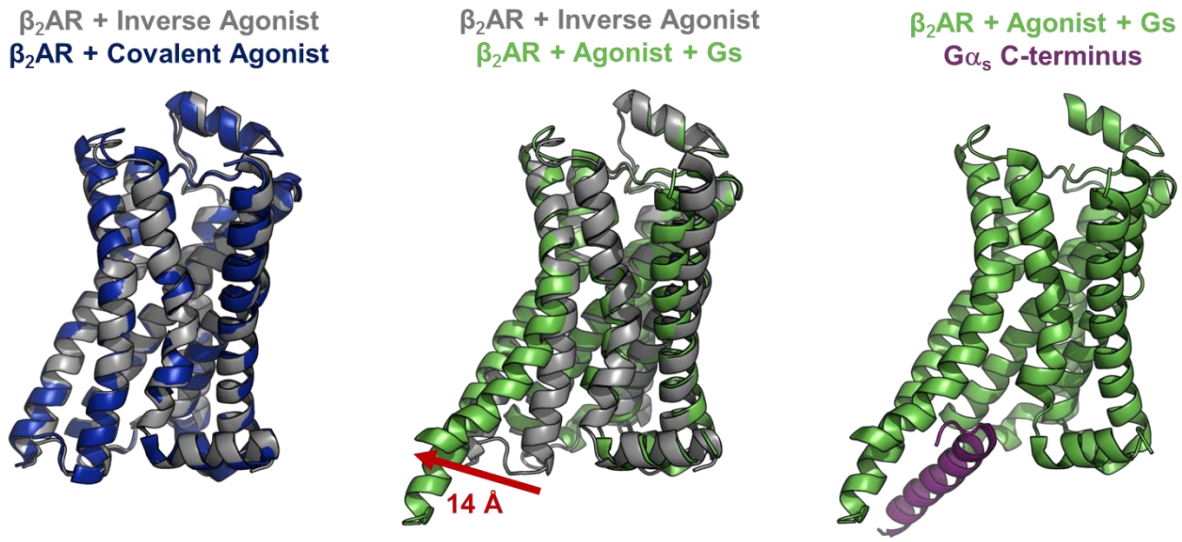

Fig. 1-3. Structural models of GPCR activation and the allosteric coupling between agonist and G protein.
The structure of β_2AR bound to a covalent agonist (blue; PDB 3pds) did not show the large outward movement of TM6 that biophysical experiments have shown to be a fundamental part of GPCR activation. Instead, the agonist-bound structure appeared strikingly similar to the structure of the receptor bound to the inverse agonist carazolol (gray; PDB 2rh1). Full stabilization of TM6 movement required co-crystallization of β_2AR with both agonist and G protein (green; PDB 3sn6). Engagement of the Gα C-terminal helix (shown in purple) in turn stabilizes smaller conformational changes at the receptor's orthosteric site to influence agonist binding.

Structures solved by x-ray crystallography have undoubtedly provided insights into the conformational changes that occur upon GPCR activation. However, these data only provide a snapshot of one possible energetic minimum, so complementary experiments must be performed to interrogate the dynamics of GPCR activation. Recent biophysical experiments have indeed confirmed what x-ray crystallography suggested: while rhodopsin displays more rigid allosteric coupling between agonist- and G protein-binding sites and a stable active state, β_2AR agonists are not capable of fully stabilizing an active conformation of TM6[57]. Fluorescence spectroscopy experiments revealed that the agonist isoproterenol is indeed able to stabilize an outward movement of TM6 in β_2AR, but an additional change in signal was observed in the presence of both agonist and G protein, suggesting that G protein binding is accompanied by a further movement of TM6 or that G protein stabilizes a larger proportion of the receptor population in a TM6-outward state[47]. The cooperative effects of agonist and G protein on TM6 position suggested that agonist-bound β_2AR could adopt different conformations, and the ensemble of receptor conformations has been visualized in recent studies using NMR and EPR spectroscopy[58,59]. It was observed that even in the presence of a saturating concentration of agonist, a significant population of receptors still occupied inactive states at equilibrium. However, addition of Nb80 was able to trap a large proportion of receptors in the active state. Investigation of β_1-adrenergic receptor (β_1AR) and mu opioid receptor (MOPr) activation by NMR also revealed that full stabilization of an active state required binding of a G protein mimetic nanobody[60,61]. Taken together, the recent structural data highlight the allosteric nature of GPCRs, namely, that for many receptors, stabilization of the fully active receptor conformation is achieved by the concerted action of two ligands, agonist and G protein.

1.6 - Focus of research

As discussed throughout this chapter, GPCR function can be modulated by many forces. The requirement for a functional change is simply an alteration in the conformational ensemble of the receptor, which produces a biological outcome by changing the ability of the receptor to interact with intracellular signaling partners. Thus, by modulating receptor conformation, orthosteric ligands are allosteric modulators of G protein activation (or GRK recruitment, arrestin binding, etc.). Small molecules labeled as "allosteric modulators" of GPCRs are no different, they also alter the receptor's conformational landscape to influence orthosteric ligand binding or recruitment of signaling partners. Furthermore, the conformational changes stabilized by G protein (or other intracellular binding partners) also affect the interaction of the receptor with orthosteric or allosteric small molecules. This thesis rests heavily on the foundation provided by recent advances in GPCR structural biology, and aims to further expand our knowledge of communication between various binding sites in β_2AR, a prototypic class A GPCR. In chapter 2 we utilize Nb80, a tool originally developed to stabilize β_2AR for crystallography, to study the effect of agonists on the dynamics of β_2AR activation in the context of the ternary complex models. Chapter 3 will focus on the structural mechanisms that allow the agonist- and G protein-binding sites to communicate with one another. Finally, chapter 4 will discuss the application of β_2AR structures as templates to identify novel allosteric modulators of β_2AR.

CHAPTER 2

Using nanobodies as conformational biosensors to study GPCR activation

2.1 - What are nanobodies?

Mammalian IgG antibodies or antibody fragments have been used widely for applications including protein purification, stabilization of proteins for structural biology, *in vitro* and *in vivo* detection of proteins, or as therapeutic agents. Traditional vertebrate antibodies are composed of multiple polypeptide chains: two heavy chains and two light chains. The antigen-recognition site, typically a large convex binding surface, is formed by contributions from domains on both the heavy and light chains (Fig. 2-1a). Minimal antigen-recognition portions of antibodies (Fab fragments and SCv fragments) have also proven to be useful tools for the applications listed above; however, traditional IgG antibodies and their fragments suffer from several drawbacks. Their binding site is relatively large and can often only recognize linearized epitopes, and in some applications they may be unstable or difficult to produce in large quantities since they are composed of multiple subunits.

In addition to traditional IgG antibodies, camelids (eg. camels, llamas, and alpacas) and sharks possess a unique type of antibody composed only of a heavy chain dimer[62,63]. Each heavy chain contains three domains: two constant domains (C_H2 and 3) and a variable domain termed V_HH (Fig. 2-1b). Included in V_HH are three hypervariable regions, which impart the V_HH domain with an antigen-binding site composed of three flexible loops, complementarity determining regions 1-3 (CDR1-3). The antigen-binding fragment derived from these antibodies

(analogous to the Fab fragment of traditional antibodies), termed a nanobody, is a single polypeptide of small size (12-15 kDa) which can be expressed and purified from several heterologous expression systems[64]. Heterologously expressed nanobodies are monomeric, stable, and retain full binding affinity for their specific antigen.

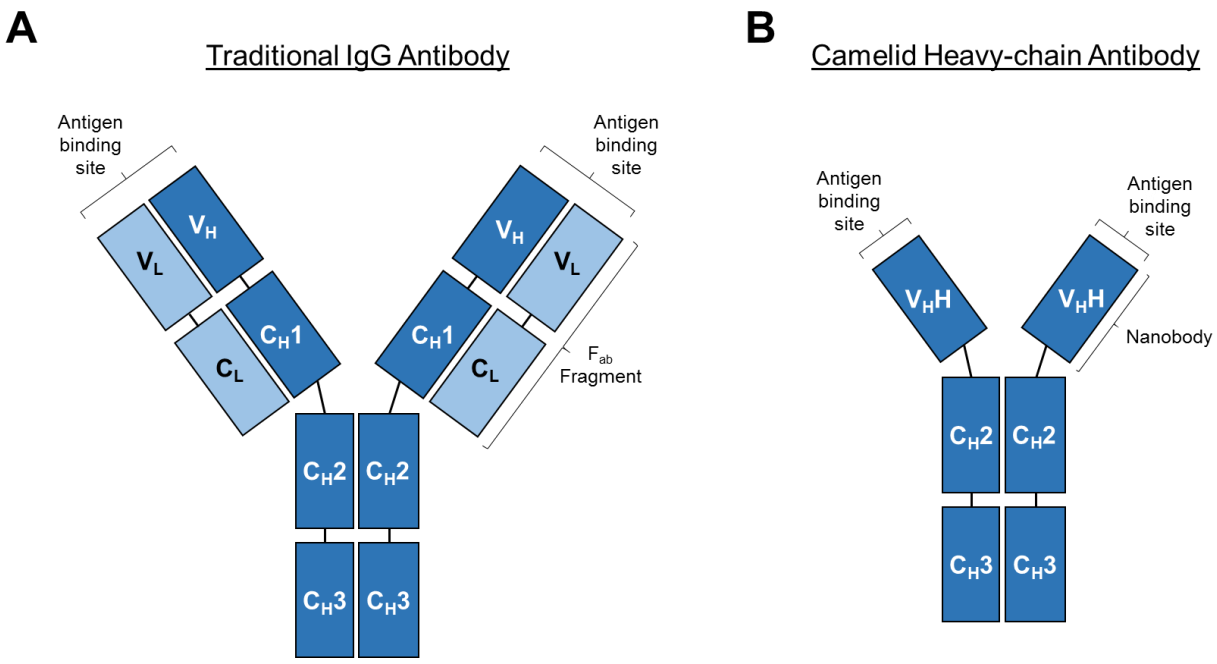

Figure 2-1. Comparison of traditional IgG and camelid heavy-chain antibodies.
Traditional vertebrate IgG antibodies (left) are comprised of four polypeptide chains: two heavy chains (dark blue) and two light chains (light blue). Both the heavy and light chains contribute to the formation of a shallow antigen binding site well-suited to bind linear epitopes. In contrast, camelid heavy-chain antibodies (right) lack the light chains of their IgG counterparts. The antigen-binding site of these antibodies is entirely located within a single variable domain on each heavy chain, and is able to bind epitopes only present in the three-dimensional structure of a protein.

2.2 - Utility of nanobodies

Nanobodies offer advantages over traditional antibodies for many experimental applications. Due to their small size and the nature of their antigen-binding sites, nanobodies are able to target epitopes inaccessible to conventional antibodies. The CDR3 loop of nanobodies is often long (20 residues or more) and quite flexible, allowing nanobodies to reach into cavities and epitopes that only exist in the protein's native state[65]. This antigen-recognition mode imparts nanobodies with a great deal of conformational selectivity in their binding. Nanobodies have been shown to bind specific states of enzymes, ion channels, and transporters, facilitating in-depth analysis of their catalytic or transport cycles[66–68]. The ability to select for specific protein conformations has proven particularly useful in structural biology. Nanobodies have been used to stabilize flexible or even intrinsically disordered proteins during crystallization and are able to trap rare protein states for X-ray crystallography studies[68–70].

The conformational selectivity of nanobodies can also be utilized in cell-based studies. Unlike Fab fragments, nanobodies can be expressed as functional proteins in the cytoplasm of living cells. Intracellularly-expressed nanobodies (intrabodies) can be used to modulate the activity of a protein or interest or to disrupt a specific protein-protein interaction[71,72]. Fusing an intrabody with a fluorescent protein allows for observation of the subcellular localization of proteins or the generation of specific protein conformations in live cells[73]. This technique has been applied to observe the translocation of the estrogen receptor and β-catenin to the nucleus and to monitor subcellular trafficking of transporters[67,74,75].

2.3 - Application of nanobodies to GPCR research

The ability of nanobodies to recognize and stabilize specific protein conformations has been useful in studying GPCR signaling. Nanobodies targeting the extracellular surface of the

chemokine receptor CXCR7 have been shown to inhibit β-arrestin2 recruitment to the receptor and slow cancer cell growth[76]. Similarly, nanobodies raised against the extracellular face of CXCR4 can attenuate HIV entry into cells. Although blockade of HIV entry may simply be due to steric inhibition of virion binding, the same nanobodies were also shown to suppress downstream CXCR4 signaling at a constitutively active CXCR4 mutant, suggesting that nanobodies can stabilize distinct recptor conformations to influence signaling outcomes[77]. Complementary to nanobody-based targeting of extracellular sites on GPCRs, intracellular expression of nanobodies may be a useful route to study downstream signaling pathways in cellular models. β_2AR-selective nanobodies can be expressed as intrabodies in HEK293 cells and block β_2AR agonist-mediated signaling[78]. In some cases, intrabody expression can dampen select pathways, suggesting that they may be useful for interrogating the role of certain signaling outcomes downstream of GPCRs.

In addition to their utility for modulating cellular signaling, nanobodies have proven instrumental in structural studies of GPCR activation. As discussed previously (chapter 1.5), the x-ray crystal structures of several agonist-bound GPCRs showed little or no movement of TM6, and an intracellular binding partner was required to stabilize a fully active receptor state during crystal formation. To visualize an active conformation of β_2AR, the receptor was crystallized in complex with an agonist and an active state-stabilizing nanobody, Nb80, which binds the cytoplasmic face of β_2AR in a cleft opened by the outward movement of TM6[55] (Fig. 2-2a). By binding at this site, Nb80 is able to allosterically enhance agonist binding to β_2AR, producing the same ~100-fold shift in agonist affinity that is seen in the presence of G protein (Fig. 2-2b). Subsequently, the structure of β_2AR bound to nucleotide-free Gs heterotrimer was solved, which

validated the receptor conformation stabilized by Nb80 (overall RMSD ~0.6 Å between the two β_2AR structures)[56].

Active-state stabilizing nanobodies have also facilitated structural studies of agonist-bound M2 muscarinic acetylcholine receptor (M2R) and mu-opioid receptor (MOPr)[79,80]. Like Nb80, the M2R and MOPr nanobodies bound the cytoplasmic face of their respective receptors to stabilize the movement of TM6 and were discovered based on their ability to stabilize high-affinity agonist binding in a manner similar to G proteins. Because of the absence of a M2R- or MOPr-G protein complex structure for comparison, however, the specific conformational changes stabilized by these nanobodies have not been validated.

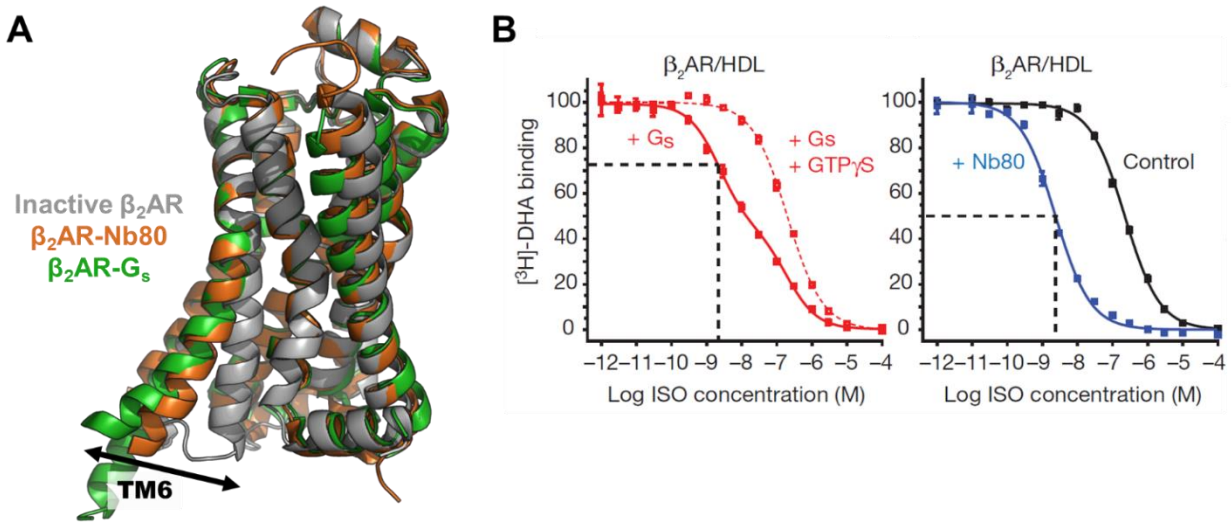

Figure 2-2. Nb80 mimics Gs in its stabilization of active β2AR and its effects on agonist affinity. A) By binding to a site opened by the outward movement of TM6, Nb80 is able to stabilize an activated conformation of β_2AR similar to the conformation stabilized by Gs. **B)** The conformational similarity translates to similar pharmacology, as Nb80 and Gs both stabilize high-affinity binding of the agonist isoproterenol. Panel B is reprinted from Nature Publishing Group with permission (see Rasmussen *et al.* 2011)[55].

2.4 - Using Nb80 to monitor spatial and temporal aspects of β_2AR activation

The ability to express nanobodies as functional fluorescently-labeled intracellular proteins, together with the conformational selectivity of Nb80, raised the possibility that Nb80 could be used as a tool to monitor the location of activated β_2AR in living cells. In the classical model of GPCR signaling, G protein activation by an agonist-bound receptor is short-lived, as GRKs and arrestins are rapidly recruited to an active receptor and block further G protein signaling. Furthermore, since arrestin-bound receptors are targeted to clathrin-coated pits and internalized, the activation of G proteins was thought to occur solely at the plasma membrane. Thus in traditional models, GPCR signaling was thought to progress in waves: an initial G protein-mediated signal from the plasma membrane, followed by a second arrestin-mediated signal from internalized receptors[81]. However, work on the parathyroid hormone and thyroid-stimulating hormone (PTH and TSH, respectively) receptors showed showed that disruption of the receptor-arrestin interaction paradoxically shortened cAMP generation following agonist application[82–84]. This finding raised the possibility that internalized receptors may still be able to stimulate G protein signaling.

In order to assert that co-localization of Nb80 and β_2AR observed in cells is indeed indicative of β_2AR activation, we developed an *in vitro* binding assay to characterize the affinity of Nb80 for various ligand-stabilized conformational states of β_2AR. Agonist-bound β_2AR has been shown to maintain significant conformational flexibility[58,85,86], therefore the possibility exists that Nb80 may bind multiple states of agonist-occupied receptor, including inactive-like states. Thus an *in vitro* characterization of the β_2AR-Nb80 interaction was critical to demonstrate the requirement of Nb80 binding on β_2AR activation. Furthermore, the ability to directly monitor

the β_2AR-Nb80 interaction allowed us to characterize the role of agonists in β_2AR activation and the allosteric communication from agonist-binding site to the intracellular face of the receptor.

Results

In order to directly measure the binding of Nb80 to β_2AR, we utilized biolayer interferometry, which can measure protein-protein and even protein-small molecule interactions[87]. In this system, the protein of interest is captured on a functionalized surface at the end of a small fiber optic probe. The probe, attached to an interferometry instrument, is dipped into buffer containing the desired small-molecule or protein binding partner to observe association. To observe dissociation, the probe is then dipped in into buffer alone.

The measurement of binding/unbinding relies on changes in mass bound to the end of the probe. White light is sent down the probe, and upon reaching the end is reflected from two surfaces back to the instrument's detector. The first surface is the end of the probe itself, the second is the layer of protein bound at the probe's surface (the "biolayer"). Light reflected from these two surfaces arrives at the detector with a certain interference pattern, and this pattern is defined as the baseline. A change in biolayer mass results in a phase shift of the light being reflected from this surface back to the detector, thus the light arriving at the detector will display an interference pattern that differs from baseline (Fig. 2-3).

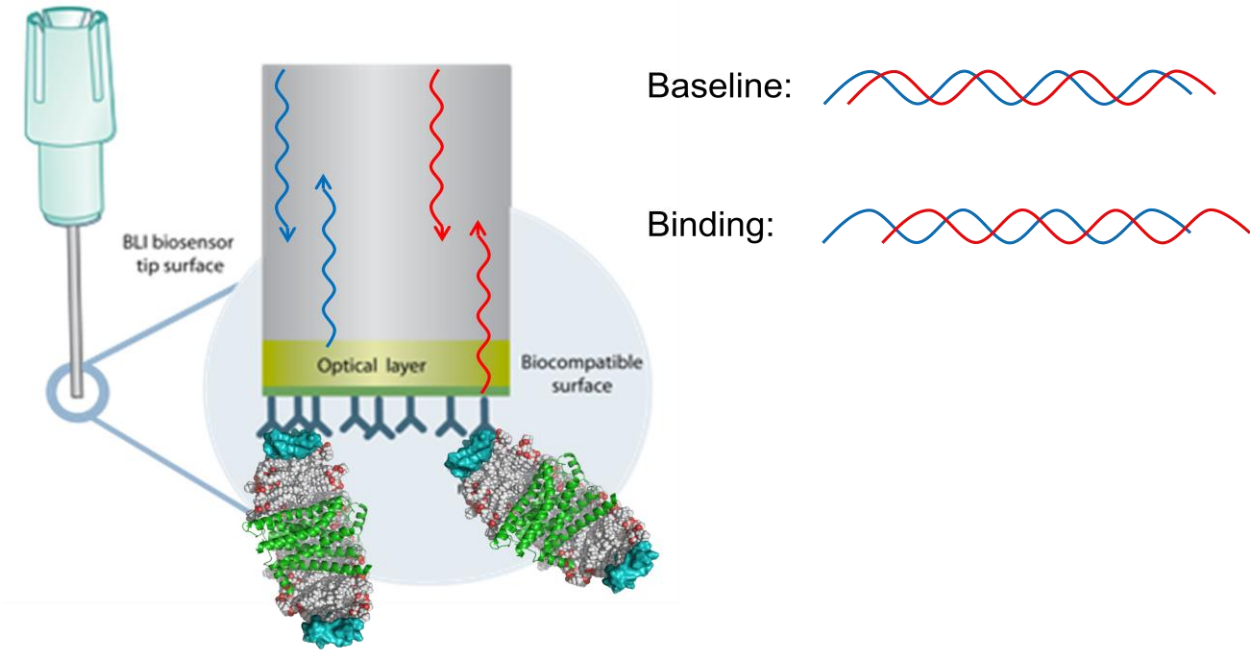

Figure 2-3. Biolayer interferometry as a means to monitor the β_2AR-Nb80 interaction.
Nb80 binding to unliganded and agonist-occupied β_2-AR was measured using the OctetRED biolayer interferometry system (Pall FortéBio). In this assay, a target protein is immobilized on the functionalized tip of a fiber optic probe that is dipped into an analyte solution to observe analyte association to the target protein. A dissociation step is then performed by transferring the biosensor into buffer lacking analyte. Analyte association/dissociation is measured by monitoring changes in the interference pattern of a light reflected from the biosensor tip as the total mass bound at the tip surface changes (blue and red waves). Figure is adapted from Pall FortéBio.

2.5 - Biotinylation of ApoAI for immobilizing reconstituted β2AR

To monitor the β_2AR-Nb80 interaction using biolayer interferometry, we needed to immobilize purified β_2AR onto the interferometry probe. Since detergent-solubilized receptors are relatively unstable and display altered ligand-binding properties, we chose to use β_2AR reconstituted into a phospholipid bilayer. However, reconstitution into traditional lipid vesicles would be problematic, as some receptors would not be accessible to Nb80 binding due to the mixed orientation of receptors that is common in these vesicles. To circumvent this obstacle we incorporated β_2AR into reconstituted high-density lipoprotein (rHDL) particles, a strategy which leaves both the extracellular and intracellular faces of the receptor accessible to solvent and able to interact with small-molecule ligands and Nb80. β_2AR inserted into rHDL particles has been shown by our lab and others to maintain its functionality, able to bind small-molecule ligands and G proteins in a manner comparable to β_2AR in native cell membranes[88,89].

Immobilization of the target protein on the interferometry tips can be achieved by multiple means, as several functionalized surfaces are commercially available (e.g. Ni-NTA, anti-FLAG, streptavidin). We chose to immobilize β_2AR-containing rHDL using the biotin-streptavidin interaction, as we anticipated that the high-affinity interaction between these two molecules would provide the most stable loading of β_2AR onto the tip. ApoAI was biotinylated using NHS-PEG4-biotin, a reagent that contains a long (~3 nm) linker between the reactive NHS-ester moiety and the biotin molecule. This linker was chosen for two reasons. First, each ApoAI monomer contains 18 lysine residues, therefore we expected efficient labeling to occur using the NHS-ester functional group. Second, the long linker provides adequate space between immobilized rHDL and the surface of the tip, as well as flexibility of orientation to ensure that Nb80 would be able to reach its binding site on β_2AR. The biotinylation reaction was performed

using a 1:1 molar ratio of NHS-PEG4-biotin:ApoAI for 30 minutes at room temperature, and any free biotin reagent was removed by gel filtration. Successful bitotinylation was confirmed by monitoring binding on OctetRED.

2.6 - Reconstitution of β_2AR for immobilization

Purified FLAG-tagged β_2AR was incorporated into rHDL particles according to methods previously published by our laboratory[88,90]. The reconstitution was performed using a 20-fold molar excess of biotinylated ApoAI compared to β_2AR. Since each rHDL particle contains two ApoAI monomers, this results in a final 10-fold molar excess of rHDL particles over β_2AR, a ratio which helps to ensure that receptors are incorporated as monomers. However, the resultant reaction mixture contains predominantly empty rHDL particles, which would occupy binding sites on the interferometry tip and decrease the maximum possible binding signal from Nb80 recruitment by β_2AR-rHDL. Therefore, receptor-containing rHDL particles were separated from empty rHDL by M1 anti-FLAG affinity chromatography. Elution fractions containing β_2AR-rHDL particles were identified by radioligand binding using a saturating concentration of [^{3}H]dihydroalprenolol ([^{3}H]DHAP), and then pooled for use in interferometry experiments.

2.7 - Determination of β_2AR-rHDL loading parameters

To maximize the total Nb80 binding signal and reduce the potential for non-specific Nb80 binding or steric effects due to receptor crowding, it was imperative to optimize the loading density of β_2AR-rHDL on the interferometry tip. Various dilutions of FLAG-purified β_2AR-rHDL particles were loaded onto streptavidin-coated tips using the OctetRED (Fig. 2-4a). At high β_2AR-rHDL concentrations, the binding proceeded rapidly ($t_{1/2} \approx 7$ seconds) with a typical maximum interference shift of 4-5 nm. At intermediate dilutions, the association rate

constant (k_{obs}) decreased with no change in maximum signal; at high dilutions both k_{obs} and the maximum interference shift decreased. The dilution chosen for further experiments was the concentration at which the observed rate constant of β_2AR-rHDL binding was slowest without decreasing the maximum binding signal, which occurred at a β_2AR-rHDL concentration of ~30 nM. The proper loading conditions were determined empirically for each batch of β_2AR-rHDL.

2.8 - Definition of non-specific Nb80 binding

Based on preliminary experiments examining Nb80 binding to tips loaded with empty rHDL, it was determined that Nb80 bound non-specifically to either the tip surface, to streptadivin, or to the empty rHDL themselves. Inclusion of BSA at 0.05% w/v final concentration in the assay buffer diminished this non-specific interaction, but at higher concentrations (≥1 μM), Nb80 still displayed non-specific binding (Fig. 2-4b). Therefore for all experiments, a parallel assay was performed using tips loaded with empty biotinylated rHDL to define non-specific binding for each Nb80 concentration. This signal was subtracted from that obtained using tips loaded with β_2AR-rHDL (Fig. 2-4c). The loading parameters for empty rHDL were optimized to match β_2AR-rHDL loading.

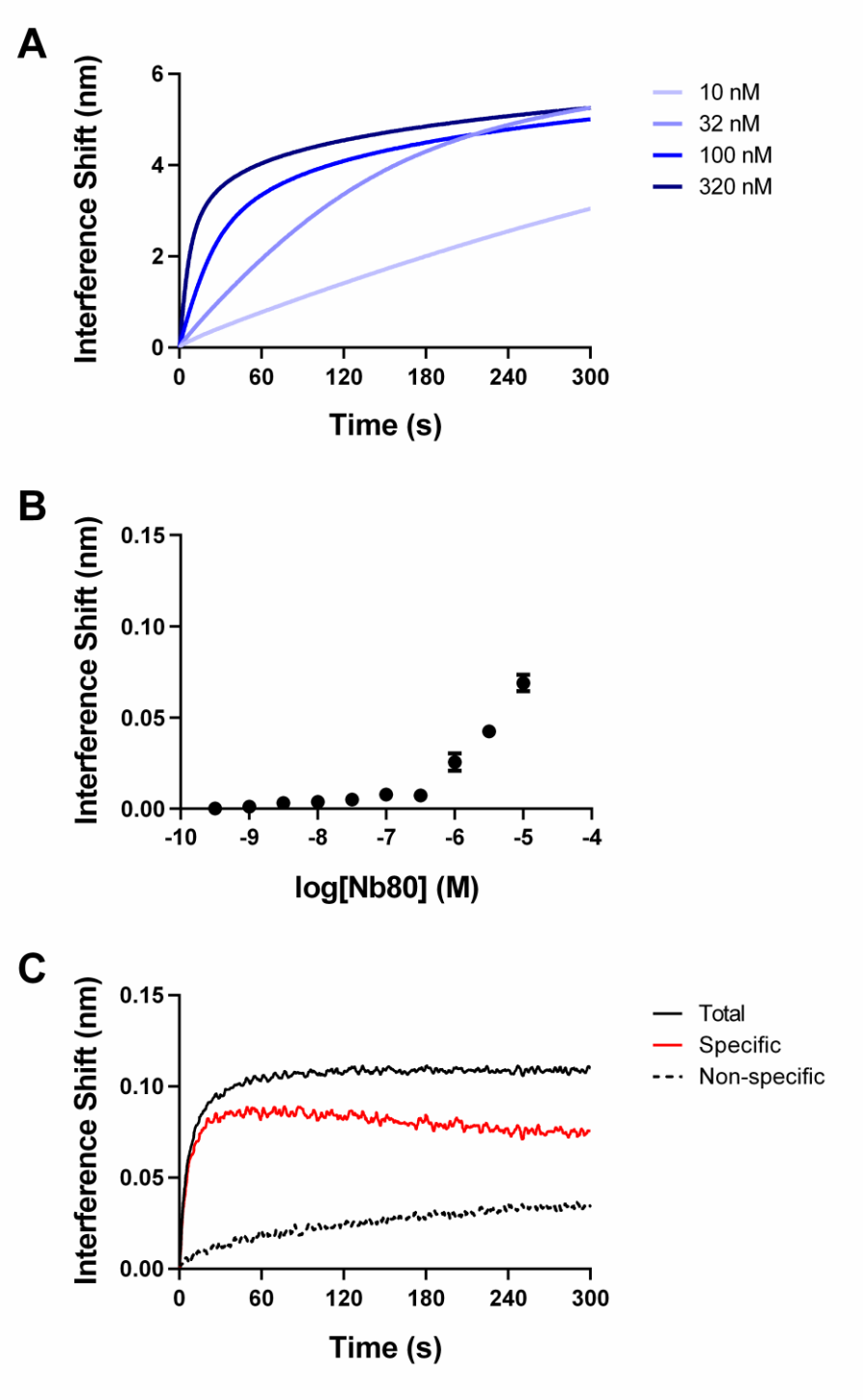

Figure 2-4. Optimization of β_2AR loading and definition of non-specific Nb80 binding.
A) Various concentrations of FLAG-purified β_2AR-rHDL were loaded onto streptavidin-coated biosensors using the OctetRED instrument. Data are a representative image of a typical loading experiment. **B)** Maximum interference shifts generated by Nb80 binding to biosensors loaded with empty biotinylated rHDL particles. Data are shown as mean ± SEM from n=3 experiments. **C)** Representative image showing total, non-specific, and specific (red) binding of 3 µM Nb80.

2.9 - Agonist enhances Nb80 affinity for β_2AR by enhancing association rate

In keeping with previously published reports demonstrating Nb80-mediated enhancement of agonist affinity for β_2AR[55], the interferometry experiments revealed an enhancement of Nb80 affinity for β_2AR in the presence of an agonist. After loading of biosensors with β_2AR-rHDL, receptor was equilibrated with either vehicle or a saturating concentration of the full agonist isoproterenol (100 μM; ISO). The association of increasing concentrations of Nb80 was monitored for 5 minutes, and dissociation of Nb80 for 30 minutes (Fig. 2-5a). The maximum association signal was plotted as a function of Nb80 concentration to determine the affinity of the β_2AR-Nb80 interaction (Fig. 2-5b). In the absence of ISO, Nb80 displayed a K_d of approximately 820 nM ($pK_d = 6.1 \pm 0.1$). However, when β_2AR was bound to ISO this value was shifted ~370-fold to an affinity of 2.2 nM ($pK_d = 8.66 \pm 0.09$). Although agonist occupancy of β_2AR slightly slowed Nb80 dissociation (Fig. 2-6a, vehicle $k_{off} = 0.0021 \pm 0.0002$ sec^{-1}; +ISO $k_{off} = 0.0014 \pm 0.0001$ sec^{-1}), the shift in Nb80 affinity was predominantly driven by a dramatic enhancement of the association rate of Nb80 in the presence of ISO.

In the absence of ISO, the relationship between the observed association rate constant and Nb80 concentration appeared hyperbolic, and thus the k_{on} for Nb80 binding could not be calculated from the available data (Fig. 2-6b). However, when β_2AR was bound to ISO, plotting the observed Nb80 association rate constant as a function of Nb80 concentration yielded a linear relationship, with a slope (k_{on}) of $1.1x10^6 \pm 4x10^4$ $M^{-1}sec^{-1}$ (Fig. 2-6c). The kinetically-derived affinity (k_{off}/k_{on}) of Nb80 for ISO-bound β_2AR was 1.9 ± 0.2 nM, in good agreement with the value calculated using the maximal Nb80 association signals.

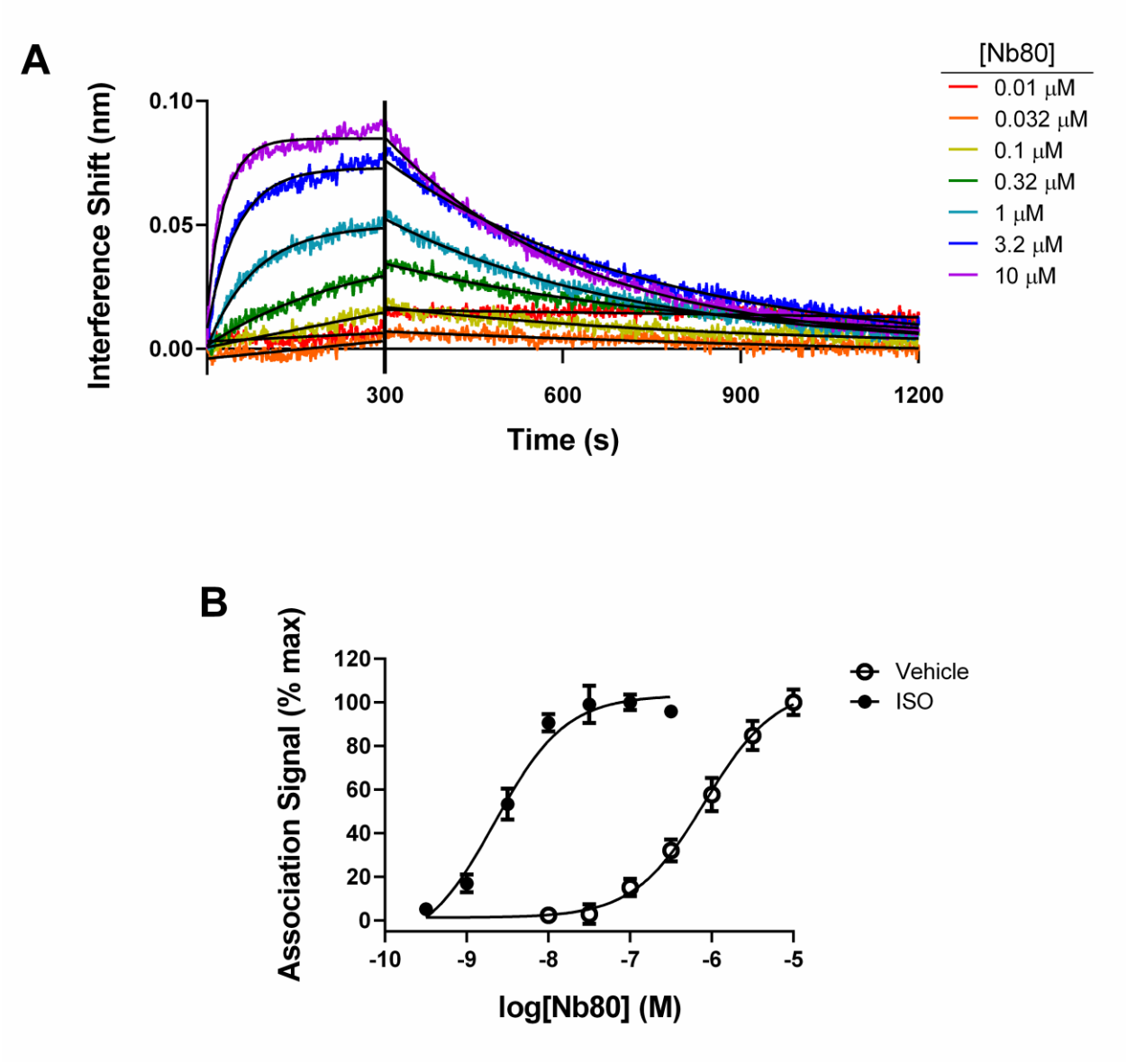

Figure 2-5. Using biolayer interferometry to measure Nb80 affinity for β_2AR.
A) Binding of Nb80 to β_2AR-rHDL in the absence of agonist. Following capture of β_2AR-rHDL, the biosensors were dipped into wells containing various concentrations of Nb80. Dissociation was initiated after 5 min (black bar) by transferring the probes into buffer alone. The data (colors) were fit to single-phase exponential association and dissociation functions (shown in black). Data shown are a representative trace of n=3 experiments. **B)** Concentration-response curves showing binding of Nb80 to β_2AR-rHDL in the absence or presence of ISO (100 μM). The affinity of Nb80 was enhanced ~370-fold in the presence of ISO (vehicle pK_d = 6.1 ± 0.1, or $K_d \approx$ 820 nM; ISO pK_d = 8.66 ± 0.09 or $K_d \approx$ 2.2 nM). Data are shown as mean ± SEM of n=3 experiments.

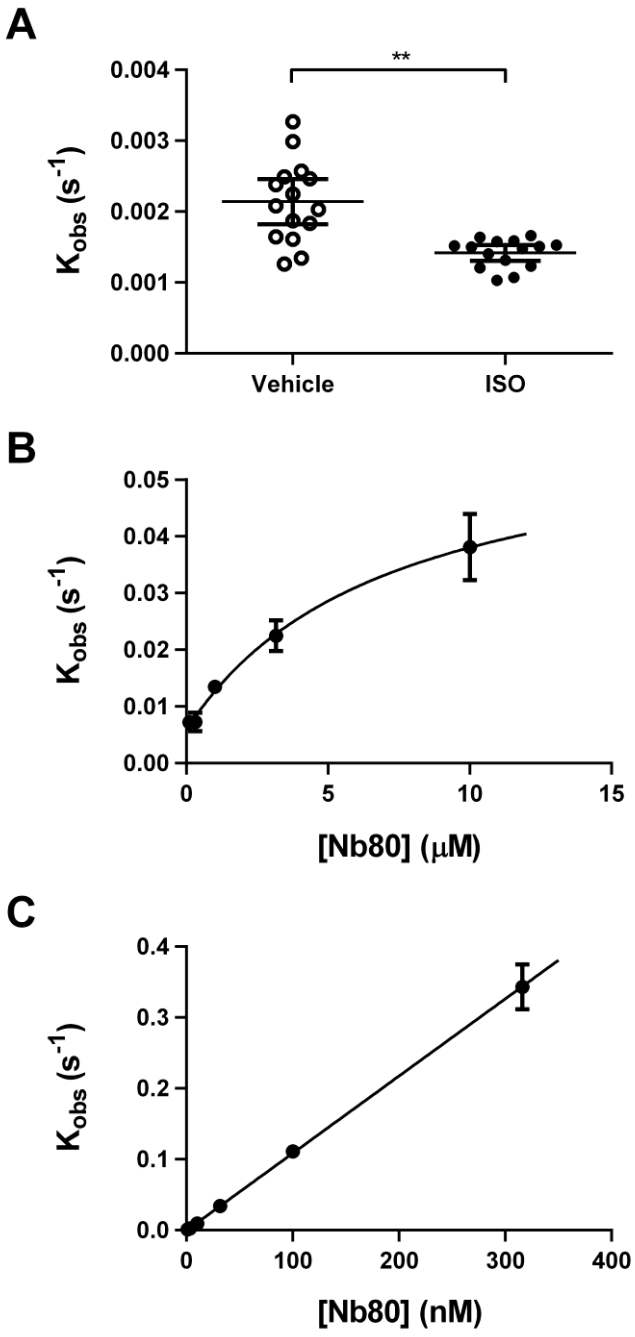

Figure 2-6. Effect of isoproterenol on the Nb80-β_2AR interaction.
A) Nb80 dissociated more slowly from ISO-bound β_2AR (k_{off} = 0.0014 ± 0.0001 sec^{-1},or $t_{1/2} \approx$ 495 sec) than from β_2AR in the absence of agonist (vehicle; k_{off} = 0.0021 ± 0.0002 sec^{-1}, or $t_{1/2} \approx$ 330 sec; p = 0.004 by a two-tailed unpaired t-test). **B)** In the absence of agonist, the relationship between Nb80 concentration and its k_{obs} for association was non-linear. **C)** When β_2AR was pre-incubated with 100 μM ISO, the relationship between Nb80 concentration and k_{obs} was linear. The second order rate constant (slope) k_{on} = $1.1x10^6$ ± $4x10^4$ $M^{-1}sec^{-1}$. All data are shown as mean ± SEM from n=3 experiments.

2.10 - Orthosteric ligands show differential cooperativities with Nb80

The enhancement of Nb80 affinity in the presence of agonist, together with the observation of a non-linear relationship between Nb80 concentration and K_{obs} in the absence of agonist, suggests that Nb80 binds selectively to an active conformation of β_2AR. To further test the hypothesis that Nb80 binding depended on transition of β_2AR into an active state, we examined orthosteric ligands of various efficacies for their ability to promote Nb80 binding to β_2AR. Pre-incubation of β_2AR with 10 μM ICI-118551, an inverse agonist, abolished measurable binding of 1 μM Nb80 (Fig. 2-7a). When β_2AR was pre-incubated with the partial agonist salmeterol (1 μM), Nb80 bound β_2AR with an affinity of approximately 15 nM (pK_d = 7.82 ± 0.04). The enhancement of Nb80 affinity was once again driven by an acceleration of Nb80 on-rate (K_{on} = $1.2x10^5$ ± $4x10^3$ $M^{-1}sec^{-1}$, K_{off} = 0.0011 ± 0.0001 sec^{-1}). Nb80 affinity and association were also enhanced by the high-affinity full agonist BI-167107 (pK_d = 8.16 ± 0.05 or $K_d \approx$ 6.9 nM; K_{on} = $4.0x10^5$ ± $2x10^3$ $M^{-1}sec^{-1}$, K_{off} = 0.0013 ± 0.0001 sec^{-1}). While the dissociation of Nb80 from β_2AR-rHDL was similar with salmeterol, isoproterenol, or BI-117167 bound, Nb80 association to salmeterol-bound receptor was markedly slower when compared to β_2AR bound by either full agonist (Table 2-1; Fig 2-7c & d).

Bound Ligand	**Nb80 K_{on} ($M^{-1}sec^{-1}$)**	**Nb80 K_{off} (sec^{-1})**
ICI-118551	No binding	
None	-	0.0021 ± 0.0002
Salmeterol	$1.2x10^5$ ± $4x10^3$	0.0011 ± 0.0001
Isoproterenol	$1.1x10^6$ ± $4x10^4$	0.0014 ± 0.0001
BI-167107	$4.0x10^5$ ± $2x10^3$	0.0013 ± 0.0001

Table 2-1. Effect of orthosteric ligands on the kinetics of Nb80 binding to β_2AR.

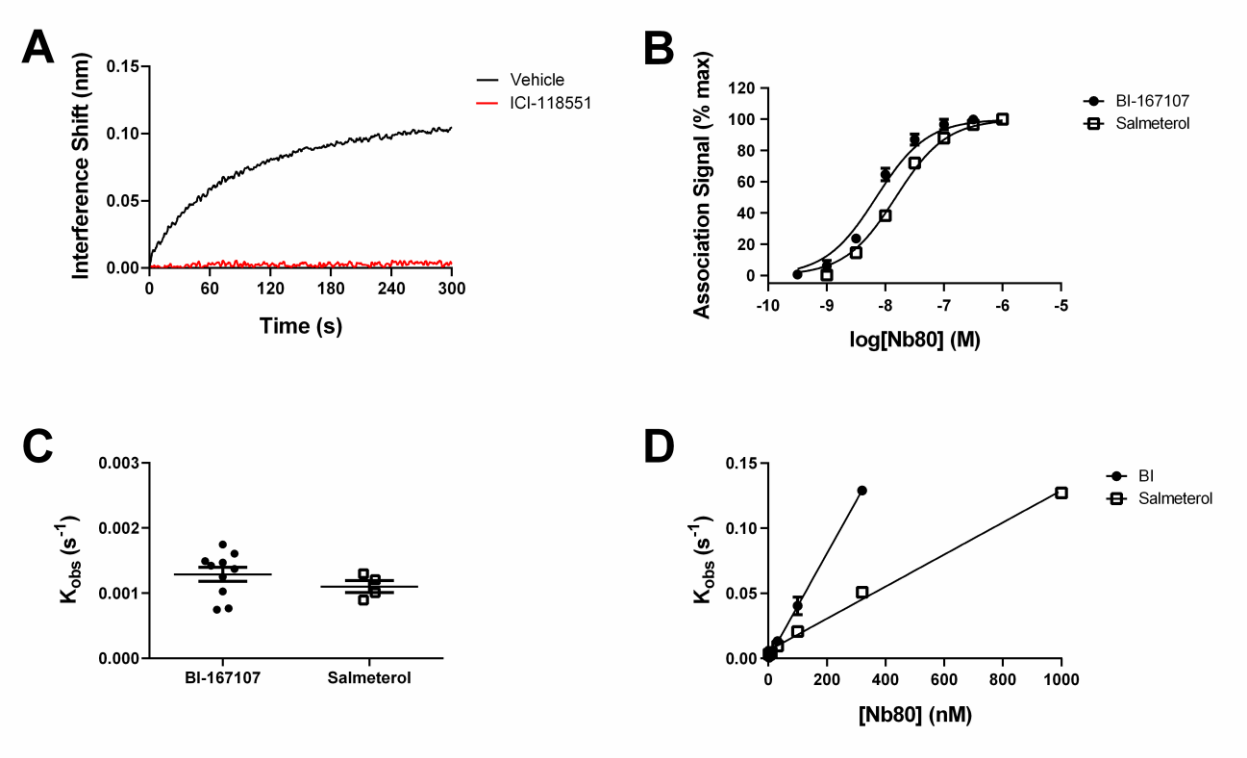

Figure 2-7. Effects of agonist efficacy on Nb80 binding to β_2AR.
A) Binding of 1 µM Nb80 was abolished by pre-incubation of β_2AR with the inverse agonist ICI-118551 (10 µM). Data are a representative image of two experiments. **B)** Nb80 bound with slightly higher affinity to β_2AR occupied by the full agonist BI-167107 compared to β_2AR bound by the partial agonist salmeterol (BI-167107 $pK_d = 8.16 \pm 0.05$ or $K_d \approx 7$ nM; Salmeterol $pK_d = 7.82 \pm 0.04$ or $K_d \approx 15$ nM). Data are shown as mean ± SEM from n=2 (BI-167107) or n=1 (salmeterol) experiments. **C)** Dissociation of Nb80 proceeds similarly from BI- or salmeterol-bound β_2AR (BI-167107 $k_{off} = 0.0013 \pm 0.0001$ sec^{-1}; Salmeterol $k_{off} = 0.0011 \pm 0.0001$ sec^{-1}). Individual values are shown along with mean ± SEM from n=2 (BI-167107) or n=1 (salmeterol) experiments. **D)** The relationship between Nb80 concentration and k_{obs} was linear in the presence of both BI-167107 and salmeterol; however Nb80 associated more slowly to salmeterol-bound β_2AR (BI-167107 $k_{on} = 4.0x10^5 \pm 2x10^3$ $M^{-1}sec^{-1}$; Salmeterol $k_{on} = 1.2x10^5 \pm 4x10^3$ $M^{-1}sec^{-1}$).

2.11 - Nb80 as a conformational sensor of β_2AR in cells

Our collaborators in Dr. Mark von Zastrow's lab at UCSF inserted the gene for Nb80 into pEGFP-N3 to append green fluorescent protein (GFP) at the C-terminus of Nb80 and expressed this construct (Nb80-GFP) in HEK293 cells. A C-terminal GFP fusion was chosen because in the structure of the β_2AR-Nb80 complex[55], the C-terminus of Nb80 is far from β_2AR and thus the addition of GFP should not alter the β_2AR-Nb80 interaction. By comparing the fluorescence intensity of Nb80-GFP in HEK293 cells to a GFP standard curve, the cytoplasmic concentration of Nb80-GFP was calculated to be approximately 20 nM. In unstimulated cells, Nb80-GFP fluorescence was diffusely distributed throughout the cytoplasm. However, upon addition of 10 μM isoproterenol, Nb80-GFP was rapidly recruited to the plasma membrane where it co-localized with FLAG-tagged β_2AR (which was visualized using an Alexa455-labeled anti-FLAG antibody). After 3 minutes, β_2AR staining became punctate as the receptor was clustered in clathrin-coated pits and internalized, but no Nb80-GFP was localized to these structures. However, following 20 minutes of agonist stimulation, Nb80-GFP showed robust recruitment to endosomal puncta, suggesting activation of internalized β_2AR at the endosomal membrane (Fig. 2-8). The ISO-mediated membrane recruitment of Nb80-GFP could be reversed by the addition of the antagonist CGP-12177 (50 μM), which returned Nb80-GFP to its original diffuse cytoplasmic distribution. Furthermore, Nb80-GFP recruitment was specific for β_2AR, since Nb80-GFP was not recruited to the plasma membrane nor to endosomes following stimulation of the closely related D1 dopamine receptor, a Gs-coupled receptor like β_2AR, with 10 μM dopamine. Our collaborators conducted many more experiments to demonstrate that β_2AR indeed engages G protein and generates cAMP signals from endosomes[91], work which is beyond the scope of this thesis.

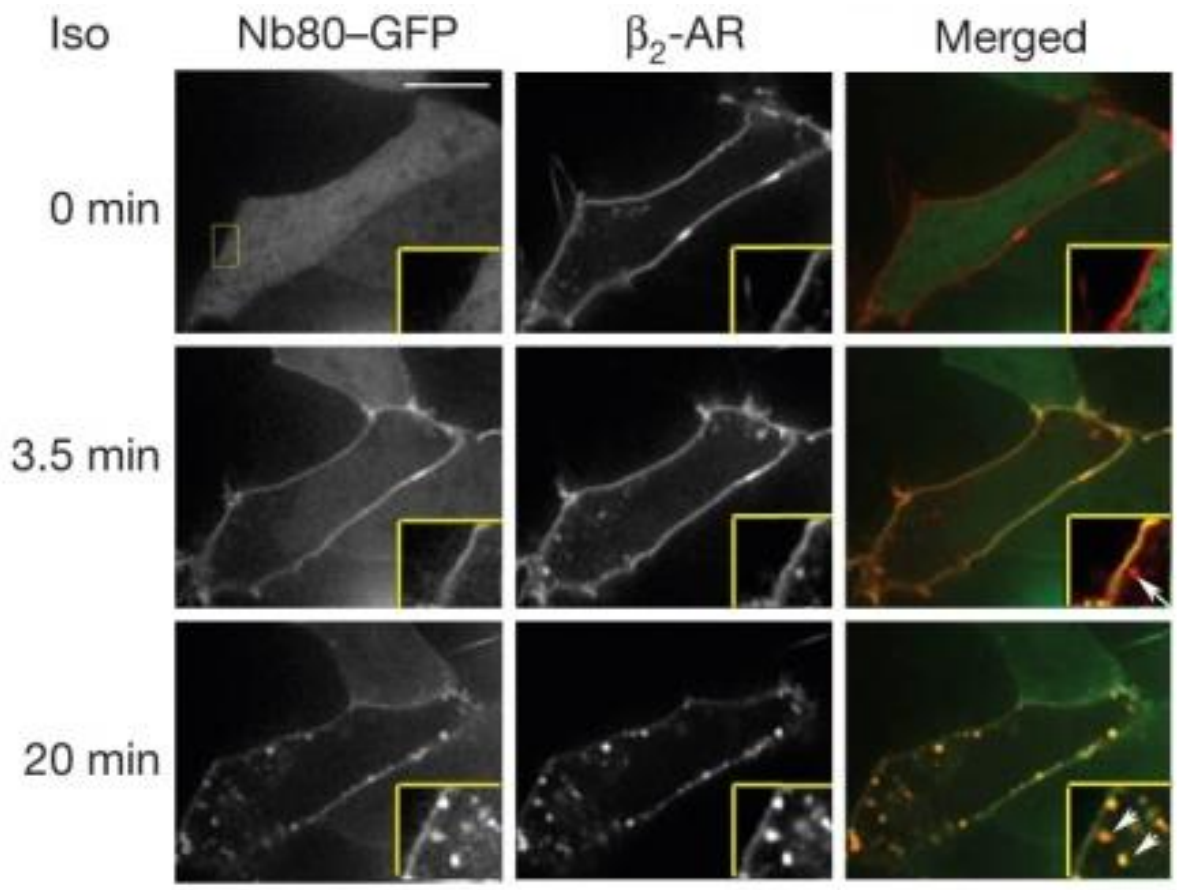

Figure 2-8. Detection of active β2AR by Nb80-GFP in living cells.
Shown are representative Nb80–GFP (green) and β_2AR (red) localization at the indicated times (left) after 10 μM isoproterenol addition (>30 Nb80–GFP positive endosomes per cell observed at 20 min; *n* = 29 cells, 10 experiments). Data were collected by Dr. Roshanak Irannejad in Mark von Zastrow's lab (see Fig. 1 of Irannejad *et al.*[91]).

Discussion

2.12 - β_2AR activation is necessary for Nb80 binding

When β_2AR was occupied by ISO, we observed a linear relationship between the observed association rate constant and Nb80 concentration, and the K_{on} derived from this fit approaches the limits of diffusion in aqueous buffer (~10^8 $M^{-1}sec^{-1}$). Thus the β_2AR-Nb80 interaction can be described as a simple bimolecular interaction (Eq. 2-1), with the main factor limiting Nb80 binding being the time it takes for Nb80 to reach the receptor.

$$R + N \underset{k_2}{\overset{k_1}{\rightleftharpoons}} RN$$

Equation 2-1. Binding of Nb80 to β_2AR in the presence of agonist.
In the presence of a saturating concentration of ISO, our data are consistent with a simple bimolecular reaction between β_2AR (R) and Nb80 (N). In this scenario, formation of the β_2AR-Nb80 complex (RN) proceeds with the second-order rate constant k_1, and the complex dissociates with the first-order rate constant k_2.

In contrast, in the absence of agonist the relationship between Nb80 concentration and observed association rate constant could not be fit to a linear function and instead appeared hyperbolic. This non-linear relationship suggests that the rate-limiting step of Nb80 binding changes as its concentration is increased (i.e. at high Nb80 concentrations, Nb80 binding is limited by something other than diffusion to its binding site). In this case, the β_2AR-Nb80 interaction cannot be described by a simple bimolecular reaction scheme and a more complex model must be invoked to describe the binding reaction. Our data are consistent with a model that requires an isomerization of the receptor to occur before Nb80 binding can proceed (Eq. 2-2). This scenario is in keeping with current models of GPCR behavior (discussed in chapter 1.4) which maintain that even in the absence of ligands, receptors are in equilibrium between inactive (R) and active (R*) conformations. The necessity of this isomerization step to occur prior to

Nb80 binding therefore suggests that Nb80 does not bind inactive β_2AR, and is indeed selective for an activated conformation of β_2AR. In support of this hypothesis, we observed no measurable Nb80 binding when β_2AR was bound to the inverse agonist ICI-118,551, which stabilizes an inactive β_2AR conformation. In contrast, the binding of an agonist is predicted to shift the R/R* equilibrium in favor of active R* conformations, thus allowing the binding of Nb80 to proceed more rapidly. To produce this effect, an agonist may either increase the rate of isomerization to R* (the rate constant k_1 shown below) or slow the decay of R* back to an inactive R conformation (k_2 below). Based on our data, we are unable to distinguish between these possibilities. However, a recent single-molecule fluorescence study of β_2AR suggests that the full agonist formoterol both increases the frequency of transitions to R* conformations and simultaneously reduces the frequency of relaxation to inactive R states[92].

1) $$\mathbf{R} \underset{k_2}{\overset{k_1}{\rightleftharpoons}} \mathbf{R^*}$$

2) $$\mathbf{R^* + N} \underset{k_4}{\overset{k_3}{\rightleftharpoons}} \mathbf{R^*N}$$

Equation 2-2. Binding of Nb80 to β_2AR in the absence of agonist.
In the absence of agonist, our data are consistent with a two-step model of Nb80 binding to β_2AR. Reaction 1 denotes the isomerization of β_2AR between inactive (R) and active (R*) conformations. The proportion of β_2AR in active R* states, competent to bind Nb80, depends on the ratio of the first-order rate constants k_2/k_1. Upon isomerization to R*, Nb80 binding is able to proceed according to reaction 2.

The reliance of Nb80 binding on receptor activation, or at least on a partial outward movement of TM6, is not unexpected based on what is known about the structural basis of Nb80 binding. In the structural model of the agonist-β_2AR-Nb80 complex reported by Rasmussen *et al.*, CDR3 of Nb80 forms contacts with residues buried within the β_2AR core that are only

exposed upon TM6 movement, including a hydrogen-bond interaction with Arg131$^{3.50}$ of the DRY motif in TM3[55]. These interactions are similar to those observed between the C-terminal α5 helix of $G\alpha_s$ and β_2AR[56], where Arg131 interacts with Tyr391 in the α5 helix, and several polar residues in TM5 (Glu225, Gln229, K232) also contribute to a hydrogen-bond network with α5. Therefore, for full Nb80 or Gα engagement, movement of TM6 is required to expose crucial residues and provide the interactions observed in crystal structures. Compared to Nb80, $G\alpha_s$ makes more extensive contacts with the receptor and forms additional contacts outside of the β_2AR TM core (e.g. with the second intracellular loop) that contribute to the binding reaction. However, the engagement of the Gα C-terminus is required for a productive β_2AR-Gs interaction that results in nucleotide exchange. Based on these structural requirements, together with our studies of Nb80 binding, we anticipate that agonists enhance receptor-G protein affinity by speeding the on-rate of G protein, rather than by slowing its dissociation from the receptor.

2.13 - Insights into agonist efficacy

In the context of a two-state model, an agonist's efficacy can be explained by its ability to shift a receptor's conformational equilibrium in favor of active (R*) states, in turn promoting G protein binding by the receptor. Under this framework, full agonists efficiently stabilize R* states of the receptor, while partial agonists do so less efficiently and thus the receptor spends less time in R* states when occupied by a partial agonist. Alternatively, it may be possible that partial agonists stabilize an entirely different subset of conformations - an "off-pathway" ensemble with a reduced ability to activate G proteins relative to R* (which we will call R' for this discussion). Nb80 represents a useful tool to interrogate these two hypotheses; because of the conformational selectivity of nanobody binding, we can use Nb80 as a tool to monitor the formation of R* states, with differences in Nb80 recruitment rate reflective of the position of the R/R* equilibrium. If

partial agonists are indeed stabilizing a unique R' ensemble of β_2AR, at the expense of R* conformations, one would predict that the affinity of Nb80 for β_2AR should be dramatically worsened (assuming poor interconversion between R' and R* states). However, if partial agonists are simply inefficient at stabilizing R*, we should still observe Nb80 binding, but at a slower rate than in the presence of a full agonist.

In the absence of agonist, when the conformational equilibrium lies in favor of inactive R states, we observed slow Nb80 association that appears dependent on an isomerization step. In the presence of the partial agonist salmeterol, Nb80 binding is more rapid, but does not reach the same rate as seen with the full agonists ISO or BI-167107. The observation that a partial agonist can recruit Nb80 suggests that the conformational ensembles of full- and partial-agonist bound receptors do overlap, and that salmeterol does not stabilize a unique partially active R' state at the expense of a fully active R* conformation. Instead, salmeterol is likely unable to stabilize β_2AR in a Nb80-binding conformation as frequently as a full agonist would, reflected in the slower association of Nb80 binding to salmeterol-occupied receptor. As previously discussed, biophysical experiments have shown that agonist-bound β_2AR maintains a great deal of conformational flexibility and agonist binding alone is not sufficient to stabilize the full outward movement of TM6 that is observed in crystal structure of β_2AR bound to Nb80 or Gs[58,85,86]. Thus, it stands to reason that salmeterol-bound β_2AR should still retain enough flexibility to transition to a state able to bind Nb80.

2.14 - Validation of intracellular Nb80-GFP binding experiments

By establishing a technique to directly measure affinity of Nb80 for β_2AR, we were able to validate the behavior of Nb80-GFP our collaborators observed in living cells. Based on the concentration of Nb80-GFP in the cytoplasm (~20 nM), and assuming that the binding of Nb80-

GFP in cells proceeds similarly to what we measured *in vitro* using interferometry, few receptors should be bound by Nb80 in the absence of agonist. However, based on the dramatic enhancement of Nb80 affinity in the presence of agonist, it is predicted that the majority of receptors will be occupied by Nb80 upon addition of ISO. Furthermore, our kinetic analysis demonstrated the selectivity of Nb80 for active conformations of β_2AR. It is therefore unlikely that the observed recruitment of Nb80 to the plasma membrane or to endosomal membranes represented Nb80 binding to inactive β_2AR. However, it is unknown whether the active state of β_2AR in endosomes is generated by basal activity, or by the binding of agonist co-internalized with the receptor.

2.15 - Application of interferometry to study other GPCRs

The assay developed in this chapter serves as a versatile template to study the interactions between a broad array of receptors and their binding partners. Many GPCRs have been incorporated into rHDL particles by several laboratories and have been shown to be functional[79,80,88,90,93–96]. Since the immobilization strategy described here captures receptor-containing rHDL particles via their ApoAI "belt," any GPCR that can be inserted into rHDL can be studied in this system without the need to covalently modify the receptor for immobilization. Indeed, we have used the procedures described here to immobilize MOPr-rHDL and investigate the role of orthosteric and allosteric ligands in the binding of Nb39, an active-state stabilizing nanobody for MOPr (Livingston *et al.*, manuscript in preparation). Furthermore, GPCRs interact with an array of cytoplasmic proteins: G proteins, GRKs, β-arrestins, RGS proteins, PDZ domain-containing proteins, and many more. As we will discuss in chapter 5.2, the interactions between GPCRs and these diverse binding partners could potentially be studied quantitatively using interferometry techniques similar to what we have described here.

Conclusion

We developed an interferometry platform to monitor the binding of nanobody Nb80 to β_2AR in rHDL particles and applied this method to use Nb80 as a reporter of β_2AR conformational states. Our data demonstrate the selectivity of Nb80 for an active conformation of β_2AR and provide support for the current models used to describe receptor activation. Furthermore, we have gained insight into the role of agonists in stabilizing various states of β_2AR and the mechanism by which they allosterically enhance protein binding at the cytoplasmic face of β_2AR.

CHAPTER 3

Allosteric communication between the G protein- and agonist-binding site in GPCRs

Just as agonists are able to allosterically promote G protein or Nb80 recruitment to β_2AR, the binding of G protein at the receptor's cytoplasmic face has been shown to enhance agonist affinity for many GPCRs. This chapter proposes a structural basis to explain this phenomenon, and what follows is the pre-print version of a manuscript submitted for publication. Several members of our lab, as well as collaborating labs, made important contributions to this work. The initial observations of Nb80- and G protein-mediated effects on radiolabeled antagonist binding were made by Gisselle Vélez-Ruiz, and the structural characterization of β_2AR bound to Nb80 and to nucleotide-free G protein (done by Brian DeVree in collaboration with Soren Rasmussen in the Kobilka Lab) allowed us to develop a structural hypothesis to explain the allosteric communication between agonists and G protein. Brian went on to characterize the effects of Nb80 and nucleotide-free G protein on antagonist binding kinetics. I followed his studies with a set of similar experiments using radioligands of varying efficacies (inverse agonist, partial agonist, full agonist) and characterized the behavior of mu opioid receptor and M2 muscarinic acetylcholine receptor bound to nucleotide-free G protein or their respective G protein-mimetic nanobodies.

G protein-coupled receptors (GPCRs) remain the primary conduit by which cells detect environmental stimuli and communicate with each other. Sequencing of the human genome revealed the magnitude of the GPCR superfamily, identifying over 800 genes encoding GPCRs, making this class of receptors the third-largest gene family[97]. Despite the varying nature of the chemical stimuli, which range from photons to small-molecule odorants and hormones to larger peptides and proteins, the generation of G protein-mediated signals proceeds by a common mechanism. Upon activation by extracellular agonists, these seven transmembrane domain (7TM)-containing receptors interact with heterotrimeric G proteins to regulate downstream second messenger and/or protein kinase cascades. We recently used x-ray crystallography[56], hydrogen-deuterium exchange mass spectrometry[98], and electron microscopy[99] to characterize a prototypic GPCR, the β_2-adrenergic receptor (β_2AR), in complex with its cognate G protein, Gs.

Our studies of the nucleotide-free agonist-β_2AR-Gs ternary complex revealed dramatic conformational changes in Gα that are stabilized by binding to agonist-activated receptor and provided insight into the mechanism by which GPCRs catalyze GDP release, the key step required for GTP binding and activation of G proteins[56]. The structural data also offer hints on how G protein binding is associated with conformational changes that propagate in the opposite direction to allosterically influence ligand binding.

Here, we suggest an explanation for the allosteric communication which links the nucleotide binding site on the G protein to the hormone binding site on the receptor, with a focus on conformational changes in the extracellular face of the receptor that alter access to the hormone binding site. Specifically, we provide functional evidence that G protein coupling to β_2AR stabilizes a 'closed' receptor conformation characterized by restricted access to and egress from the hormone binding site. Surprisingly, the effects of G protein on the hormone binding site

can be observed in the absence of a bound agonist, where G protein coupling driven by basal receptor activity impedes the association of agonists, partial agonists, antagonists and inverse agonists. The ability of bound ligands to dissociate from the receptor is also hindered, providing a structural explanation for the G protein-mediated enhancement of agonist affinity, which has been observed for many GPCR-G protein pairs. Our studies also suggest that in contrast to agonist binding alone, coupling of a G protein in the absence of an agonist stabilizes large structural changes in a GPCR. The effects of nucleotide-free G protein on ligand binding kinetics are shared by other members of the superfamily of GPCRs, suggesting that a common mechanism may underlie G protein-mediated enhancement of agonist affinity.

Results

3.1 - Nucleotide-free G protein limits antagonist binding to β_2AR

GPCR-G protein interactions have historically been monitored using radioligand binding assays. Observations as early as the 1970s suggested that G protein coupling enhances agonist affinity for the receptor, and can be abolished by uncoupling the G protein from the receptor with guanine nucleotides[33]. These and other data formed the basis for the ternary complex model of agonist-receptor-G protein interactions[35,100]. In this paradigm, the active state of the receptor is stabilized by both the agonist and G protein, and enhancement of agonist affinity arises due to the positive cooperativity between agonist and G protein. However, using purified β_2AR•Gs complexes, we observed peculiar binding characteristics of the antagonist [^{3}H]dihydroalprenolol ([^{3}H]DHAP) to β_2AR (Fig. 3-1a). As illustrated, addition of GDP increases the observed binding of a saturating concentration of [^{3}H]DHAP, whereas removal of GDP using a nucleotide lyase, apyrase, decreases [^{3}H]DHAP binding. The apyrase-mediated decrease in [^{3}H]DHAP binding is

reversed upon addition of excess GDP, suggesting that the decrease is indeed due to the formation of nucleotide-free β_2AR·Gs complexes. Removal of GDP from the β_2AR·Gs complex relies on the constitutive activity of β_2AR and the rapid hydrolysis (by apyrase) of GDP released from the α-subunit of Gs, Gsα. The nucleotide-free status of Gsα in these β_2AR•Gs complexes was confirmed by rapid [^{35}S]GTPγS binding kinetics[47]. The observed deficit in [^{3}H]DHAP binding to nucleotide-free β_2AR•Gs is the result of slower [^{3}H]DHAP association (Fig. 3-1b). GDP enhances [^{3}H]DHAP association in a concentration-dependent manner, with similar effects achieved by complete β_2AR•Gs uncoupling with GTPγS. Although nucleotides do not significantly affect the affinity (K_d) of [^{3}H]DHAP, their modulatory capacity is gamma phosphate-dependent since GTPγS is ~10-fold more potent than GDP (Fig. 3-2). Thus, β_2AR bound to nucleotide-free G protein adopts a conformation characterized by restricted access to the hormone binding site.

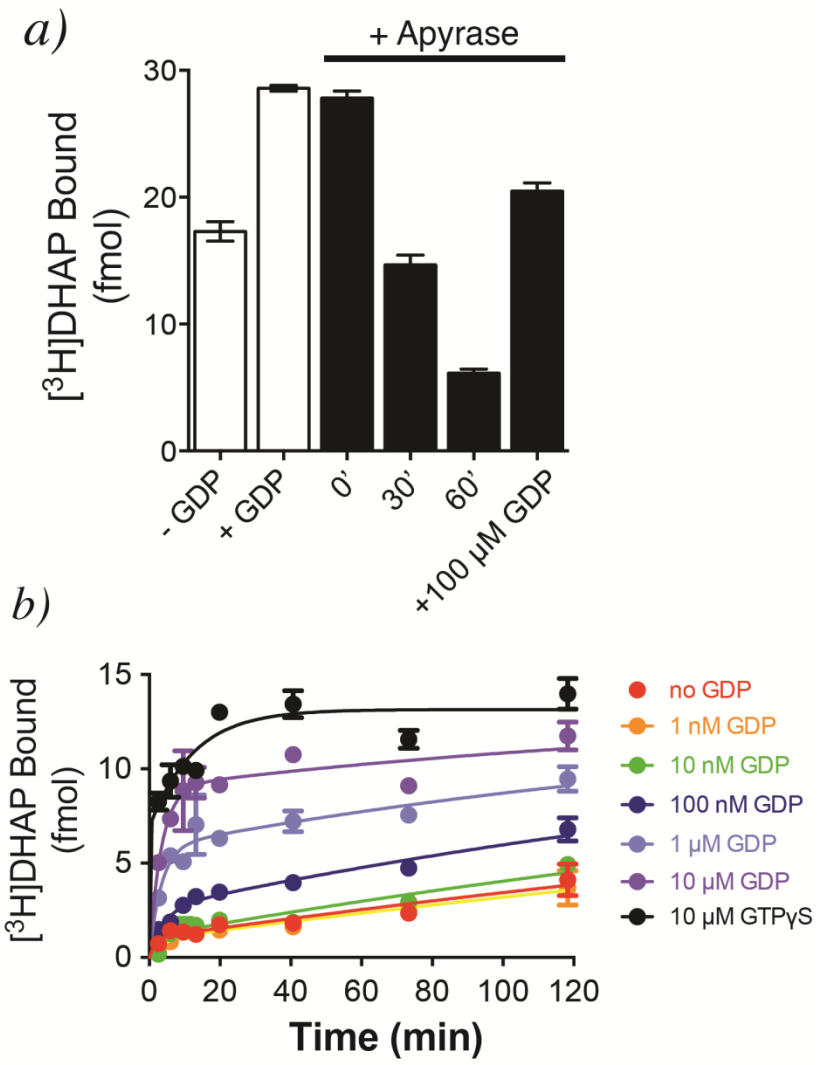

Figure 3-1. Guanine nucleotides influence antagonist binding to β_2AR·Gs complexes.
a) Binding of 2 nM [^{3}H]DHAP to β_2AR•Gs in the absence or presence of GDP. Addition of apyrase to GDP-bound β_2AR·Gs led to a progressive decrease in [^{3}H]DHAP binding over time, which could be restored by the addition of excess GDP. ***b)*** Addition of increasing concentrations of GDP enhanced both the rate and extent of [^{3}H]DHAP binding to apyrase-treated β_2AR·Gs complexes. Data in both ***a*** and ***b*** are shown as mean ± SEM from n=3 independent experiments performed in duplicate. Experiments were performed by Dr. Gisselle Vélez-Ruiz and Dr. Brian DeVree.

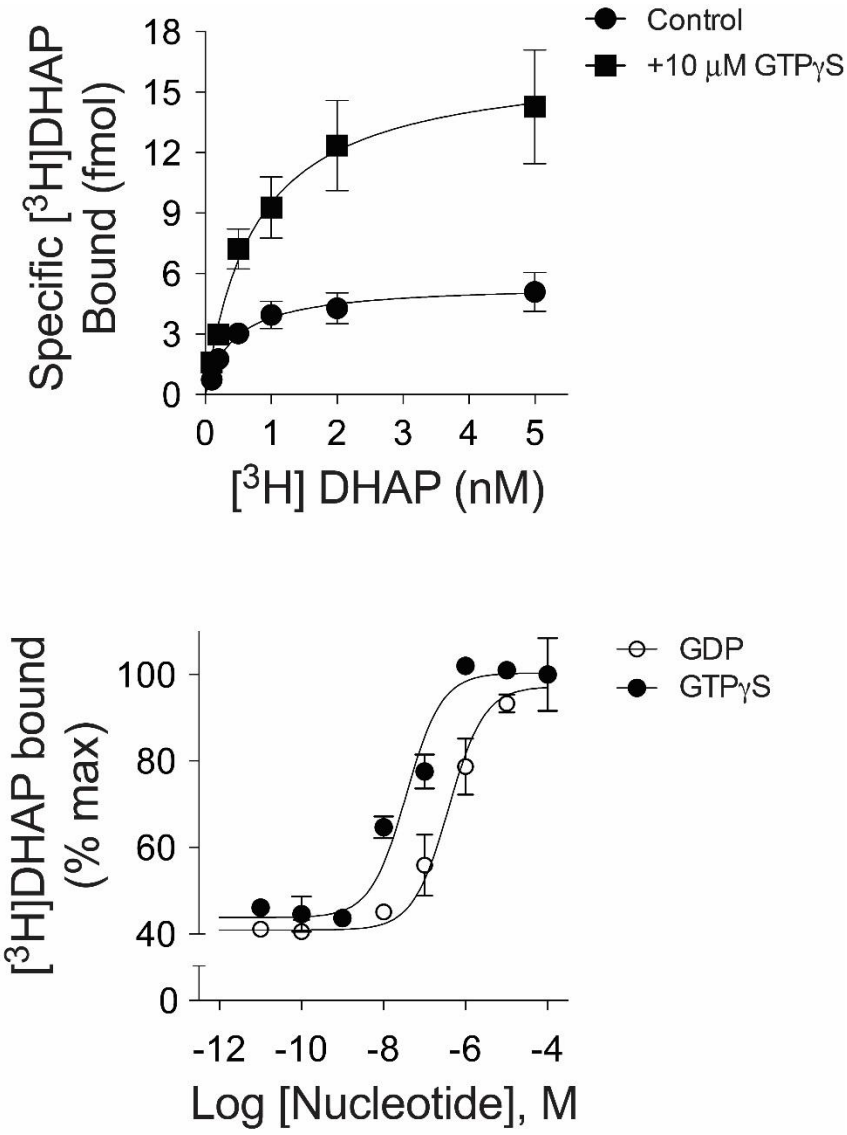

Figure 3-2. Effect of guanine nucleotides on [^{3}H]DHAP binding to β_2AR·Gs.
a) In saturation binding assays, addition of GTPγS to apyrase-treated β_2AR·Gs complexes increased the observed B_{max} for [^{3}H]DHAP without significantly altering K_d (Control: B_{max} = 5.5 ± 0.52 fmol, K_d = 0.88 nM; +GTPγS: B_{max} = 16.6 ± 1.9 fmol, K_d = 0.56 nM) ***b)*** Both GDP and GTPγS could enhance maximal [^{3}H]DHAP binding in a concentration-dependent manner (GDP Log(EC_{50}) = -6.42 ± 0.12 , or EC_{50} ~386 nM; GTPγS Log(EC_{50}) = -7.45 ± -0.16 , or EC_{50} ~35 nM). All data are shown as mean ± SEM from n=3 independent experiments performed in duplicate. Experiments were performed by Dr. Gisselle Vélez-Ruiz.

3.2 - G protein and Nb80 stabilize a "closed" orthosteric biding site in β_2AR

Crystallographic and pharmacological evidence suggests that the active conformation of β_2AR is stabilized by nucleotide-free Gs or by a single-chain camelid antibody raised against agonist-bound β_2AR (nanobody Nb80) (Fig. 3-3a)[55,56,91]. As illustrated in Fig. 3-3b, Nb80 stabilizes a conformation of β_2AR that restricts [^{3}H]DHAP association, similar to nucleotide-free Gs. Importantly, Nb80 also slows the association of a full agonist, [^{3}H]formoterol (Fig. 3-3c), as well as a partial agonist, [^{3}H]CGP-12177 (Fig. 3-3d). These data suggest that in the nucleotide-free Gs- or Nb80-stabilized active state, the β_2AR adopts a 'closed' conformation impairing access to the orthosteric binding site, regardless of the orthosteric ligand's cooperativity with G protein. These data agree with our previous observation that the inverse agonist ICI-118,551 blocks the formation of β_2AR•Gs complexes, but is unable to disrupt pre-formed complexes[47]. Nb80 also impairs binding of inverse agonist [^{3}H]carvedilol to β_2AR by modestly decreasing the observed association rate (Fig. 3-3e) but significantly decreasing total binding, suggesting that Nb80 and [^{3}H]carvedilol do not simultaneously occupy β_2AR.

Agonist-promoted G protein engagement and subsequent nucleotide loss would be expected to stabilize the active, closed receptor conformation, thus trapping the agonist in the orthosteric site and enhancing its observed affinity. Indeed, uncoupling G protein from receptor using the GTP analog GppNHp has been shown to accelerate agonist dissociation from β_2AR[101]. Such agonist-G protein cooperativity is not predicted for neutral antagonists like alprenolol, which do not stimulate G protein coupling and thus should not stabilize the closed conformation. However, we have previously demonstrated that Gs can be 'forced' to form a complex with β_2AR bound to antagonist alprenolol[47], provided that free nucleotide is removed, indicating that antagonist-bound β_2AR retains enough basal activity to engage Gs. Consistent with this model, Figures 3-3f and 3-3g clearly illustrate a progressive slowing of [^{3}H]DHAP or [^{3}H]CGP-12177

dissociation in response to increasing Nb80 concentrations, suggesting that Nb80-mediated stabilization of the closed, active receptor conformation can trap these ligands in the orthosteric binding site.

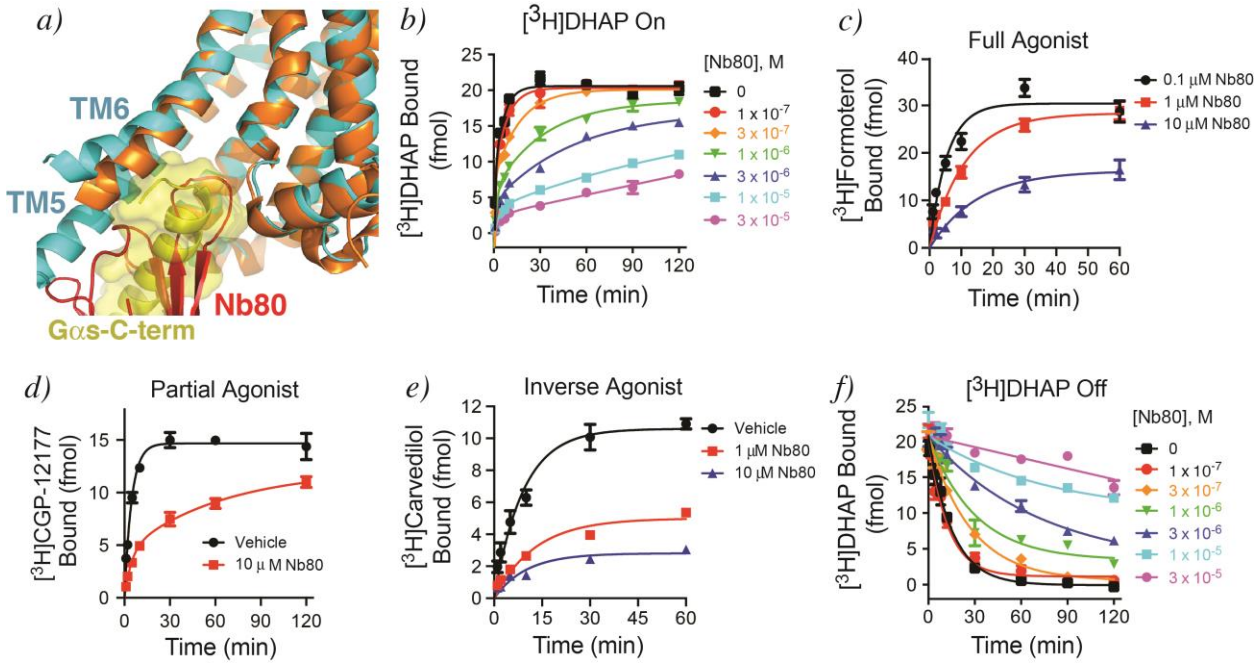

Figure 3-3. Trapping active-state β_2AR with Nb80 slows both antagonist and agonist association.

a) Nb80 (red) mimics G protein (yellow) in both its binding site and the β_2AR conformation it stabilizes. The structure of Nb80-bound β_2AR (3p0g) is shown in orange, Gs-bound β_2AR (3sn6) in cyan. ***b)*** Pre-incubation of β_2AR with increasing concentrations of Nb80 progressively slows association of neutral antagonist [^{3}H]DHAP to β_2AR. ***c)*** Nb80 also slows association of full agonist [^{3}H]formoterol, ***d)*** partial agonist [^{3}H]CGP12177, and ***e)*** inverse agonist [^{3}H]carvedilol to β_2AR. ***f)*** Nb80 stabilizes the closed, active conformation and slows [^{3}H]DHAP dissociation from β_2AR in a concentration-dependent manner. ***g)*** Nb80 is also able to slow dissociation of [^{3}H]CGP-12177. from β2AR in a concentration-dependent manner. Data in ***b)*** and ***f)*** were collected by Dr. Brian DeVree and are representative of three independent experiments. All other data are specific binding, shown as mean ± SEM from n=3 independent experiments performed in duplicate.

Analysis of access to the hormone binding sites in inactive- and active-state β_2AR structures provides a structural rationale for the slowing of agonist and antagonist association (Figs. 3-4 and 3-5). The binding of Gs or Nb80 to β_2AR stabilizes a rearrangement of the cytoplasmic end of TM7 (Fig. 3-6a & b) immediately above the ligand binding site and a change in the structure of the extracellular loop between TM4 and TM5 (ECL2). In comparison to the inactive β_2AR, the structure of the β_2AR-Gs or -Nb80 (or related Nb6B9[102]) complex demonstrates that two aromatic residues, Phe193$^{(5.25 \text{ or ECL2})}$ and Tyr308$^{7.35}$, move approximately 2-2.5 Å closer to each other to form a lid-like structure over the orthosteric binding site. Lys305$^{7.32}$ also contributes to capping the orthosteric site by trading its salt bridge[103] with Asp192^{ECL2} for an interaction with the backbone carbonyl of Phe193^{ECL2} (Fig. 3-6c). These structural changes are stabilized in the active forms of β_2AR bound to either the ultra-high affinity agonist BI-167107 or the smaller, low affinity agonist adrenaline[102], and formation of this 'lid' would be expected to sterically obstruct both ligand association and dissociation.

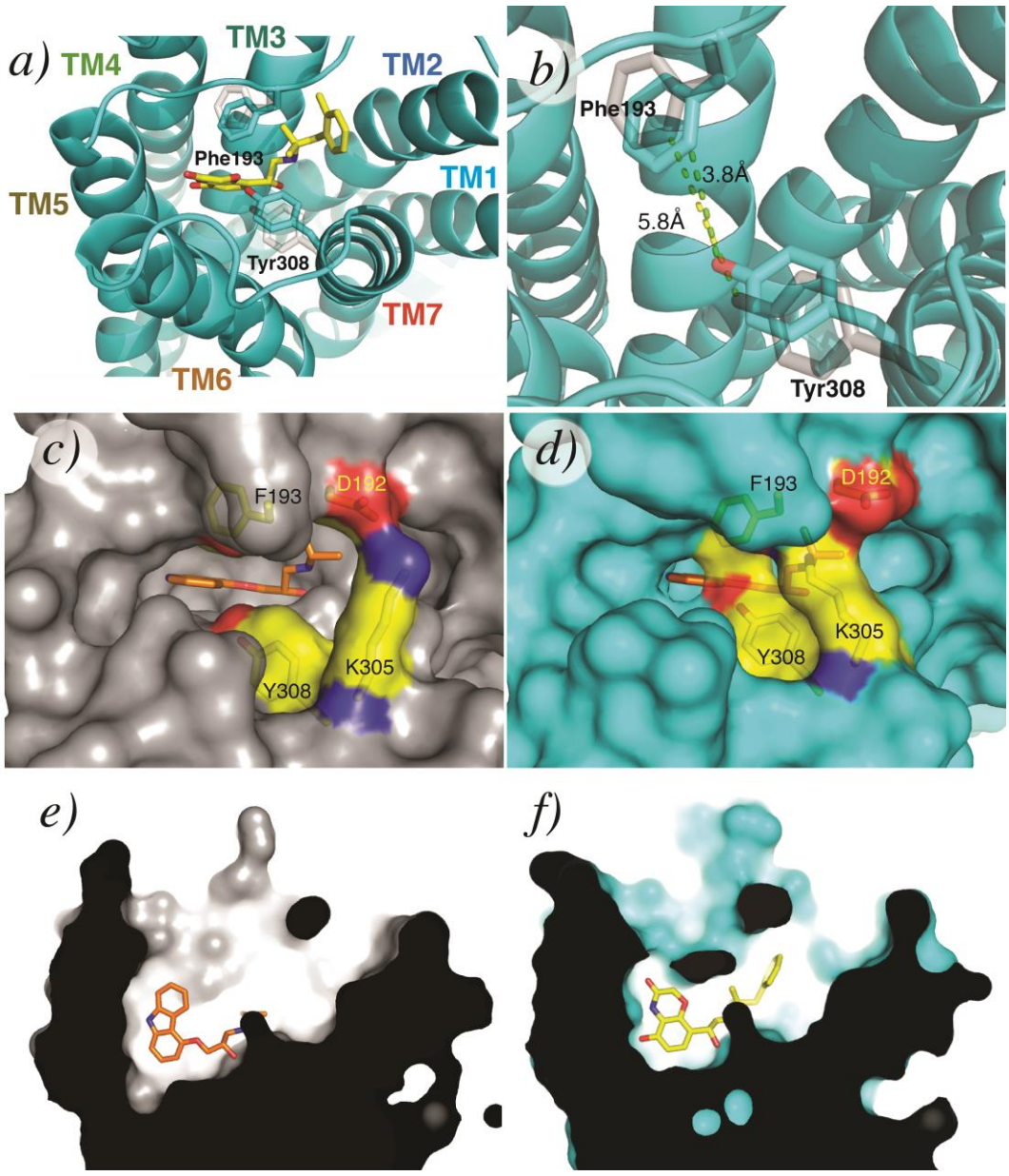

Figure 3-4. Activation of β_2AR closes the hormone binding site.
a) Stabilization of the β_2AR active conformation by Gs (or Nb80) brings the side chains of Phe193^{ECL2} and Tyr308$^{7.35}$ closer to one another compared to their positions in structures in the absence of G protein. ***b)*** Closer view of the orthosteric site, highlighting Phe193^{ECL2} and Tyr308$^{7.35}$. Distances (in Ångstroms) indicated are between the hydroxyl on Tyr308$^{7.35}$ and 2-carbon on the phenyl ring of Phe193^{ECL2}. ***c) and d)*** A surface view comparing the extracellular face of β_2AR in inactive (panel ***c***) or active (panel ***d***) conformations, showing how G protein-stabilized structural rearrangements occlude the hormone binding site in the active state. ***e) and f)*** Cutaway view illustrating closure of the hormone binding site around the bound agonist in the active state. The inverse agonist carazolol is shown in orange, the agonist BI-167107 is shown in yellow.

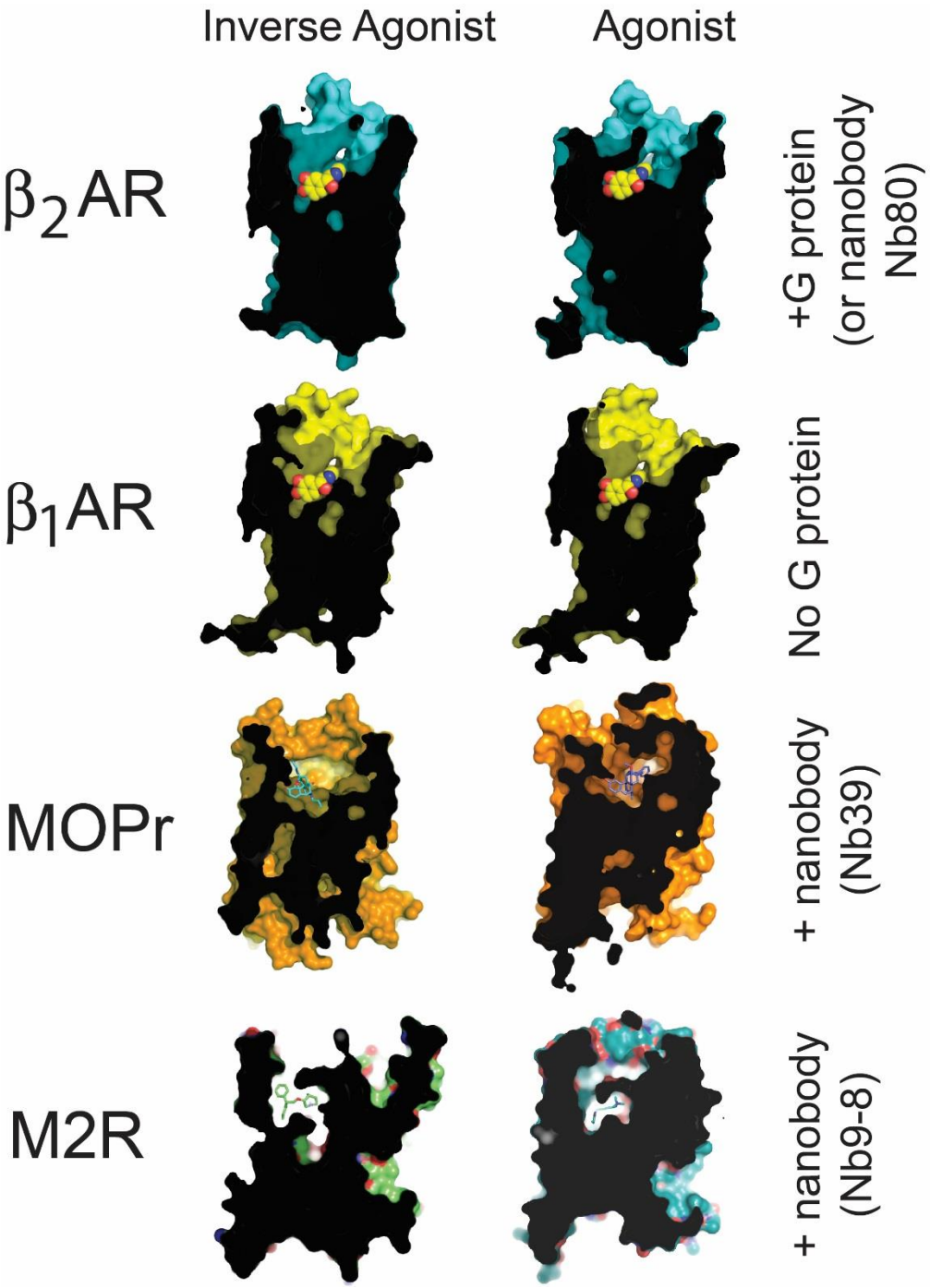

Figure 3-5. The closed conformation stabilized by agonist and G protein (or nanobody). Illustrated are the crystal structures of agonist- vs. inverse agonist-bound of the β_2AR (cyan) and β_1AR (yellow), where only β_2AR is bound to G protein. Similarly, the mu-opioid receptor (MOPr, orange) adopts a closed conformation upon binding the G protein surrogate Nb39. (β_2AR, PDB 2RH1; β_2AR-Gs, PDB 3SN6; β_1AR, PDB 2YCW; β_1AR-iso, PDB 2Y03; MOPr, PDB 4DKL; MOPr-Nb39, PDB 5C1M; M2R, PDB 3UON; M2R-Nb9-8, PDB 4MQS).

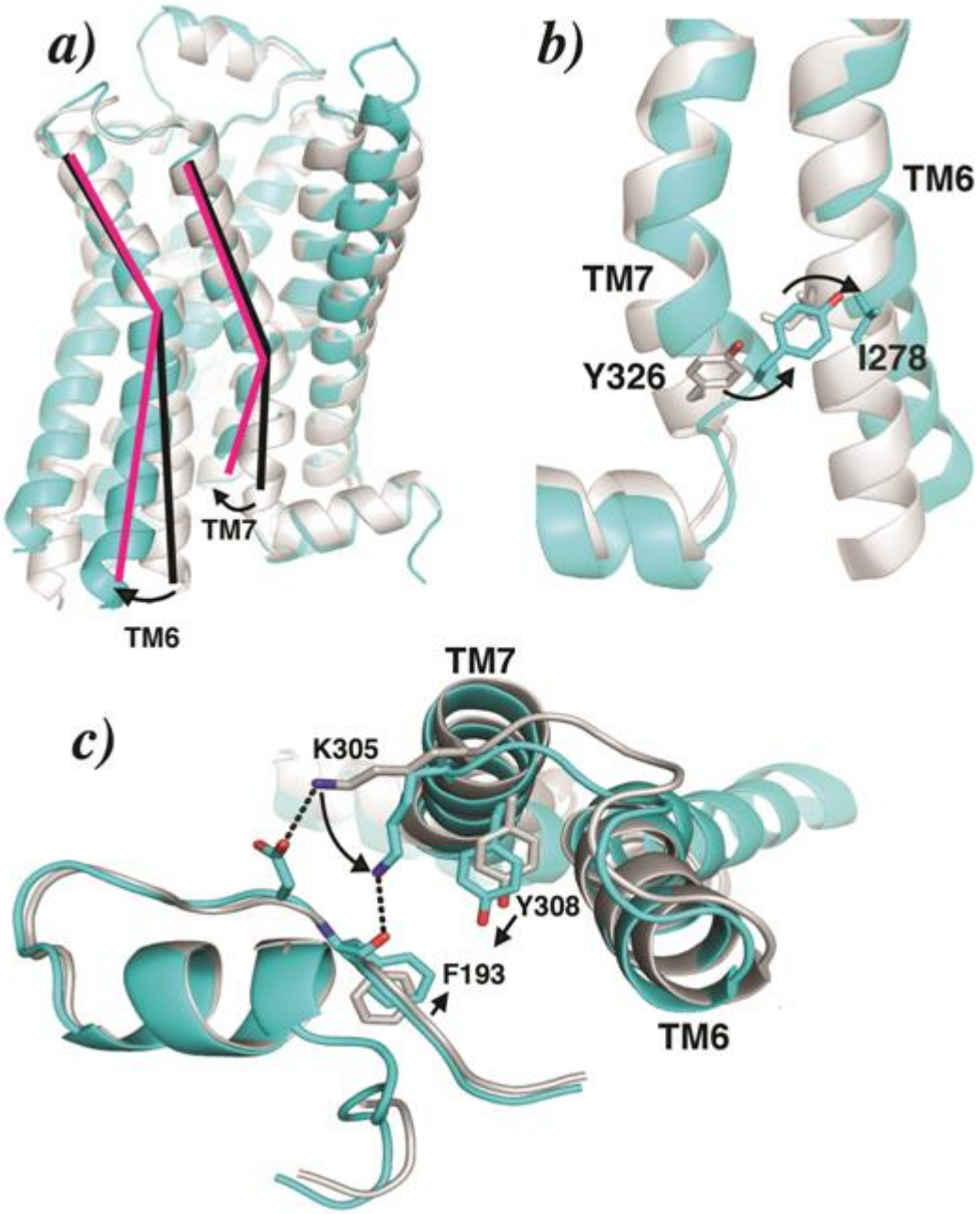

Figure 3-6. Allosteric communication between β_2AR G protein- and hormone-binding sites. ***a)*** In the β_2AR active state (cyan), the cytoplasmic end of TM6 moves away from the receptor core by ~14 Å relative to its position in the inactive-state structure, allowing for an inward movement of TM7. ***b)*** Rotation of TM7 allows Tyr326$^{7.53}$ (of the highly conserved NPxxY motif) to fill the space vacated by the conserved aliphatic residue Ile278$^{6.40}$. ***c)*** The rotation of TM7 repositions Tyr308$^{7.35}$ and Lys305$^{7.32}$. This conformational change allows Lys305$^{7.32}$ to coordinate the backbone carbonyl of Phe193^{ECL2}, stabilizing its movement toward Tyr308$^{7.35}$ to form a "lid" over the hormone binding site.

3.3 - Tyr308 in β_2AR contributes to forming a lid over the orthosteric site

To validate this structural model, we tested whether a residue smaller than tyrosine could modify the capacity of Nb80 to slow ligand association. Mutation of Tyr308$^{7.35}$ to alanine, previously shown to alter agonist affinity for β_2AR[104], significantly diminishes the ability of Nb80 to slow association of [^{3}H]DHAP and even the agonist [^{3}H]formoterol (Fig. 3-7), as suggested by recent molecular dynamics simulations[105]. Of interest, pre-incubation with 10 μM Nb80 increases the extent of [^{3}H]formoterol binding to the Y308A mutant, suggesting that Nb80 is still capable of slowing *dissociation* of the bound agonist (Fig. 3-7d). Thus, while Tyr308$^{7.35}$ limits access to the orthosteric site in the active β_2AR conformation, other residues may work in concert with Tyr308$^{7.35}$ to slow agonist dissociation.

It is noteworthy that the movement of Phe193^{ECL2} and Tyr308$^{7.35}$ is not fully observed in the crystal structure of β_2AR bound to an agonist alone[49], nor in the inactive-state structure of β_1AR bound to the agonist isoprenaline[50] (Fig. 3-5). Binding of G protein or G protein-mimetic (nanobody) is sufficient to stabilize the closed, active conformation since their effects on ligand binding kinetics (as in Figs. 3-1 and 3-3) are agonist-independent. An agonist may enhance G protein engagement but cannot stabilize the closed, active conformation by itself. Additionally, the data presented here suggest that formation of the closed, active conformation stabilized by the nucleotide-free G protein can occur due to basal receptor activity, in keeping with predictions of more recent models of GPCR pharmacology such as the extended and cubic ternary complex models[37,38] (see section 3.5 for further discussion). Moreover, conformational changes stabilized by the nucleotide-free G protein influence not only agonist binding, but ligand binding in general, implying that the role of nucleotides needs to be included in an updated version of ternary complex model.

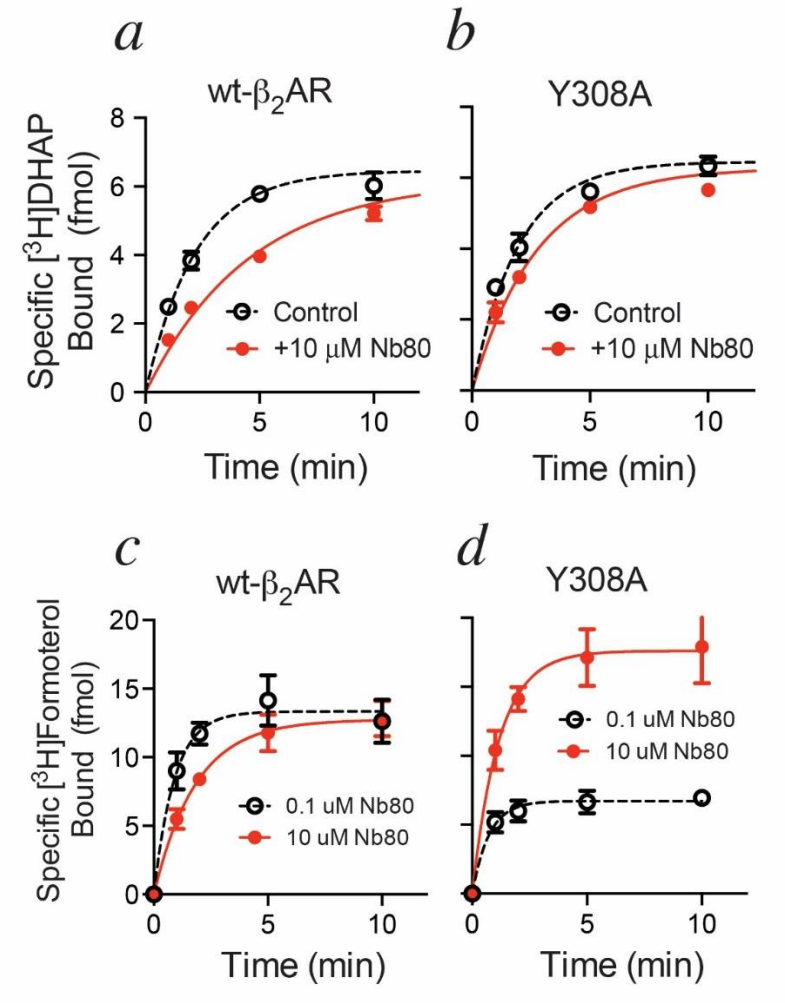

Figure 3-7. Y308A mutation abolishes the rate-slowing effects of Nb80.
a) and b) Time course of [^{3}H]DHAP binding to wild-type β_2AR **(*a*)** or β_2AR-Y308A **(*b*)** following pre-incubation of receptor with Nb80. Nb80 significantly slowed [^{3}H]DHAP association to wild-type β_2AR (-Nb80 k_{obs} = 0.45 ± 0.05 min^{-1} or t½ = 1.5 ± 0.2 min, +Nb80 k_{obs} = 0.20 ± 0.03 min^{-1} or t½ = 3.5 ± 0.5 min; p = 0.011 by an unpaired two-tailed *t*-test), but less effectively slowed [^{3}H]DHAP association to β_2AR-Y308A (-Nb80 k_{obs} = 0.50 ± 0.06 min^{-1} or t½ = 1.4 ± 0.2 min; +Nb80 k_{obs} = 0.32 ± 0.01 min^{-1} or t½ = 2.2 ± 0.1 min; p = 0.05 by an unpaired two-tailed t-test. All data are shown as mean ± SEM from n=4 (-Nb80) or n=3 (+Nb80) independent experiments performed in duplicate. ***c)*** and ***d)*** Time course of [^{3}H]formoterol binding to wild-type β_2AR **(*c*)** or β_2AR-Y308A **(*d*)** following pre-incubation of receptor with Nb80. Nb80 slowed [^{3}H]formoterol association to wild-type β_2AR (0.1 μM Nb80 k_{obs} = 0.68 ± 0.13 min^{-1} or t½ = 1.0 ± 0.2 min, 10 μM Nb80 k_{obs} = 0.27 ± 0.05 min^{-1} or t½ = 2.6 ± 0.5 min; p = 0.031 by an unpaired two-tailed *t*-test). However, with β_2AR-Y308A, Nb80 had little effect on the observed association rate constant but enhanced the amount of [^{3}H]formoterol bound (0.1 μM Nb80 k_{obs} = 0.37 ± 0.11 min^{-1} or t½ = 1.9 ± 0.6 min with a plateau of 10 ± 0.8 fmol, 10 μM Nb80 k_{obs} = 0.53 ± 0.13 min^{-1} or t½ = 1.3 ± 0.4 min with a plateau of 21 ± 1.2 fmol; unpaired two-tailed *t*-test of the k_{obs} values showed p = 0.4). All data are shown as mean ± SEM from n=4 independent experiments performed in duplicate.

3.4 - Other GPCRs adopt a closed conformation in their active states

The capacity of G proteins to stabilize a closed receptor conformation explains the poorly defined GTPγS-mediated increase in radiolabeled antagonist binding observed with several GPCRs, including muscarinic, α-adrenergic, adenosine, and opioid receptors[106–109] (as in Fig. 3-8 and 3-9). We analyzed the behavior of the M2 muscarinic acetylcholine receptor (M2R) and the μ-opioid receptor (MOPr) to determine whether GTPγS-mediated uncoupling relieves a G protein-stabilized closed conformation. We focused on these receptors since structural models are available for both inactive and active conformations[79,80,110,111] and to determine whether the mechanism we propose for β_2AR is shared among other GPCRs. The active-state structure of the M2R, in particular, revealed similar conformational changes to the β_2AR in that a 'lid-like' structure is formed above the orthosteric site[79]. Although the structural changes are not identical, the effect of G proteins (or nanobodies) on the association and dissociation of ligands at the orthosteric sites is shared among β_2AR, M2R, and MOPr (Fig. 3-9), suggesting that the allosteric effects of G proteins on orthosteric agonists may be manifested by conceptually common mechanisms (See section 3.6 for more discussion).

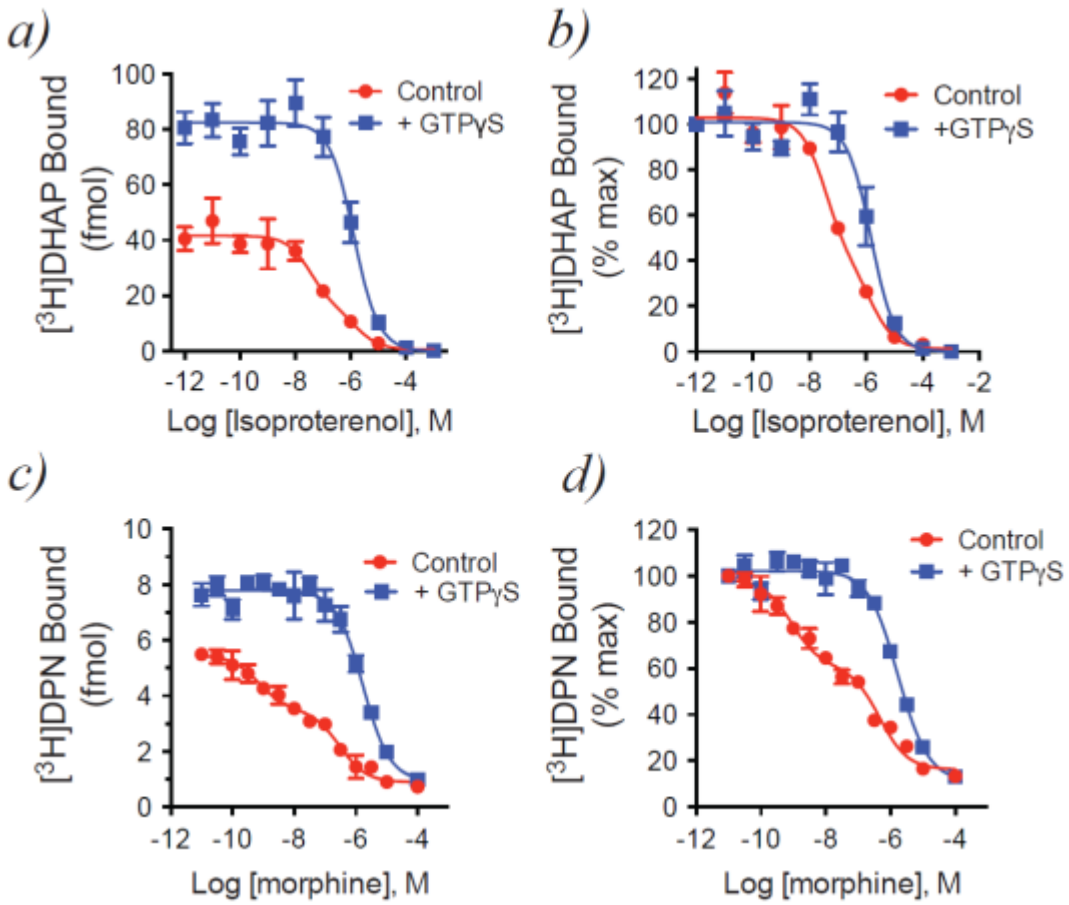

Figure 3-8. Effect of guanine nucleotides on [^{3}H]antagonist binding are also seen in competition binding assays.
a) Agonist (isoproterenol) competition binding using apyrase-treated β_2AR•Gs complexes shows the characteristic G protein-dependent shift in agonist affinity, along with a dramatic increase in total [^{3}H]DHAP binding, upon the addition of 10 μM GTPγS. ***b)*** Normalization of the data from ***a)*** yields a plot representative of what is commonly reported in the literature. ***c)*** Similar to β_2AR, agonist (morphine) competition binding using MOPr•Go complexes shows the characteristic G protein-dependent shift in agonist affinity, along with a dramatic increase in total [^{3}H]DPN binding, upon the addition of 10 μM GTPγS. ***d)*** Normalization of the data from ***c).*** All data are shown as mean ± SEM from n=3 independent experiments performed in duplicate. Isoproterenol competition assays were performed by Dr. Gisselle Vélez-Ruiz, and experiments with MOPr were conducted by Dr. Adam Kuszak.

a)

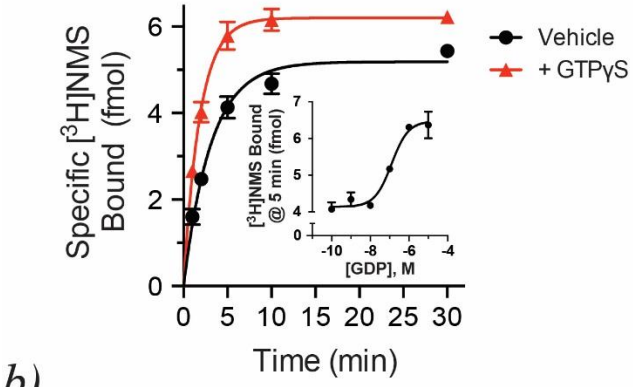
Specific [3H]NMS Bound (fmol)
Time (min)
Vehicle
+ GTPγS
[3H]NMS Bound @ 5 min (fmol)
[GDP], M

b)

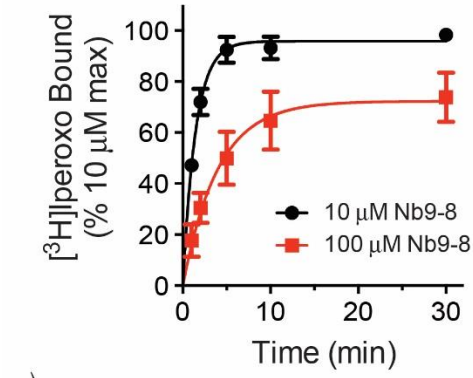
[3H]Iperoxo Bound (% 10 µM max)
Time (min)
10 µM Nb9-8
100 µM Nb9-8

c)

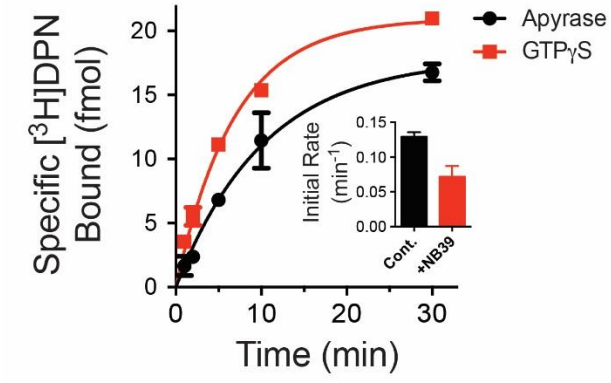
Specific [3H]DPN Bound (fmol)
Time (min)
Apyrase
GTPγS
Initial Rate (min-1)
Cont.
+NB39

Figure 3-9. Mu opioid receptor and M2 muscarinic acetylcholine receptor behave similarly to β_2AR when bound to nucleotide-free G protein or an active-state stabilizing nanobody.
a) Following apyrase treatment of M2R•Go complexes, addition of 10 μM GTPγS enhances association of [^{3}H]N-methylscopolamine ([^{3}H]NMS) to M2R (Vehicle k_{obs} = 0.32 ± 0.02 min^{-1} or $t_{½}$ = 2.2 ± 0.1 min, +GTPγS k_{obs} = 0.54 ± 0.02 min^{-1} or $t_{½}$ = 1.3 ± 0.1 min; p = 0.002 by an unpaired two-tailed *t*-test). Data are shown as mean ± SEM from n=3 independent experiments performed in duplicate. Addition of GDP was also able to increase the rate of [^{3}H]NMS binding (inset; pEC_{50} = 6.91 ± 0.18 or EC_{50} ~123 nM; mean ± SEM from n=2 independent experiments performed in duplicate). ***b)*** Pre-treatment of M2R with either 10 μM (black circles) or 100 μM (red squares) Nb9-8[26] impairs association of [^{3}H]iperoxo to M2R (10 μM Nb9-8 k_{obs} = 0.68 ± 0.09 min^{-1} or $t_{½}$ = 1.0 ± 0.2 min, 100 μM Nb9-8 k_{obs} = 0.25 ± 0.04 min^{-1} or $t_{½}$ = 2.8 ± 0.5 min; p = 0.04 by an unpaired two-tailed *t*-test). Data are shown as mean ± SEM from n=3 (10 μM Nb9-8) or n=2 (100 μM Nb9-8) independent experiments performed in duplicate. ***c)*** Addition of 10 μM GTPγS to apyrase-treated MOPr•Go complexes hastened association of the antagonist [^{3}H]diprenorphine ([^{3}H]DPN) to MOPr (Apyrase k_{obs} = 0.06 ± 0.02 min^{-1} or $t_{½}$ = 9.8 ± 1.3 min, +GTPγS k_{obs} = 0.12 ± 0.01 min^{-1} or $t_{½}$ = 5.6 ± 0.6 min; p = 0.1 by an unpaired two-tailed *t*-test). The effect of nucleotide-free G protein was recapitulated by pre-incubating MOPr with Nb39[28] (inset; control k_{obs} = 0.13± 0.01 min^{-1}, +100 μM Nb39 k_{obs} = 0.07 ± 0.02 min^{-1}). Data are shown as mean ± SEM from n=2 (MOPr·Go) or n=3 (MOPr + Nb39) independent experiments performed in duplicate.

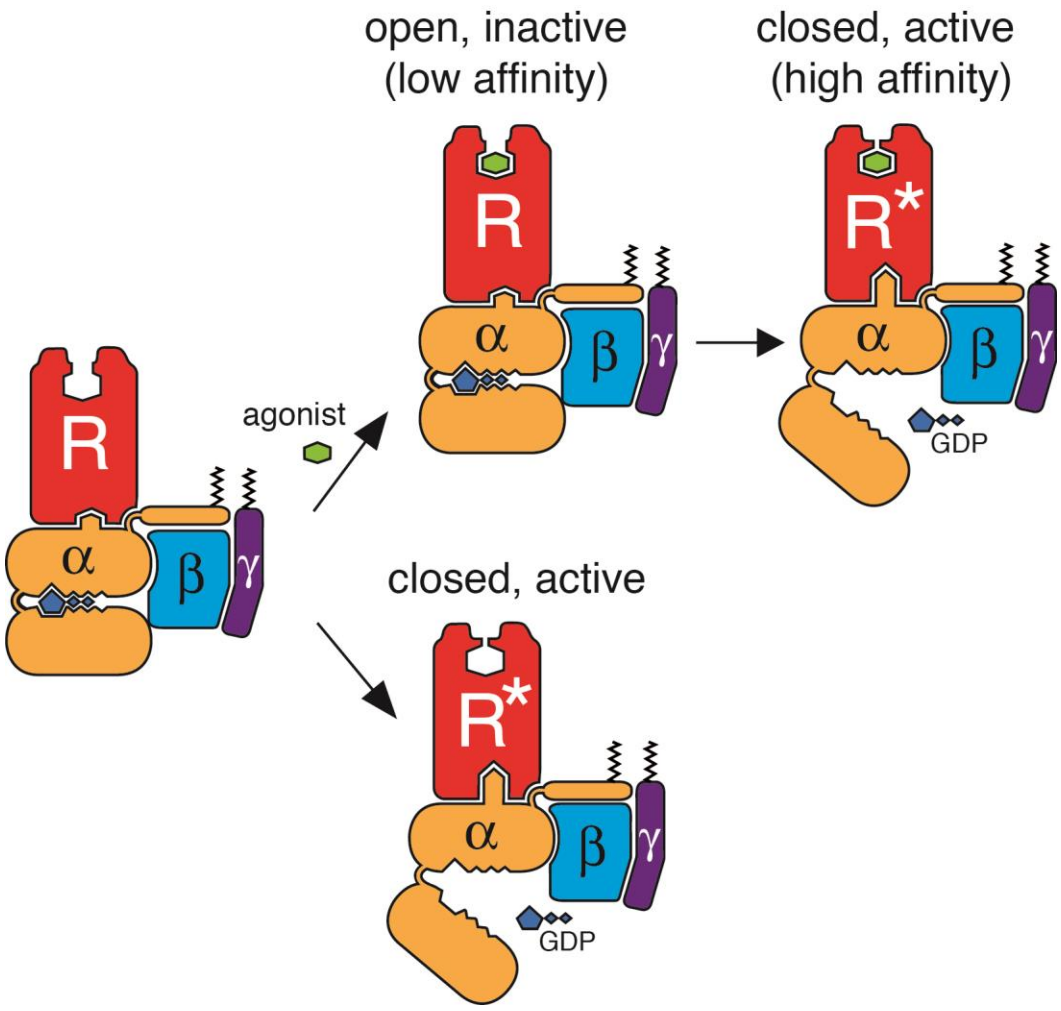

Figure 3-10. Model to explain G protein-dependent high-affinity agonist binding.

Agonist binding promotes the receptor-G protein interaction and GDP release from Gα. In this nucleotide-free state, the C-terminal helix of Gα remains embedded in the receptor core, stabilizing the conformational changes at both the intracellular and extracellular faces of the receptor. At the extracellular side, the orthosteric binding site closes around the bound agonist, sterically opposing agonist dissociation and thereby enhancing the observed affinity. Constitutive (basal) receptor activity may also activate the G protein, releasing GDP and thereby stabilizing the 'closed' conformation of the receptor in the absence of an agonist.

Discussion

3.5 - The ternary complex

Taken together, the data in this report provide an integrated pharmacological and structure-based mechanism for how G proteins stabilize high affinity agonist binding and how agonists are capable of promoting G protein coupling to GPCRs. As predicted by the *simple* ternary complex model, agonist-bound receptors exist in equilibrium between inactive and active states[33,35,100]. The probability of adopting an active state and, by extension, an agonist's efficacy to activate G proteins can be described in terms of the allosteric free energy coupling between the agonist- and G protein-binding sites. This energetic linkage is ultimately a representation of conformational changes within the receptor[112] that are stabilized by the concerted actions of both ligands (agonist and G protein). Indeed, recent biophysical studies suggest that GPCRs are highly dynamic, but the movement of the cytoplasmic end of TM6 to the fully active conformation, a hallmark of GPCR activation, cannot be stabilized by agonists alone, even by saturating concentrations[58,60,85,86]. Even a full agonist covalently bound to β_2AR revealed an inactive receptor conformation by x-ray crystallography[49], together suggesting that the Agonist-bound active Receptor complex (A·R*) is transient and unstable. Only upon G protein or nanobody coupling (A·R*·G) can populations in the fully active conformation be observed using biophysical and pharmacological approaches.

An alternative hypothesis that perhaps explains why picomolar affinity full agonists and even covalent full agonists fail to stabilize the active conformation may be the existence of sub-states. Here the traditional ternary complex model A·R* may actually be composed of A•R' and A·R* states, where the R* state is rare and unstable. Such activation intermediates are described by Kim *et al.* in which binding of the picomolar affinity full agonist BI-167107 to β_2AR could

not fully stabilize a population of receptors in the active conformation without a G protein or G protein mimetic nanobody. The fully active state was only stabilized in the presence of both agonist and nucleotide-free G protein or G protein mimetic nanobody (A·R*·G). This is also consistent with the fact that most agonist-bound GPCR crystal structures appear in their inactive conformations or display only some aspects of a partially active conformation. The subtle differences likely reflect the difference in the energy landscapes of activation for individual receptors, where certain receptors (e.g. the adenosine A2A receptor[51]) are able to adopt meta-stable activation intermediate states.

The *extended* ternary complex model further postulates that active receptor states, and in turn receptor-G protein interactions, can either be achieved spontaneously (i.e. basal receptor activity) or be stabilized by agonist binding. In support of this prediction, we found that G protein or nanobody binding even in the absence of agonist was sufficient to stabilize a closed, active conformation of the receptor, here demonstrated with a variety of GPCRs. We propose that the closed, active receptor conformation we observe in this case corresponds to the active, coupled states of the receptor (R*·G or A·R*·G) put forth by the ternary complex models. However, neither the *extended* nor the more thorough *cubic* ternary complex models take into account the effect of nucleotides on the receptor-G protein interaction and agonist affinity[37,38]. In the current study we demonstrate that the presence or absence of nucleotide has a profound effect on receptor conformation, particularly in the agonist-free, basally active state. To this end these data suggest that the extended ternary complex model be further refined to include both the concepts of receptor sub-states of the active conformation (e.g. R' and R*), as well as the role of nucleotides in regulating or stabilizing the A·R*·G complex.

3.6 - The closed, active conformation: specific to β_2AR or applicable to other GPCRs?

The capacity of G proteins to stabilize a closed receptor conformation explains the poorly defined GTPγS-mediated increases in radiolabeled antagonist binding that has been observed with GPCRs of several families, including muscarinic, α-adrenergic, adenosine, and opioid receptors[106–109] (as in Fig. 3-8 & 3-9). We speculate that this observation arises from accumulation of nucleotide-free receptor-G protein complexes formed from basal receptor activity in an environment where free GDP is depleted, such as in isolated plasma membranes. Populations of receptors in their closed, active conformation thus accumulate, thereby limiting accessible antagonist binding sites unless the receptor-G protein complexes are uncoupled with nucleotides (GDP, GTP, or GTPγS). Consistent with this model, purified M2 muscarinic acetylcholine receptor (M2R) stabilized in its active conformation with nucleotide-free G_o heterotrimer displays slow association of the antagonist [^{3}H]N-methylscopolamine unless GDP or GTPγS are present. Additionally, an active state-stabilizing nanobody, Nb9-8, was able to slow association of the agonist [^{3}H]iperoxo to M2R (Fig. 3-9a & b). We also observe slower association rates of [^{3}H]diprenorphine to purified mu-opioid receptor (MOPr) in complex with either nucleotide-free G_o heterotrimer or Nb39, a nanobody selective for the active state of MOPr (Fig. 3-9c). These data support previous observations that MOPr agonist association and dissociation were enhanced by GTP[113], and the finding that the G protein mimetic nanobody Nb39 was able to slow dissociation of the agonist BU72 from MOPr[80].

The slower binding characteristics are consistent with the recent crystal structure of agonist- and nanbody-bound M2R, which demonstrates a pronounced lid-like structure over the orthosteric site. The lid, composed of three aromatic residues (Y104$^{3.33}$, Y403$^{6.38}$ and Y426$^{7.39}$) forms largely through the inward movements of TM6 and TM7[26] and can conceivably affect

ligand association and dissociation in a manner conceptually similar to what we propose for β_2AR. In contrast, the crystal structures of peptide receptors such as MOPr or the neurotensin receptor NTS-R1 reveal binding sites that are considerably larger and more open at the extracellular surface than for receptors for small molecules (e.g. monoamines), including β_2AR[52,111]. However, structures of the nanobody-stabilized MOPr and partially activated (through mutagenesis) NTS-R1 reveal subtle changes in the structure of extracellular face around a peptide ligand that may in essence "pinch" the ligand rather than cap the ligand binding site[80,114]. Formation of the active receptor state (Figures 3-11 & 3-1) could promote more favorable peptide-receptor interactions that enhance agonist affinity and alter orthosteric ligand association and dissociation.

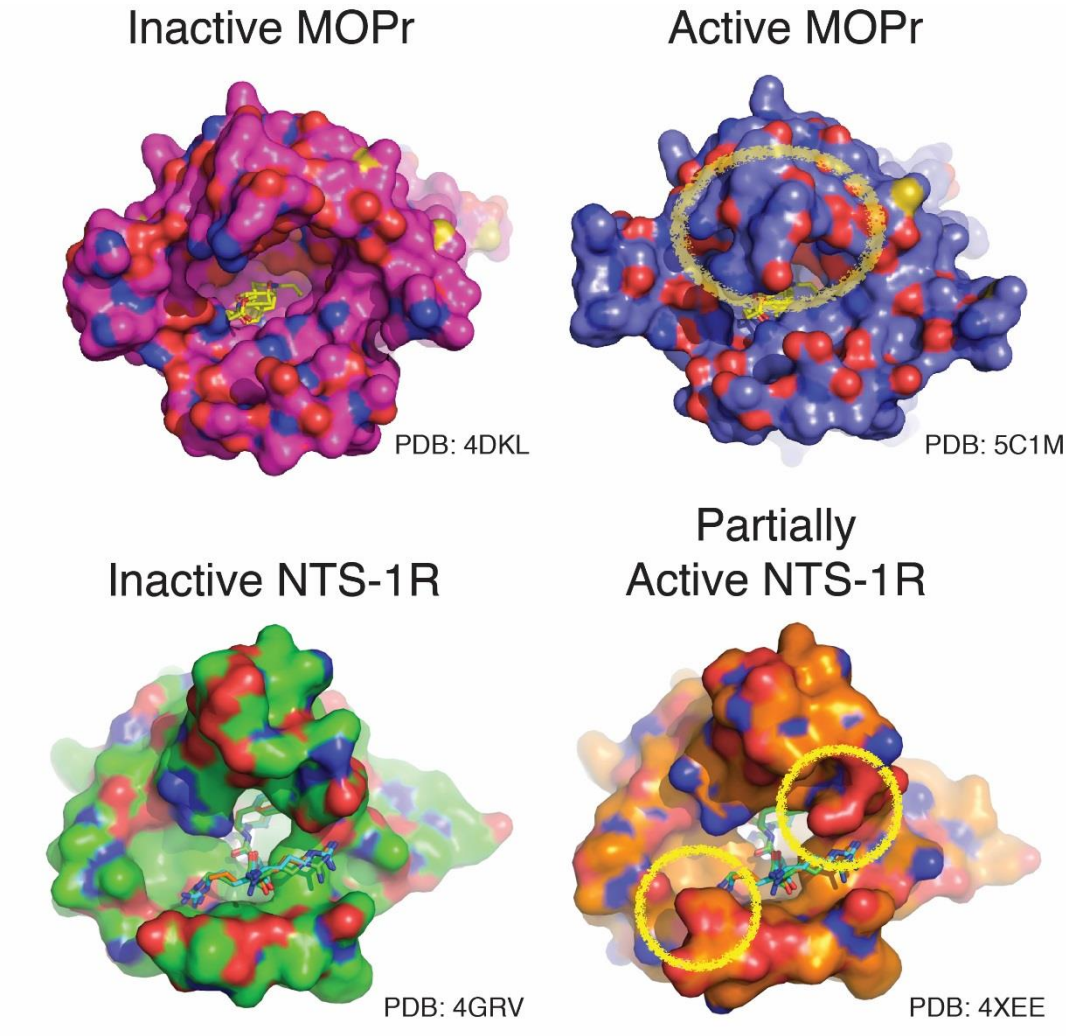

Figure 3-11. The extracellular regions in the active conformations of the peptide receptors MOPr and NTS-R1. Illustrated are the crystal structures of the inactive and active (or partially active NTS-R1) conformations of the MOPr and NTS-R1 from the top or extracellular view of the receptor. The surface rendering highlights residues or structure on the extracellular face that change upon receptor activation (circled). The mu-opioid receptor (MOPr) in its inactive conformation (purple) is compared to the Nb39-bound (G protein mimic) form in blue. Similarly, the inactive NTS-R1 (green) is compared with a mutant NTS-R1 that adopts a partially active conformation (orange). (MOPr PDB 4DKL, MOPr-Nb39 PDB 5C1M, NTS-R1 PDB 4GRV and active-like NTS-R1 PDB 4XEE).

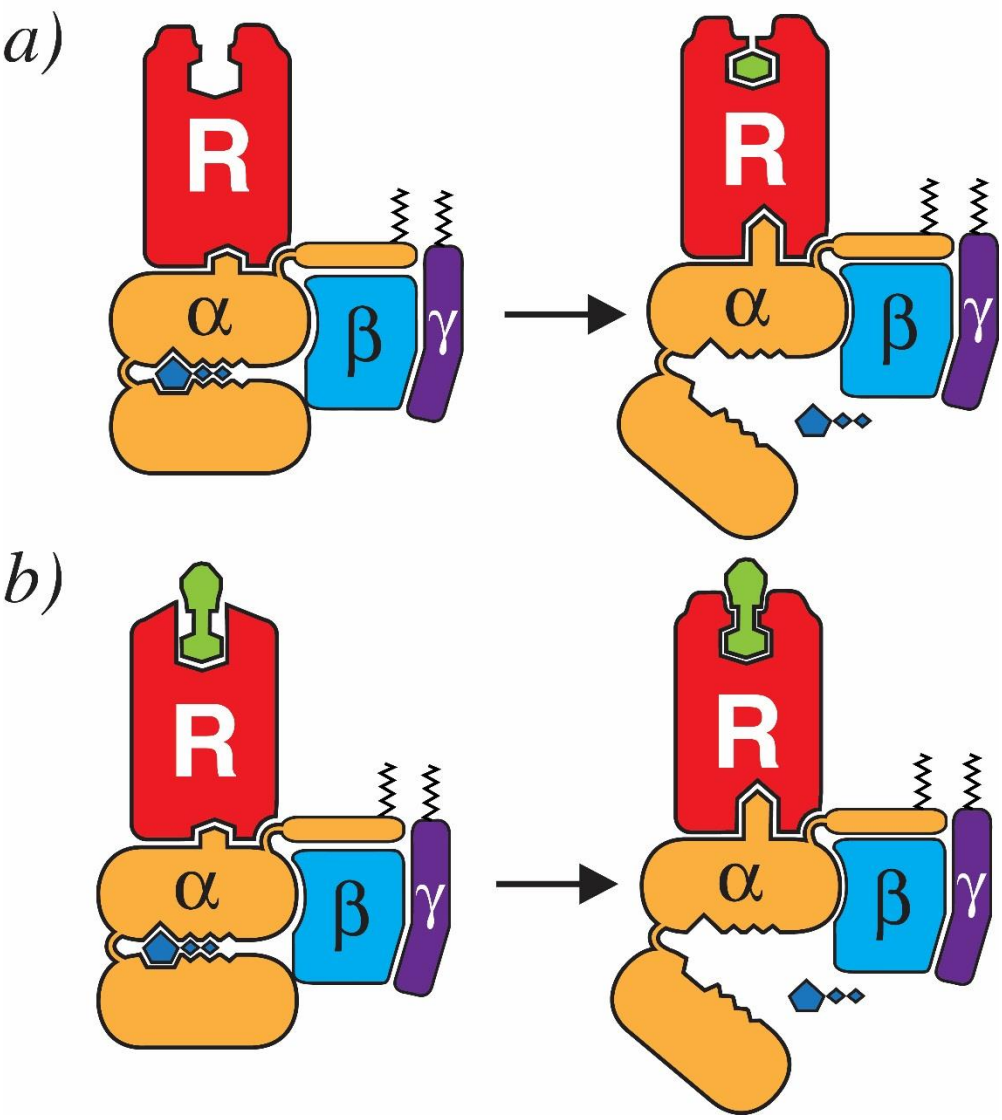

Figure 3-12. Model of G protein-dependent high-affinity agonist binding in peptide receptors.
a) As in Figure 3-10, nucleotide-free G protein-stabilized family A GPCRs experience alterations in the extracellular face of the receptor, thus affecting orthosteric binding site. In a monoamine receptor like the β_2AR, G protein binding and GDP loss accompanies the stabilization of a closed, active conformation of the receptor. ***b)*** For receptors such as MOPr or NTS-R1, where the peptide hormones/agonists are considerably larger, the influence of the G protein-mediated changes in the extracellular domain structure result in similar effects on orthosteric ligand dissociation. Rather than closing over the orthosteric site as with monoamine receptors as in ***a)*** the extracellular face may contain structures and residues that 'pinch' the larger ligands.

Thus, despite the subtle structural differences, the influence of G proteins (or nanobodies) on the association and dissociation of ligands at the orthosteric sites are shared, suggesting that the allosteric effects of G proteins on orthosteric agonists may be manifested by conceptually common mechanisms. Interestingly, class A GPCRs with very lipophilic agonists (e.g. rhodopsin, sphingosine-1-phosphate receptor 1 (S1PR1), and free fatty acid receptor 1 (FFAR1)) have a "lid-like" structure over their orthosteric sites even in the inactive state, suggesting that ligand entry occurs from the lipid bilayer[44,115,116]. Although the mechanism remains unclear, receptors for membrane-partitioned agonists still exhibit nucleotide-dependent shifts in agonist affinity and in some cases accelerated agonist association and dissociation in response to GTP, like the β_2AR[117–121].

Several family B and C GPCRs also show G protein-dependent changes in agonist affinity[32,122–125], including recent studies with the metabotropic glutamate receptor mGluR2, where the active conformation of the 7TM domain allosterically stabilizes the active conformation of the extracellular ligand-binding domain[126]. Thus, while the GPCR superfamily exhibits a great deal of structural diversity, reciprocal allosteric communication between the G protein-binding site and the orthosteric site appears to be fundamental to GPCR function. The specific structural mechanisms that allow G proteins to communicate with the orthosteric site of each GPCR will need to be investigated and may differ from the mechanisms described here.

3.7 - The closed conformation and GPCR-arrestin coupling

One of the hallmarks of GPCR activation, first demonstrated with *meta*II-rhodopsin, is the outward movement of the intracellular regions of the TM domains, most notably TM6. Evidence from EPR spectroscopy[127] as well as x-ray crystallography support the outward

movement of TM6. This outward movement of TM6 in rhodopsin is necessary in order to open a binding cavity capable of accommodating the G protein C-terminus and facilitate GDP release on Gα[53,54,128]. Similar movements of TM6 were observed in the active conformation structures of the β_2AR, MOPr and M2R[56,79,80]. The large TM movements on the intracellular face are accompanied by conformational changes on extracellular regions, which for many GPCRs form a 'lid-like' structure over the orthosteric site, as described in this current study. Similarly, the recent crystal structures of activated rhodopsin bound to the finger loop peptide of arrestin[129] and of activated opsin bound to arrestin[130] reveal similar outward conformational rearrangements of TM6 to accommodate the finger loop region of arrestin. The role of arrestin in stabilizing only the active, chromaphore-bound Meta IIb-rhodopsin and not the dark state, nor opsin (retinal-free), suggests an active conformation-specific arrestin interaction[131]. As we have seen with G protein coupling, the conformational changes that accompany arrestin binding could stabilize rearrangements at a receptor's extracellular face to form a lid-like structure over the orthosteric site of Class A GPCRs such as hormone receptors. Arrestin has been shown to enhance agonist binding to the β_2AR and M2R in a manner similar to G proteins, and therefore agonist-receptor-arrestin has been described as an alternative ternary complex[132]. It is thus plausible that arrestin coupling, like G protein coupling, will stabilize a closed receptor conformation and alter agonist dissociation, thereby enhancing agonist affinity for the receptor.

3.8 - Therapeutic implications of the closed conformation

The formation of the closed conformation has particular significance to the development of allosteric modulators targeting Class A GPCRs. Most allosteric modulator binding sites have focused on the extracellular vestibule located above the orthosteric binding sites. For the

muscarinic M2R for example, the potent allosteric positive modulator LY2119620 utilizes residues that form the 'lid' in the active, closed conformation as described here, as the floor of the vestibule[79]. Stabilization of this closed conformation may therefore be an important aspect on the differentiation between positive allosteric modulators, which enhance agonist binding and activation, and negative allosteric modulators, which decrease agonist binding.

Conclusion

In summary, we provide pharmacological and biochemical evidence suggesting that the closed, active conformation of GPCRs is stabilized by the nucleotide-free G protein, allowing G proteins to influence passage of ligands to the orthosteric binding site. The dramatic effect of G proteins on either ligand association or dissociation is consistent with, and in fact validates, structural models generated from x-ray crystallography where G protein coupling on the intracellular face of the receptor allosterically influences the structure of the extracellular face. Agonist or hormone binding enhances G protein engagement, whereby formation of the active receptor conformation is accompanied by nucleotide loss from the G protein. Therefore, the capacity of G proteins to enhance agonist binding affinity is structurally and energetically linked to the agonist's capacity to promote nucleotide loss from Gα.

CHAPTER 4

Structure-based identification of small-molecule allosteric modulators of β_2AR

GPCRs are excellent therapeutic targets given their localization on the plasma membrane, their widespread distribution throughout many tissues and organs in the body, and their involvement in many physiological processes. Most current drugs that target GPCRs bind to the receptor's orthosteric site, or the site at which the receptor's endogenous ligand binds[14,133]. While this site is often well-suited to binding small molecules, adding to the ease of GPCR druggability, targeting the orthosteric site of GPCRs can present its own set of challenges. For example, the orthosteric site is often highly conserved between receptor subtypes within a given family (e.g. adrenergic receptors, see Fig. 4-1) due to the need to bind a common endogenous ligand[134]. Thus, achieving selectivity for a single receptor subtype has often required exhaustive medicinal chemistry campaigns, with mixed success[134–136].

Allosteric modulation of GPCRs using small molecules is an attractive therapeutic strategy due to the potential for superior subtype selectivity and improved safety profiles compared to orthosteric drugs[137]. Small-molecule allosteric ligands have been discovered for many receptors across all the human GPCR subclasses (class A,B,C, and F) and show a spectrum of activities[15]. Allosteric modulators have the potential to bind to sites where the sequence of closely-related receptors can be quite divergent and thus have may significantly different effects on closely related receptors. Indeed, the few structures of class A GPCRs bound to allosteric ligands have demonstrated an extreme diversity in the location of allosteric binding sites[79,115,138–

[140]. Furthermore, allosteric modulation preserves the spatial and temporal signaling aspects of a receptor's natural signaling profile, minimizing potential side-effects that may arise from chronic activation or blockade of GPCRs[141].

	3.29	3.32	3.33	3.36	3.37	ECL2.52	ECL2.54	5.38	5.42	5.43	5.46	6.48	6.51	6.52	6.55	6.58	7.35	7.39	7.43
α_{1A}	A	D	V	C	T	I	E	Y	S	A	S	W	F	F	M	G	F	F	Y
α_{1B}	A	D	V	C	T	V	E	Y	S	S	S	W	F	F	L	G	F	F	Y
α_{1D}	A	D	V	C	T	I	E	Y	S	S	S	W	F	F	L	G	F	F	Y
α_{2A}	L	D	V	C	T	I	D	Y	S	C	S	W	F	F	Y	T	F	F	Y
α_{2B}	L	D	V	C	T	L	Q	Y	S	S	S	W	F	F	Y	G	F	F	Y
α_{2C}	L	D	V	C	T	L	D	Y	S	C	S	W	F	F	Y	Y	F	F	Y
β_1	T	D	V	V	T	F	T	Y	S	S	S	W	F	F	N	K	F	N	Y
β_2	T	D	V	V	T	F	T	Y	S	S	S	W	F	F	N	H	Y	N	Y
β_3	T	D	V	V	T	F	S	Y	S	S	S	W	F	F	N	R	F	N	Y

Figure 4-1. Comparison of orthosteric site residues in adrenergic receptor subtypes.
The residues chosen for comparison form the binding site for epinephrine in the structure of β_2AR bound to epinephrine and the active state-stabilizing nanobody Nb6B9 (PDB 4ldo). Residue positions are shown according to Ballesteros-Weinstein numbering.

4.1 – Methods of GPCR ligand identification

Discovery of novel GPCR ligands - both orthosteric and allosteric - has often relied on high-throughput screening approaches to identify candidate molecules. While these screening campaigns have tremendous potential for discovery and have yielded many novel ligands, they are expensive to perform, requiring access to large physical libraries of compounds and the robotics to handle testing on a large scale. Virtual screening approaches offer a less expensive alternative to physical high-throughput screening. Using virtual screening, small molecules that do not bind to the target protein *in silico* can be dismissed without purchasing them for testing, and only the top-scoring hits (typically tens of compounds) are purchased. Additionally, virtual screens often identify ligands of diverse chemotypes that do not resemble currently-known scaffolds, translating into the potential for novel biological effects[142]. As computing power has improved in recent years, the reliability and predictive power of virtual screening has also improved and hit rates for virtual screening campaigns are now often better than from conventional high-throughput screens[142].

Virtual screening has proven to be an especially robust method for structure-based identification of orthosteric GPCR ligands. Several groups have performed docking studies with a variety of GPCRs where typically 20-30% (and even as high as 70%) of the compounds tested showed biological activity, some with low-nanomolar affinity for their receptor[143–147]. However, there is a structural bias in the *in silico* discovery of orthosteric ligands. Screens performed on inactive-state structures have yielded antagonist or inverse agonist compounds, and only the screens performed using active-state templates have yielded novel agonists[148]. These results emphasize the importance of thoroughly characterizing the structure-function relationship that underlies GPCR activity.

4.2 – Targeting GPCR allosteric sites using virtual screening

Based on currently available structural data, it seems that virtual screening campaigns targeting allosteric sites will also be heavily affected by the conformational state of the receptor template. Perhaps the most well-characterized example is the allosteric site for the M2 muscarinic acetylcholine receptor (M2R), in which the allosteric site has been visualized using x-ray crystallography[79]. Decades of research on M2R has thoroughly characterized its allosteric binding site, located in the extracellular vestibule directly above the orthosteric site. As seen in chapter 3, the conformational changes that occur during receptor activation affect both the cytoplasmic and extracellular faces of GPCRs. The structure of M2R bound to the agonist iperoxo and the active state-stabilizing nanobody Nb9-8 showed that the overall shape of the extracellular vestibule was dramatically different than the vestibule of inactive-state M2R. However, no further changes in the vestibule site were observed upon binding of LY-2119620, a positive allosteric modulator (PAM) that binds to the vestibule site. It therefore appears that the LY-2119620 binding site is largely formed by the process of M2R activation, and that LY-2119620 produces its potentiating effects by lending stability to this same active state. Thus, changes in the extracellular face of GPCRs that accompany receptor activation provide the opportunity to selectively stabilize certain receptor conformations with allosteric ligands.

In M2R, the bottom of the LY-2119620 binding site is formed by the tyrosine 'lid' (residues $Y104^{3.33}$, $Y403^{6.38}$ and $Y426^{7.39}$) that caps the orthosteric binding site in the active conformation (see chapter 3.8). Our work in the preceding chapter suggests that a similar site may exist in β_2AR; the 'lid' made up of $Phe193^{ECL2}$ and $Tyr308^{7.35}$ may form the 'floor' of an allosteric binding site. This hypothesis is supported by molecular dynamics simulations where the antagonist alprenolol was seen to bind transiently in the extracellular vestibule, immediately

above Tyr308$^{7.35}$, before entering the receptor's orthosteric site[105]. Furthermore, the extended 'tail' of the β_2AR-selective partial agonist salmeterol (Fig. 4-1) is known to project from the receptor's orthosteric site into a secondary binding pocket in the receptor's extracellular face, termed the exosite. A recent study by Baker, Proudman, and Hill[149] employed extensive mutagenesis to identify the location of the exosite on β_2AR and implicated both Lys305$^{7.32}$ and Tyr308$^{7.35}$ as important components of this exosite, again suggesting that residues which cap the orthosteric site of β_2AR may contribute to formation of a pocket amenable to biding small molecules.

Here, we embarked on a virtual screening campaign to identify novel allosteric modulators of β_2AR binding at this site in the receptor's extracellular vestibule. Despite decades of pharmaceutical interest surrounding β_2AR, there are no known allosteric modulators targeting this receptor. Our goal was to provide proof-of-concept that novel allosteric sites can be defined based on available GPCR structures, and that molecules complementary to these novel sites can then be reliably identified using virtual screening. We envisioned an iterative cycle of *in silico* docking, pharmacological testing, and synthetic chemistry to generate allosteric ligands of suitable affinity, culminating with a crystallographic interrogation of the validity of the docking poses. Our initial screens yielded a several potential modulators with poor affinity and/or weak effects, however the remainder of this chapter will focus on a negative allosteric modulator of β_2AR that inhibited agonist binding and downstream signaling. We identified analogs of this compound with improved affinity for the receptor, but we have yet to verify the predicted binding modes in structural studies.

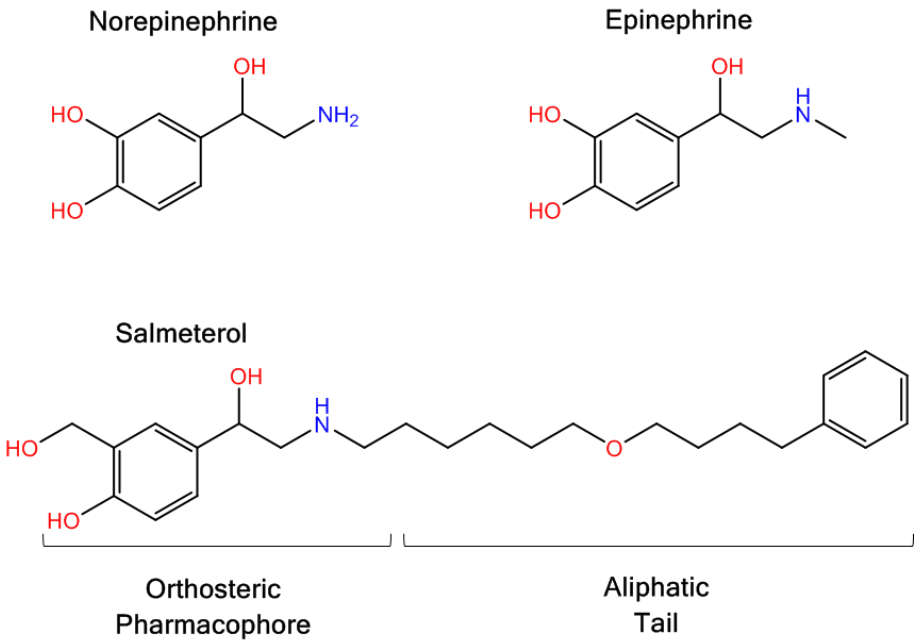

Figure 4-2. Structures of endogenous adrenergic agonists and the β_2AR partial agonist salmeterol.
By definition, the orthosteric site of β_2AR is the binding pocket occupied by the catecholamine hormones epinephrine and norepinephrine. Salmeterol retains a slight variation of this orthosteric pharmacophore, trading the catechol for a saligenin moiety. Salmeterol also contains an extended aliphatic tail that extends to fill a secondary binding pocket commonly referred to as the exosite.

Results

4.3 – Identification of lead compounds

Starting with the x-ray crystal structure of β_2AR bound to salmeterol (solved by Dr. Cheng Zhang, Kobilka lab, Stanford University), the ligand was removed and over 4,000,000 lead-like molecules from the ZINC library (zinc.docking.org) were docked into the extracellular vestibule of β_2AR (All virtual screening in this chapter was performed by Dr. Magdalena Korczynska, Shoichet Lab, UCSF). Because virtual screening hits often have low affinity for the target protein, we chose to first analyze the behavior of the compounds in assays using purified proteins, thereby avoiding any false positives based on compound binding to off-target proteins. Twenty-six of the top-scoring hits were initially tested by Dr. Cheng Zhang for their ability to modulate activation of purified G protein (G_s heterotrimer) by purified β_2AR in rHDL particles. In this assay, the compounds were tested for their ability to enhance or suppress [^{35}S]GTPγS binding in response to 5 μM norepinephrine. Two compounds showed weak activity in the initial screening, here we will focus on one compound that enhanced norepinephrine-stimulated G protein activation (BRAC1; Fig. 4-3).

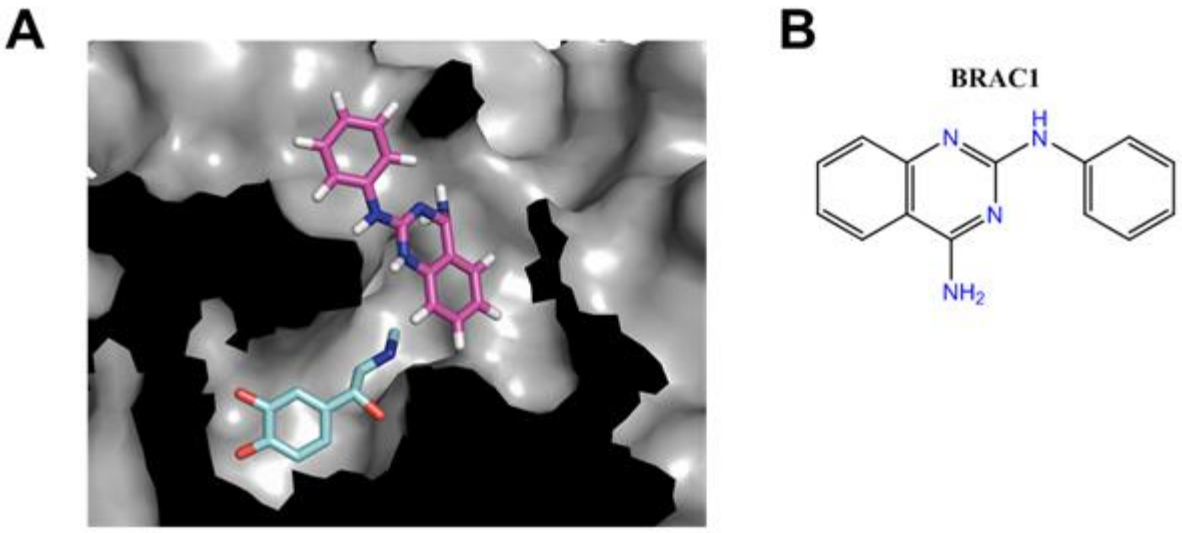

Figure 4-3. Location of the extracellular vestibule site in β_2AR targeted by virtual screening.
A) Cross section of the extracellular portion of β_2AR showing the spatial relationship of the orthosteric site (marked by the position of epinephrine, shown in cyan, from PDB 4ldo) and the extracellular vestibule site that we targeted using virtual screening. BRAC1 is shown in magenta, docked into the vestibule site. **B)** Structure of BRAC1.

4.4 – BRAC1 inhibits agonist binding and downstream signaling

Our initial tests identified BRAC1 (β-receptor allosteric compound 1), a compound which suppressed agonist-stimulated G protein activation by β_2AR. In keeping with the effects we observed in our preliminary experiments, BRAC1 showed concentration-dependent antagonism of epinephrine-stimulated [^{35}S]GTPγS binding and cAMP accumulation (Fig. 4-4a & b). Furthermore, BRAC1 itself demonstrated inverse agonist activity, suppressing basal [^{35}S]GTPγS binding levels (Fig. 4-4c). BRAC1 also inhibited arrestin recruitment in response to multiple agonists, but did not appear biased towards preferential inhibition of G protein or arrestin pathways (Fig. 4-4d). Unfortunately, inhibition of functional responses by BRAC1 required very high concentrations of compound, and at these concentrations BRAC1 showed an apparent competitive displacement of the antagonist [^{3}H]DHAP in saturation binding assays, worsening [^{3}H]DHAP affinity for β_2AR without affecting B_{max} (Fig 4-5a). BRAC1 was also unable to alter [^{3}H]DHAP dissociation from β_2AR (Fig. 4-5b), a commonly observed attribute of allosteric modulators. However, BRAC1 did demonstrate allosteric effects on orthosteric ligand binding to β_2AR. BRAC1 decreased epinephrine affinity for β_2AR ~3-fold at the highest concentration tested (100 μM), but slightly enhanced the affinity of the inverse agonist ICI-118551 for the receptor (Fig. 4-5c & d). Therefore, we sought to identify analogs of BRAC1 with improved affinity for the allosteric site on β_2AR, preserving the allosteric actions without binding at the orthosteric site.

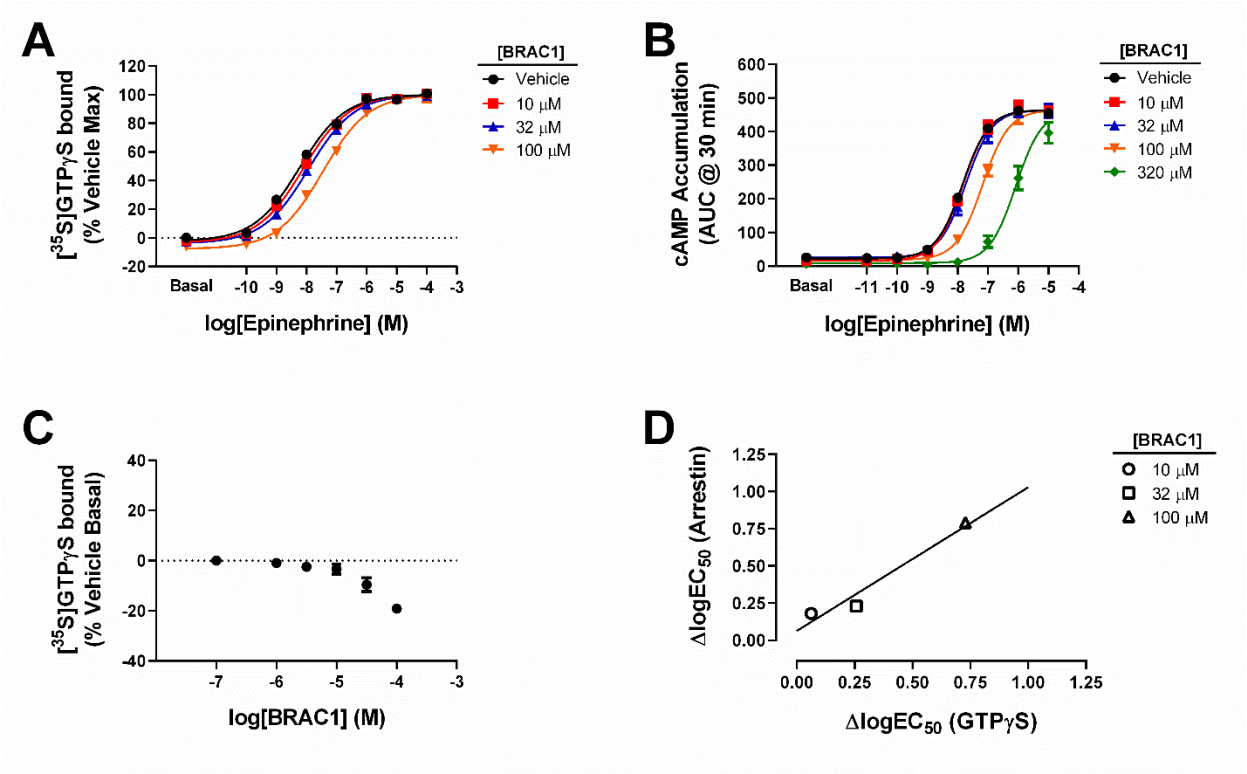

Figure 4-4. BRAC1 inhibits G protein and arrestin signaling downstream of β_2AR.
A) Increasing concentrations of BRAC1 antagonized [^{35}S]GTPγS binding in response to epinephrine (Vehicle pEC_{50} = 8.23 ± 0.05; 100 μM pEC_{50} = 7.46 ± 0.05, or EC_{50} ≈ 6 nM vs. 35 nM, respectively). **B)** In keeping with its effects on G protein activation, BRAC1 also inhibited epinephrine-stimulated cAMP accumulation in a concentration-depended manner (Vehicle pEC_{50} = 7.84 ± 0.04; 100 μM pEC_{50} = 7.18 ± 0.05, or EC_{50} ≈ 14 vs. 66 nM). **C)** BRAC1 showed inverse agonist activity, suppressing basal [^{35}S]GTPγS binding in a concentration-dependent manner. **D)** Comparison of the capability of BRAC1 to inhibit G protein- and arrestin-mediated responses suggests that BRAC1 does not preferentially inhibit one pathway over the other. The shifts in isoproterenol EC_{50} (BRAC1 relative to vehicle) from each assay were plotted as a set of *x,y* coordinates, and the resulting plot could be fit to a straight line with slope = 0.96 ± 0.2 (r^2 = 0.95). Arrestin recruitment was measured by Dr. Harald Hübner. Data are shown as mean ± SEM from n=3 experiments performed in duplicate.

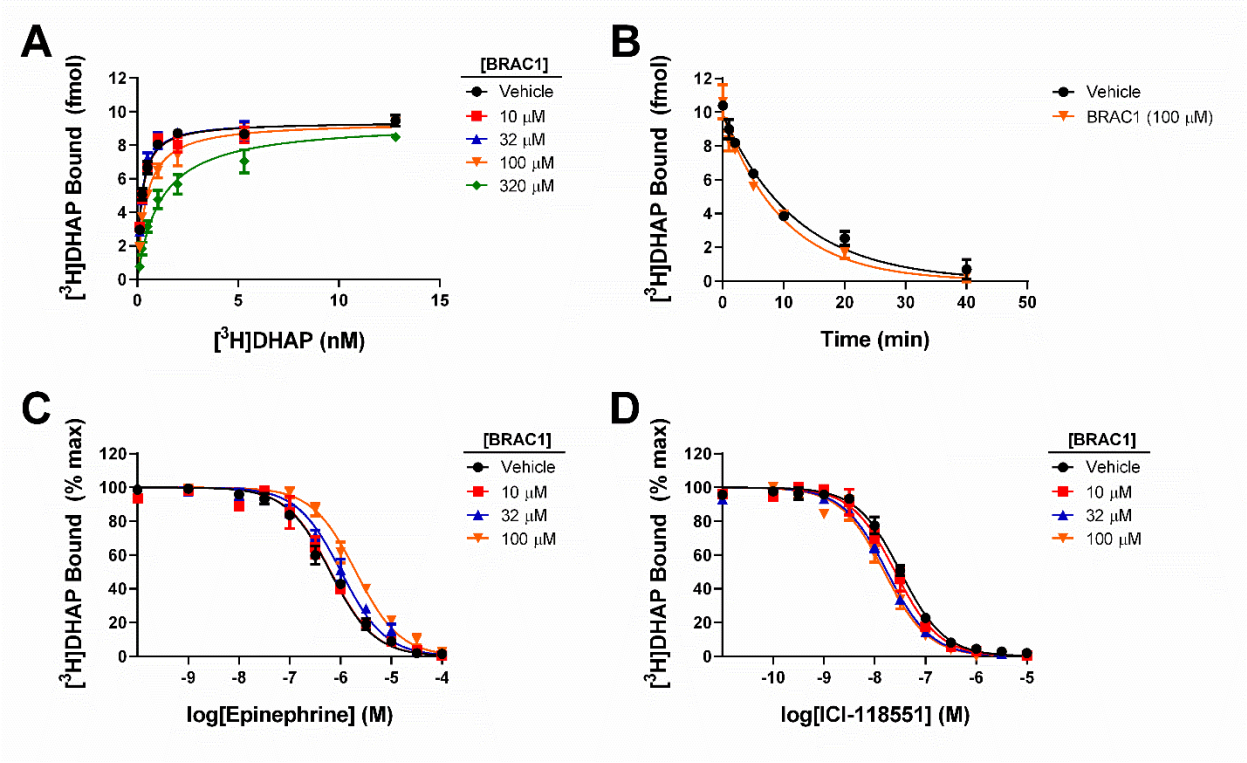

Figure 4-5. BRAC1 shows combined orthosteric and allosteric effects at β_2AR.
A) At concentrations ≥100 μM, addition of BRAC1 resulted in an apparent competitive displacement of [^{3}H]DHAP, decreasing its affinity without altering the observed B_{max} (Vehicle K_d = 0.21 ± 0.02 nM; 320 μM K_d = 1.2 ± 0.1 nM). **B)** The presence of 100 μM BRAC1 did not influence the dissociation kinetics of [^{3}H]DHAP. **C)** BRAC1 produced a concentration-dependent decrease in epinephrine affinity as assessed in competition binding assays (Vehicle pK_i = 6.70 ± 0.03; 100 μM pK_i = 6.17 ± 0.04, or K_i ≈ 210 vs. 670 nM). **D)** Conversely, BRAC1 slightly enhanced the ability of the inverse agonist to compete for binding to β_2AR (Vehicle pK_i = 7.97 ± 0.03; 100 μM pK_i = 8.29 ± 0.04, or K_i ≈ 11 vs. 5 nM). Data are shown as mean ± SEM from n=3 experiments performed in duplicate.

4.5 – Identification of BRAC1 analogs with higher affinity for β_2AR

Based on docking of commercially available BRAC1 analogs, we purchased 35 BRAC1 analogs and examined their effects on direct displacement of [^{3}H]DHAP, agonist affinity, and agonist-stimulated signaling. We identified four BRAC1 analogs with improved potency compared to the parent compound (Fig. 4-6a). Of particular interest, BRAC1-13 inhibited [^{35}S]GTPγS binding in our screening assay with an IC_{50} of ~7 μM and only slightly displaced [^{3}H]DHAP at 32 μM (data not shown). Increasing concentrations of BRAC1-13 produced saturable rightward shifts of the epinephrine concentration-response curve in [^{35}S]GTPγS binding assays (Fig. 4-6b). Fitting this family of curves using an allosteric ternary complex model predicted an affinity of ~1 μM for BRAC1-13 binding to β_2AR. Furthermore, this analysis yielded a cooperativity factor (αβ) of ~0.08 for the modulation of epinephrine response by BRAC1-13, indicating a predicted maximum 12-fold shift in the epinephrine EC_{50} at a saturating concentration of BRAC1-13. Although this modulator was able to produce more than a 10-fold shift in epinephrine's EC_{50} for stimulation of [^{35}S]GTPγS binding, BRAC1-13 had only a small effect on epinephrine affinity ($\alpha = 0.5$, or a 2-fold maximum shift in affinity) and did not affect the affinity of ICI-118551 for β_2AR (Fig 4-6b & c). However, these estimates of affinity and cooperativity are likely skewed by the fact that BRAC1-13 was poorly soluble at concentrations >32 μM. In an attempt to improve the solubility of BRAC1-13, Dr. Anne Stoessel (Gmeiner lab) synthesized several analogs containing bioisosteres of the methyl ester group on BRAC1-13. Unfortunately, none of these compounds were as effective as the parent (Fig. 4-6d).

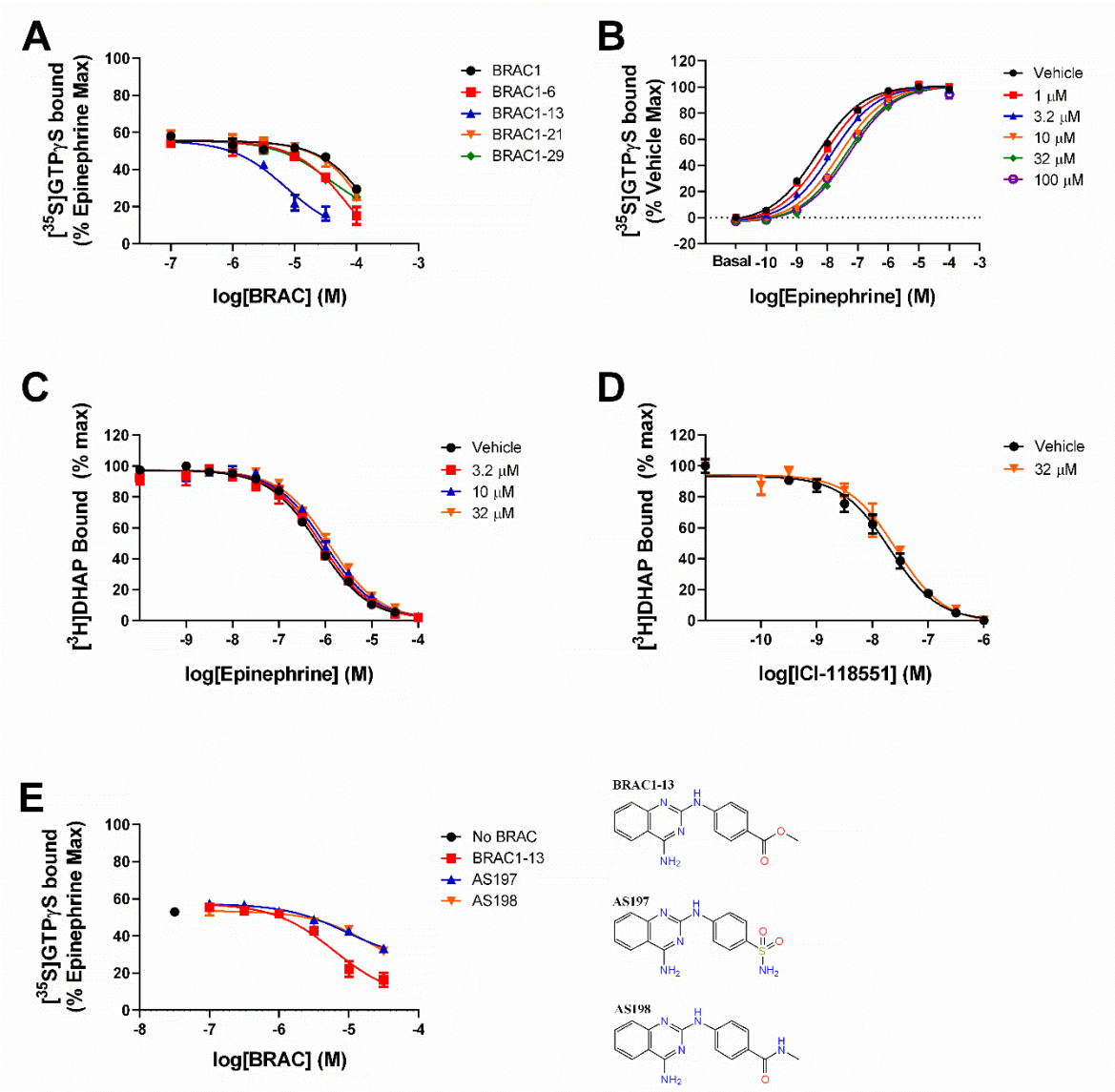

Figure 4-6. BRAC1-13 showed enhanced affinity for β2AR, but produced small shifts in orthosteric ligand affinity. A) Several BRAC1 analogs suppressed the [^{35}S]GTPγS binding produced by 10 nM epinephrine, with BRAC1-13 displaying the highest potency (pIC_{50} = 5.1 ± 0.1, IC_{50} ≈ 7 μM). Data are normalized to the response generated by 10 μM epinephrine. **B)** BRAC1-13 antagonized epinephrine-stimulated [^{35}S]GTPγS binding in a concentration-dependent, saturable manner. The data were globally fit using an allosteric ternary complex model to quantify the negative cooperativity between BRAC1-13 and epinephrine (logαβ = -1.10 ± 0.05, or αβ ≈ 0.08, indicating a maximum ~12-fold shift in epinephrine EC_{50} in response to a saturating concentration of BRAC1-13) and calculate the affinity of BRAC1-13 for the receptor (pK_b = 5.91 ± 0.09, or K_b ≈ 1.2 μM). **C)** BRAC1-13 had minimal effect on the ability of epinephrine to compete for binding to β_2AR (Vehicle pK_i = 6.68 ± 0.04; 32 μM pK_i = 6.47 ± 0.06; Ki = 210 vs 340 nM), and **D)** did not alter the affinity of ICI-118,551. **E)** Analogs of BRAC1-13 with improved solubility did not maintain the ability to inhibit [^{35}S]GTPγS binding in response to 10 nM epinephrine. Data are shown as mean ± SEM from n=3 experiments performed in duplicate.

We also discovered a halogenated series of BRAC1 derivatives that inhibited epinephrine-stimulated [^{35}S]GTPγS binding less potently than BRAC1-13, but produced larger shifts in agonist affinity. In our initial screening of BRAC1 analogs, the fluorinated compound BRAC1-29 displayed a potency of ~30 μM. We investigated the role of the halogen in this compound's action by testing synthesized analogs of BRAC1-29 containing chlorine or bromine atoms at the same position, or added instead at the *para* position relative to the original placement of the halogen (Fig. 4-7a). All analogs tested showed similar potency to inhibit [^{35}S]GTPγS binding in response to 10 nM epinephrine (Fig. 4-7b). However, investigation of their effects on ligand binding to β_2AR revealed differences in their behavior that were dependent on the position of the halogen modification. None of the Cl- or Br-substituted BRAC1 analogs displaced [^{3}H]DHAP from β_2AR, even at a concentration of 100 μM, and neither AS241 nor AS328 significantly affected affinity of the partial agonist [^{3}H]CGP-12177 (Fig 4-8a & b). However, AS94 decreased the observed affinity and B_{max} of [^{3}H]CGP-12177 (Fig. 4-8c), suggesting a non-competitive effect on binding of the radioligand. Furthermore, both AS241 and 328 slowed dissociation of both [^{3}H]DHAP and [^{3}H]CGP-12177 from β_2AR, an effect not produced by AS94 or AS98 (Fig 4-8d-e).

Satisfied that the halogenated BRAC1 derivatives were not acting at the orthosteric site of β_2AR, we next examined the effects of these compounds on agonist affinity. We observed similar ~10-fold shifts in agonist affinity in response to 32 μM AS94 and AS98 (Fig. 4-9a). However, AS241 was able to lower epinephrine affinity almost 100-fold, and produced a similar ~30-fold rightward shift in norepinephrine competition curves in rHDL particles (Fig 4-9a & b). Fitting the competition binding data using an allosteric ternary complex model predicted an affinity of ~1 μM for AS241 binding to β_2AR.

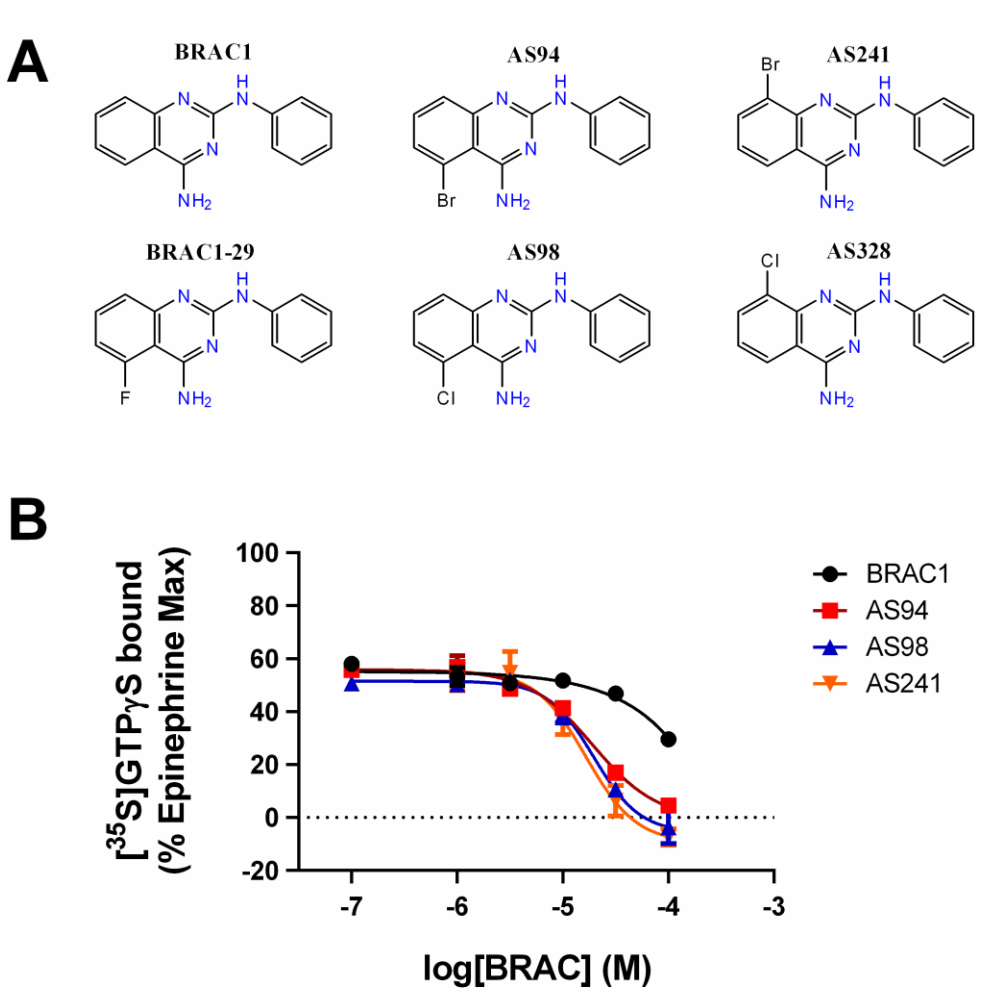

Figure 4-7. Halogenated BRAC1 analogs show similar potency to inhibit G protein activation.
A) Structures of halogenated BRAC1 analogs. **B)** Comparison of the behavior of AS94, 98, and 241 showed that all compounds displayed similar potency to inhibit [^{35}S]GTPγS binding in response to 10 nM epinephrine.

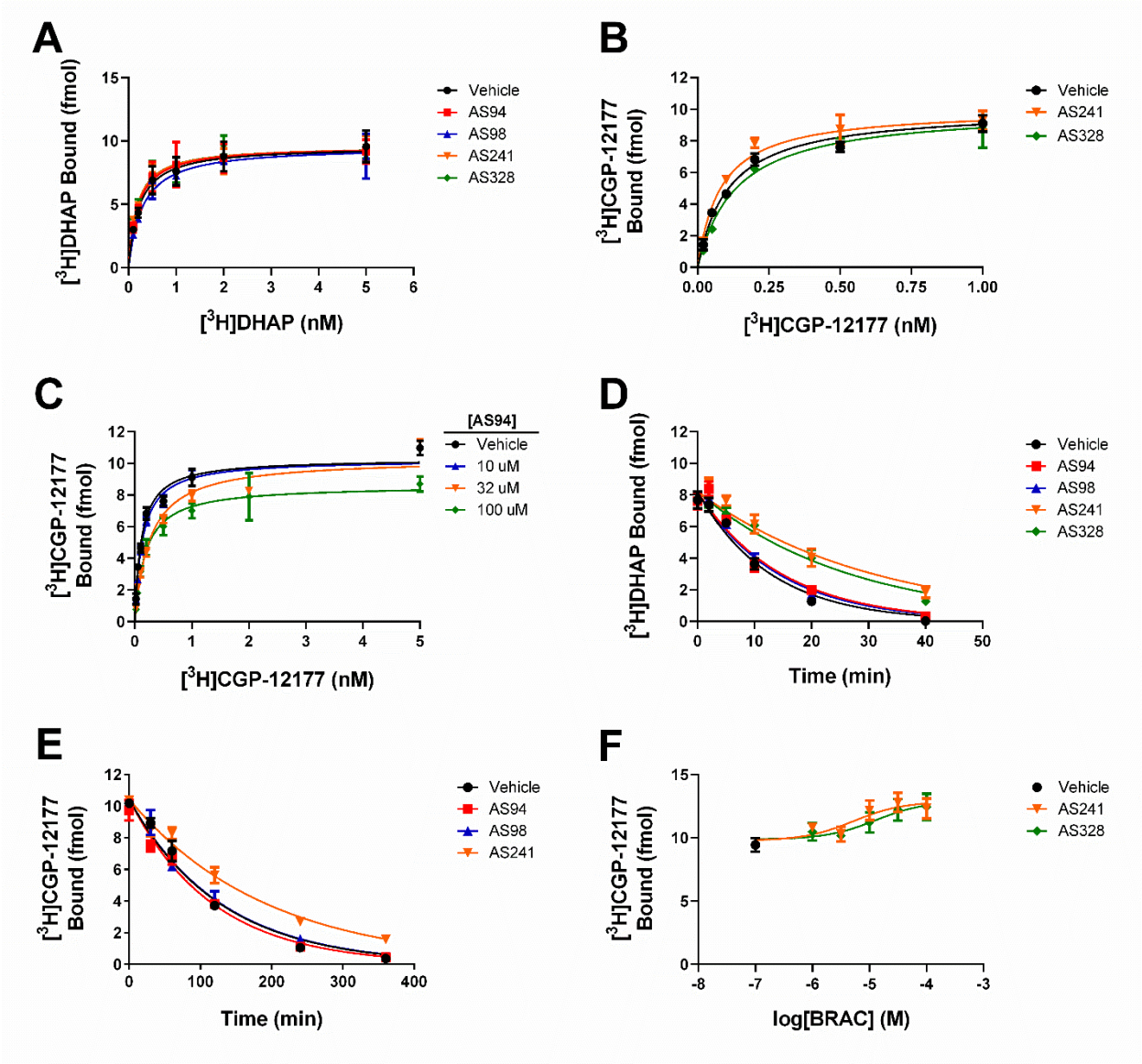

Figure 4-8. Effects of halogenated BRAC1 analogs on antagonist binding to β_2AR.
A) Presence of the halogenated analogs at 100 µM did not alter binding of the antagonist [^{3}H]DHAP. **B and C)** Although AS241 and AS328 did not affect binding of the partial agonist [^{3}H]CGP-12177, AS94 produced a concentration-dependent decrease in observed affinity and B_{max}. **D)** While AS94 and AS98 did not alter dissociation kinetics of [^{3}H]DHAP, AS241 and 328 slowed its off-rate almost 3-fold (Vehicle k_{obs} = 0.079 ± 0.007 min^{-1}; +AS241 k_{obs} = 0.033 ± 0.004 min^{-1}; +AS328 k_{obs} = 0.038 ± 0.004; $t_{1/2}$ ≈ 8.8, 21, and 18 min, respectively). **E)** Similarly, AS94 and AS98 did not influence dissociation of [^{3}H]CGP-12177 from β_2AR, but AS241 maintained its effect (Vehicle k_{obs} = 0.0079 ± 0.005 min^{-1}; +AS241 k_{obs} = 0.0052 ± 0.0003 min^{-1}; $t_{1/2}$ ≈ 88 vs. 133 min). **F)** Dissociation of [3H]CGP-12177 120 min after initiation of the timecourse. Increasing concentrations of AS241 or AS328 were added at t=0 along with unlabeled [^{3}H]CGP-12177. The compounds were able to slow dissociation with similar potency (AS241 pEC_{50} = 5.3 ± 0.8; AS328 pEC_{50} = 4.9 ± 0.8). Data are shown as mean ± SEM from n=3 experiments (panel F is n=4) performed in duplicate.

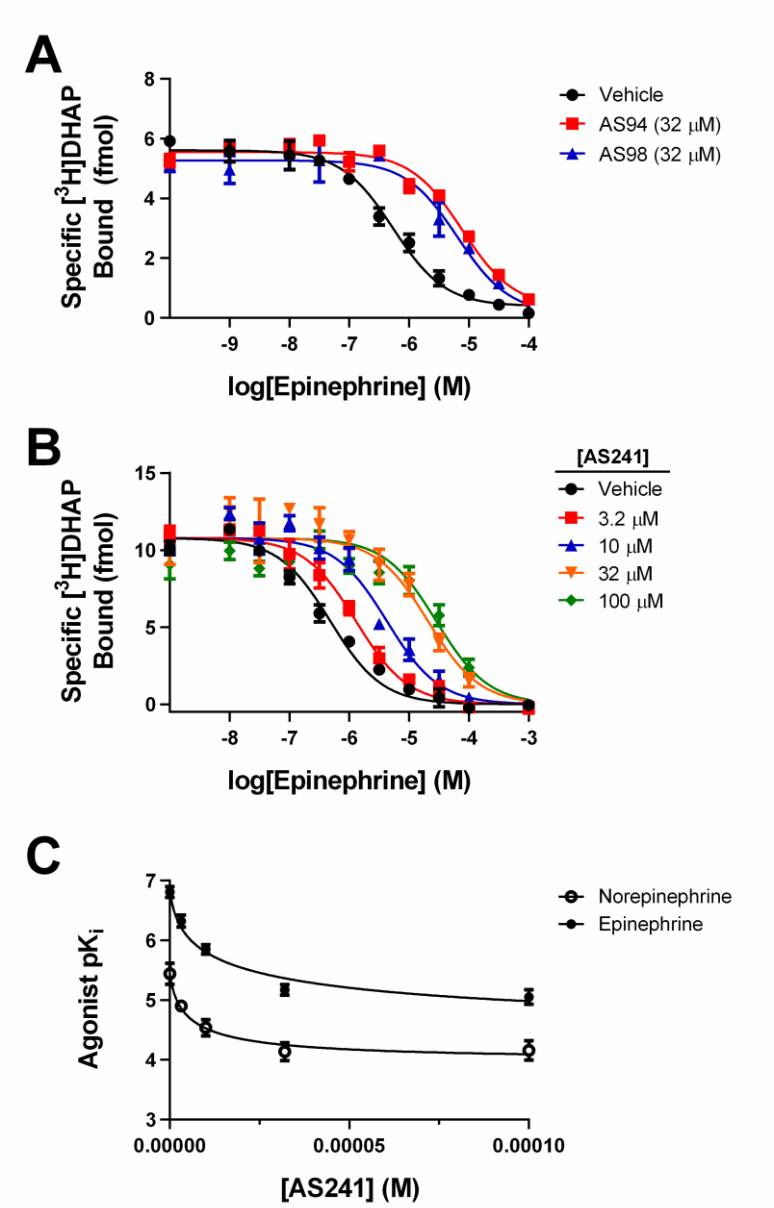

Figure 4-9. Effects of halogenated BRAC1 analogs on agonist affinity for β_2AR.
A) AS94 and AS98 produced similar shifts in epinephrine affinity when tested at 32 μM (Vehicle pK_i = 6.64 ± 0.09; +AS94 pK_i = 5.53 ± 0.09; +AS98 pK_i = 5.65 ± 0.7; $K_i \approx$ 270 nM, 3.0 μM , and 2.2 μM, respectively). **B)** AS241 produced a concentration-dependent, saturable shift in epinephrine affinity. **C)** Shifts in agonist pK_i were plotted as a function of AS241 concentration, and the data were fit to a hyperbolic function derived from the allosteric ternary complex model to determine the cooperativity factor α (i.e. the maximum predicted shift in agonist affinity), and the affinity of AS241. AS241 shows robust negative cooperativity with both epinephrine and norepinephrine (α_{EPI} = 0.008 ± 0.004, or ~125-fold maximum shift; α_{NE} = 0.034 ± 0.006, or ~30-fold maximum shift) and is predicted to bind with an affinity of ~1 μM to unoccupied β_2AR (pK_b = 5.99 ± 0.03). Data are shown as mean ± SEM from n=3 experiments performed in duplicate.

Based on the behavior of the halogenated BRAC1 analogs, we hypothesized that these compounds stabilized an inactive receptor conformation to exert their effects on agonist binding. In keeping with this idea, the degree of affinity shifts observed in response to AS94 was roughly correlated with agonist efficacy: full agonists such as epinephrine and isoproterenol experienced greater shifts (~13-fold) in affinity compared to partial agonists like dopamine and pindolol (~2 fold; Table 4-1). The shifts in formoterol and salmeterol affinity (Table 4-1) also correlate with their efficacy (full agonist and partial agonist respectively), however these ligands contain larger substituents extending from the orthosteric pharmacophore and thus the affinity shift we observe could alternatively be due to a steric clash between AS94 and the agonist, rather than an allosteric effect of AS94 on their binding. The halogenated BRAC1 derivatives also displayed inverse agonist activity in [^{35}S]GTPγS binding assays and inhibited agonist-stimulated [^{35}S]GTPγS binding (Fig. 4-10a & b). Furthermore, AS241 enhanced the affinity of the inverse agonist atenolol for β_2AR, however AS94 had no effect (Fig. 4-10c & d).

4.6 - Combination of BRAC1 modifications worsens compound performance

Armed with a modulator of increased potency (BRAC1-13) and a modulator that produced large shifts in agonist affinity (AS94/98), we attempted to combine these modifications to create allosteric compounds that possessed the desirable attributes of both compounds. However, addition of both a chlorine and methyl ester substituent on the BRAC1 scaffold yielded a compound neither as potent as BRAC1-13 nor as efficacious as AS98 (Fig 4-11a). Other combinations of modifications resulted in a similar loss of activity (Fig. 4-11b-d). Based on preliminary electron density maps of β_2AR bound to BRAC1 and the inverse agonist carazolol (determined by Dr. Xiangyu Liu, Kobilka Lab), it appeared that two molecules of

BRAC1 may be able to occupy the extracellular vestibule. We tested a series of dimeric BRAC1 compounds with the individual BRAC1 molecules linked in different orientations (Fig. 4-12a). AS193, AS194, and AS195 displaced [^{3}H]DHAP from β_2AR in an apparently competitive manner (Fig. 4-12b). All three compounds displayed approximately a threefold shift in IC_{50}, as predicted by the Cheng-Prusoff equation for competitive inhibition, when the concentration of [^{3}H]DHAP was increased from 0.5 to 2 nM. Futhermore, AS194 and 195 completely displaced both concentrations of radioligand, an effect not shared by AS193 likely due to its insolubility at concentrations >10 μM. However we cannot rule out a saturable inhibition of [^{3}H]DHAP binding by AS193, which would indicate an allosteric mode of action. These compounds also inhibited agonist-stimulated [^{35}S]GTPγS binding, except for AS195, which demonstrated partial agonism in this assay but not in cAMP accumulation assays (Fig. 4-12c; cAMP data not shown). Because of the potential that these compounds bound the orthosteric site of β_2AR, we did not pursue them further. Overall, our attempts to modify BRAC1 beyond the addition of a single substituent resulted undesirably, either decreasing the modulator's performance or introducing an apparent ability to bind the orthosteric site.

	Vehicle		***+32 μM AS94***		**K_i shift (fold change)**
Agonist	**pK_i**	**K_i**	**pK_i**	**K_i**	
Epinephrine	6.64 ± 0.09	230 nM	5.53 ± 0.09	3 μM	13
Isoproterenol	7.76 ± 0.09	23 nM	6.55 ± 0.09	280 nM	12
Isoetharine	6.68 ± 0.05	210 nM	5.54 ± 0.06	2.9 μM	14
Formoterol	8.60 ± 0.05	2.5 nM	7.85 ± 0.05	14 nM	6
Salmeterol	9.35 ± 0.04	0.47 nM	8.93 ± 0.06	1.2 nM	3
Dopamine	3.85 ± 0.09	140 μM	3.5 ± 0.1	340 μM	2
Pindolol	9.60 ± 0.06	0.25 nM	9.33 ± 0.06	0.47 nM	2

Table 4-1. Effects of AS94 on agonist affinity.
AS94 displayed a probe-dependent modulation that varied with agonist efficacy. Data are shown as mean ± SEM from n=2 experiments.

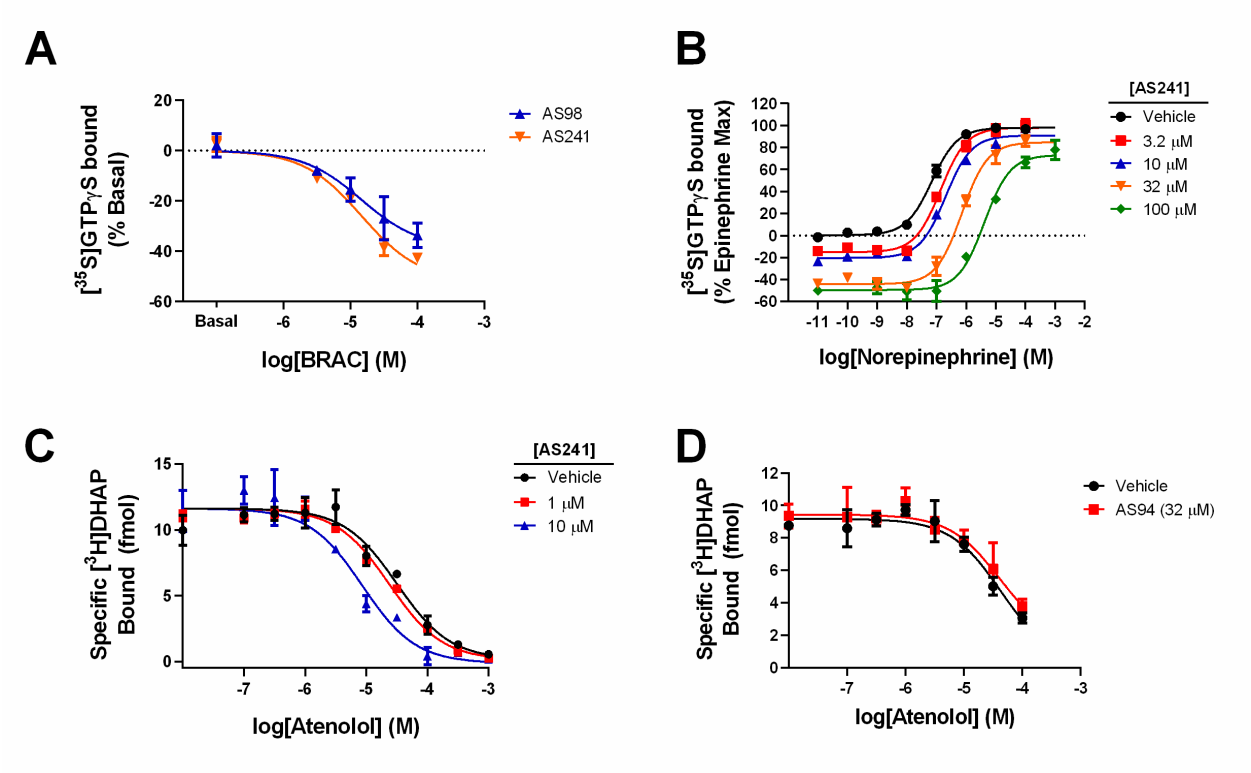

Figure 4-10. Halogenated BRAC1 analogs stabilize an inactive conformation of β_2AR.
A) Both AS98 and AS241 displayed inverse agonist activity in [^{35}S]GTPγS binding assays (AS98 pIC_{50} = 4.8 ± 0.3; AS241 pIC_{50} = 4.8 ± 0.1; IC50 ≈ 15 μM for both compounds). **B)** AS241 antagonized norepinephrine-stimulated [^{35}S]GTPγS binding in a concentration-dependent manner, producing an approximately 60-fold shift in norepinephrine EC_{50} (Vehicle pEC_{50} =7.15 ± 0.06; 100 μM pEC_{50} = 5.4 ± 0.1; EC_{50} ≈ 70 nM vs. 4 μM). **C and D)** AS241 enhanced the affinity of the inverse agonist atenolol (Vehicle pIC_{50} = 5.0 ± 0.1; 10 μM pIC_{50} = 5.5 ± 0.1; IC_{50} ≈ 10 μM vs. 3 μM), however AS94 did not produce the same effect. All data are shown as mean ± SEM from n=3 experiments performed in duplicate.

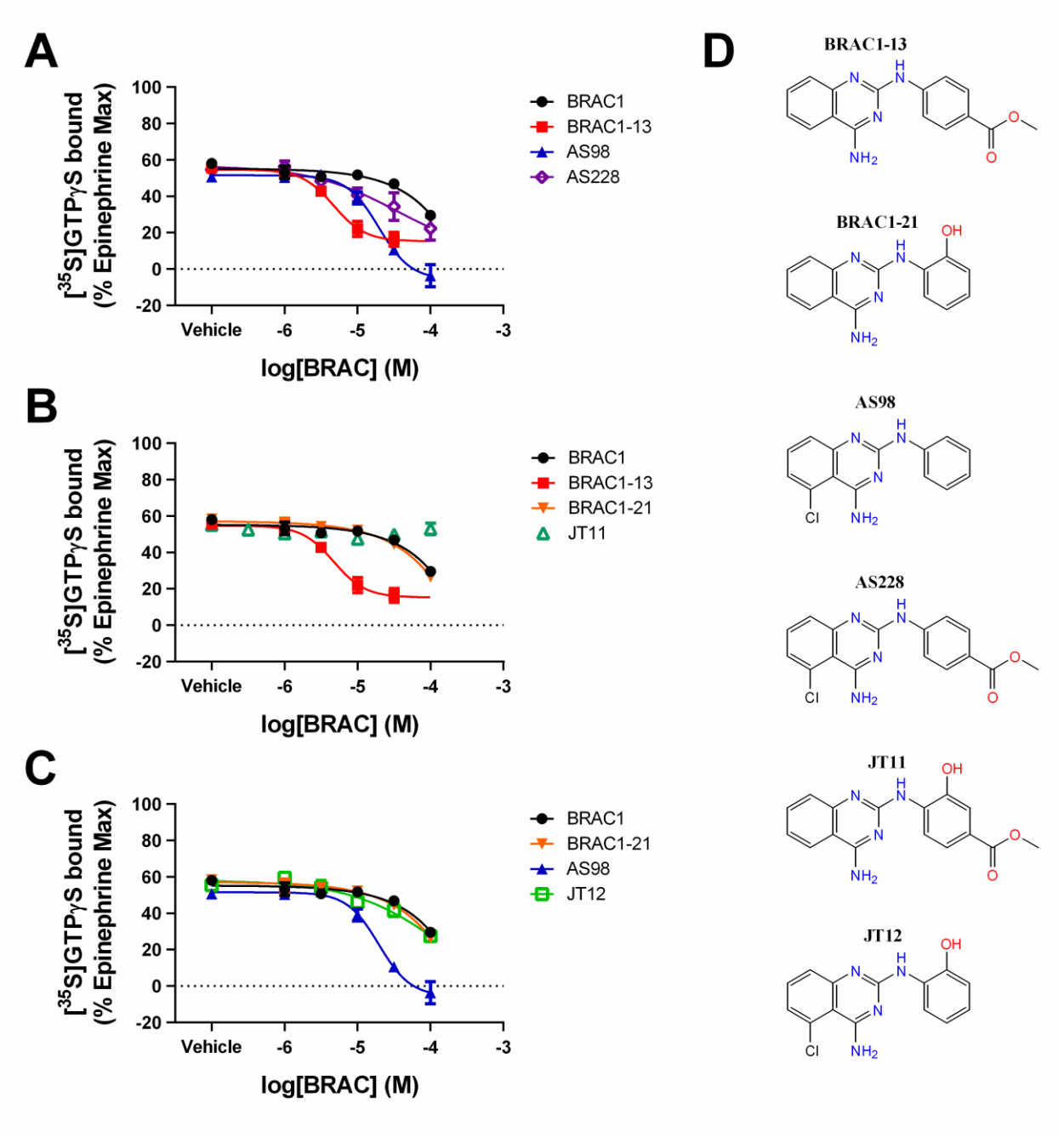

Figure 4-11. Combination of BRAC1 modifications is detrimental to activity.
A) Inhibition of [^{35}S]GTPγS binding (stimulated by 10 nM epinephrine) by BRAC1 analogs. Combination of the substituents on BRAC1-13 and AS98 produced a compound, AS228, that was less potent than the parent molecules and inhibited [^{35}S]GTPγS less effectively. **B and C)** Similar attempts to generate BRAC1 analogs bearing multiple substituents resulted in compounds with little ability to inhibit [^{35}S]GTPγS binding. **D)** Structures of BRAC1 analogs. All data are shown as mean ± SEM from n=3 experiments performed in duplicate.

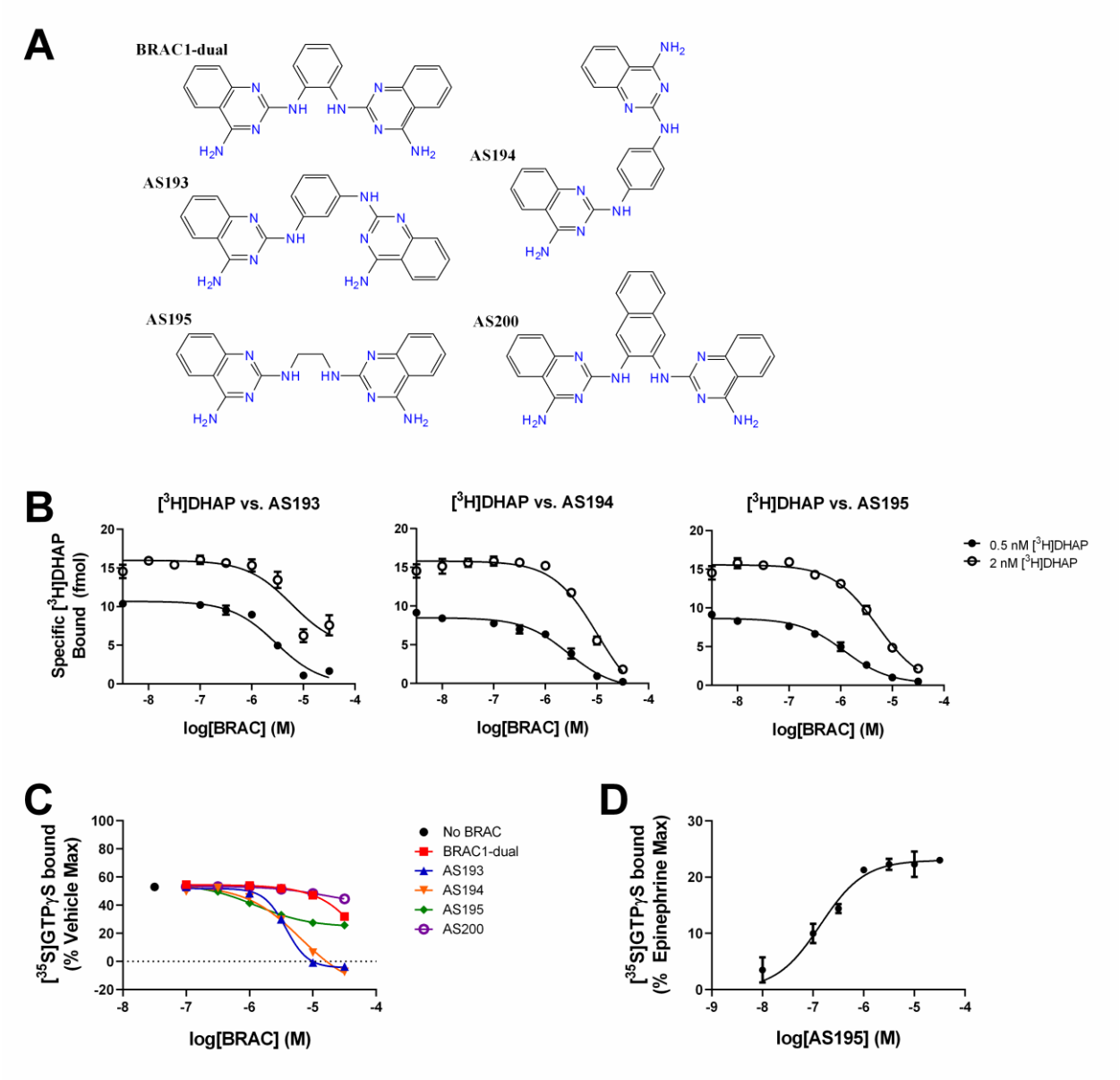

Figure 4-12. Dimeric BRAC1 compounds compete for orthosteric binding and suppress G protein activation.

A) Structures of dimeric BRAC1 compounds. **B)** AS193, AS194, and AS195 displaced [^{3}H]DHAP from β_2AR in a manner consistent with a competitive interaction. **C)** Inhibition of 10 nM epinephrine-stimulated [^{35}S]GTPγS binding by the dimeric BRAC1 analogs. Inhibition by AS195 displayed a non-zero plateau, an effect that can be explained by its partial agonist activity shown in **D**. All data are shown as mean ± SEM from n=2 (panels C & D) or n=3 (panel B) experiments.

Discussion

4.7 - BRAC1 likely binds both orthosteric and allosteric sites

Taken together, the effects we observed with BRAC1 suggest that this compound can act allosterically to influence the affinity of orthosteric ligands, but that BRAC1 itself can occupy the orthosteric site at the same concentrations that produce these allosteric effects. BRAC1 decreased the affinity of the agonist epinephrine but enhanced binding of the inverse agonist ICI-118551, suggesting that BRAC1 is an allosteric modulator that stabilizes an inactive state of β_2AR. However, we observed a progressive decrease in [^{3}H]DHAP K_d in response to increasing concentrations of BRAC1, without a change in the observed B_{max} for [^{3}H]DHAP binding. This observation could be explained by a competitive interaction between BRAC1 and [^{3}H]DHAP at the receptor's orthosteric site, or by an allosteric effect of BRAC1 on β_2AR conformation that leads to a decrease in [^{3}H]DHAP affinity. We failed to observe saturation of BRAC1-induced shifts in affinity, which would indicate saturation of an allosteric site by BRAC1. Therefore, based on the available data we cannot exclude the possibility that at high concentrations ($\geq$100 μM), BRAC1 is able to bind the orthosteric site of β_2AR, acting as a direct competitor of [^{3}H]DHAP binding. Our observation that BRAC1 does not alter the dissociation kinetics of [^{3}H]DHAP also suggests that the effects of BRAC1 on [^{3}H]DHAP affinity are not produced by an allosteric effect. Thus, we sought to identify BRAC1 analogs with a purely allosteric mode of action.

4.8 - BRAC1 analogs bind only an allosteric site

By docking and testing commercially available analogs of BRAC1, we identified several compounds that modulated agonist affinity and functional responses without displacing

[^{3}H]DHAP. Although 32 μM BRAC1-13 did slightly displace [^{3}H]DHAP, this compound produced shifts in epinephrine competition-response curves at concentrations below 10 μM, and its affinity for unoccupied β_2AR was calculated to be ~1 μM. Therefore, the addition of the methyl ester group in BRAC1-13 greatly improves the affinity for its allosteric site, but at higher concentrations BRAC1-13 may still bind weakly at the orthosteric site. However, the halogenated BRAC1 derivatives AS94, AS98, AS241, and AS328 did not displace [^{3}H]DHAP at any concentration tested. Even without measurable affinity for the orthosteric site, these compounds maintained the capacity to negatively impact agonist-stimulated responses and also produced shifts in agonist affinity, consistent with an allosteric mechanism of action.

4.9 - BRAC1 analogs modulate different components of agonist action

Our data suggest that even though BRAC1-13 and the halogenated BRAC1 congeners both allosterically antagonize agonist responses, these compounds may produce their suppression of β_2AR signaling by different mechanisms. The large (~10-fold) shifts in agonist EC_{50} values suggest that BRAC1-13 predominantly decreases agonist *efficacy*, since it did not produce great shifts (~2-fold) in agonist binding affinity. Initial docking poses suggested that BRAC1-13 may occupy a site in the extracellular vestibule of β_2AR and form interactions with Lys305$^{7.32}$. As this region is known to undergo rearrangement upon agonist binding and activation of β_2AR[103] (see chapter 3), the binding of BRAC1-13 may thus interfere with important conformational changes that occur during β_2AR activation, but this hypothesis remains to be examined. In contrast to the efficacy-based modulation of BRAC1-13, the inhibition of agonist-driven functional responses by the halogenated BRAC1 analogs is likely dominated by the large shifts in agonist *affinity* produced by these compounds (10-100 fold). The effect of the halogenated analogs on agonist

affinity suggests that this series of compounds stabilizes an inactive receptor conformation, a hypothesis supported by the observation of inverse agonist activity of these compounds in [^{35}S]GTPγS binding assays. Therefore it appears that by binding at an allosteric site, these compounds are able to directly influence the conformations sampled at the intracellular face of β_2AR.

4.10 - Halogen position modulates the properties of BRAC1 analogs

Addition of a halogen to BRAC1 precludes its binding at the orthosteric site of β_2AR, but the type of halogen (Cl or Br) does not seem substantially modify the allosteric modulation displayed by the compound. Rather, halogen position seems to be the critical variable in defining the characteristics of the modulator, and we are able to group the analogs into two functional classes based on the position of halogen addition: AS94/98 and AS241/328. The functional similarity between Cl- and Br-substituted compounds was a somewhat surprising result, given the size difference between these atoms and their overall effects on electrostatic potential when present in an organic molecule[150]. Based on docking results, the halogen substitution on AS94/98 points towards the receptor's orthosteric site, while in AS241/328 the halogen lies at a position facing the extracellular space. Thus we may be able to introduce other modifications at this position to further enhance the affinity and/or efficacy of these modulators.

Conclusion

In this chapter, we focused on applying our knowledge of the structural changes that occur in β_2AR activation, attempting to define a novel allosteric site on β_2AR and identify small molecules to complement this site. Using virtual screening methods, we discovered BRAC1, a novel allosteric modulator of β_2AR. Through the complementary application of docking, pharmacological assays, and medicinal chemistry, we uncovered a variety of effects in response to this compound and its congeners. Our data suggest that BRAC1 and its derivatives are negative modulators of both G protein and arrestin signaling. Structural studies to verify the virtually-predicted binding modes of these compounds are ongoing. The discovery of these molecules provide, to our knowledge, the first allosteric ligands of β_2AR, which serves as an important proof-of-concept that novel allosteric sites on GPCRs can be identified and targeted using structure-based methods. Furthermore, the characterization of these compounds has yielded further insights into the allosteric behavior of β_2AR and illustrate the potential of allosteric ligands to modulate signaling pathways downstream of this receptor.

CHAPTER 5

Extended discussion and conclusions

5.1 - Overall summary

Our studies focused on characterizing the allosteric communication within β_2AR that is fundamental to its transmission of biological signals, and how the principles of allostery can be used to pharmacologically manipulate receptor signaling for experimental or therapeutic outcomes. We highlight the versatility of nanobodies and their applications to studies of GPCRs beyond structural biology. In this work, we utilized these tools to study the role of agonists in GPCR activation and the allosteric communication between agonists and Nb80 binding. We found that agonists enhance Nb80 (and presumably G protein) affinity for β_2AR predominantly by enhancing its *association* kinetics, while Nb80 or nucleotide-free G protein in turn enhance the affinity of the bound agonist predominantly by slowing its *dissociation*. By examining structures of β_2AR recently solved by x-ray crystallography, we provided a structural explanation for these kinetic observations: the binding of Nb80 or nucleotide-free G protein stabilizes conformational changes at the extracellular face of the receptor, constricting the binding pocket around the bound agonist and thereby slowing its dissociation. Based on these activation-dependent conformational changes in the extracellular vestibule, we utilized β_2AR structures as templates to identify novel allosteric ligands using virtual screening.

This work provides an important characterization of Nb80, a tool that has already proven useful in studying the structure of β_2AR, quantifying its selectivity for active states of β_2AR and illustrating its utility in probing the biological behavior of β_2AR. Furthermore, we provide a mechanism to explain the G protein-mediated enhancement of agonist affinity that has been observed with many GPCR-G protein pairs since the 1970s. Our discovery of allosteric ligands for β_2AR adds the first allosteric modulators to an extensive pharmacological toolbox for this receptor, providing another set of probes to interrogate β_2AR function experimentally. Our work has largely focused on β_2AR, which has served as a prototype class A GPCR for decades. Thus we anticipate that the principles outlined in this thesis will be useful in studying GPCRs at large.

5.2 - Application of interferometry to other GPCR binding partners

In this work we developed a method to directly monitor the interaction of GPCRs with G protein-mimetic nanobodies. As briefly discussed in chapter 2.15, the modular nature of this assay provides it with a broad applicability to many future studies with β_2AR and other receptors. An ideal use of this system would be to monitor the receptor-G protein interaction directly. However, G proteins are lipid-modified and therefore must be purified in buffers containing detergent, the addition of which would likely solubilize the rHDL particles used for receptor reconstitution. Even if we could keep the detergent concentration to a minimum and avoid deleterious effects on rHDL integrity, the presence of a lipid moiety would drive G protein recruitment to the rHDL. Thus it would be difficult to separate receptor-mediated recruitment from lipid-mediated recruitment events. In an attempt to address this complication, we have constructed a mutant $G\alpha_s$ lacking its palmitoylation site by mutating Asn6 to Ser. Similarly, $G\beta\gamma$ can be expressed as a soluble complex by mutation of the prenylation site on $G\gamma$ (e.g. Cys68 to

Ser in $G\gamma_2$)[151]. Thus these mutants may be useful reagents for studying receptor-G protein interactions directly with interferometry, providing a method to quantify the effects of nucleotides on the kinetics of receptor-G protein interactions, to study receptor-G protein selectivity, or the effect of co-reconstituted membrane proteins such as receptor activity modifying proteins (RAMPs) on G protein recruitment.

This technology can also be applied to various other intracellular binding partners of GPCRs. We attempted to use this system to study the effects of ligands on binding of arrestin 2 (β-arrestin 1) by β_2AR. However, these assays were complicated by a high non-specific binding signal generated by arrestin. The intensity of the non-specific binding signal was negatively correlated with the loading density of rHDL particles, suggesting that arrestin was binding non-specifically to the interferometry probe. We screened various blocking conditions and buffer additives in an attempt to decrease the non-specific binding, to no avail. However, a report by Li *et al.* used interferometry to measure an interaction between $G\alpha_s$ and arrestin[152]. Their assay was performed in a detergent-containing buffer, a condition we did not attempt due to the presence of rHDL. Beyond G proteins and arrestins, GPCRs interact directly with a number of cytoplasmic binding partners such as kinases, RGS proteins, PDZ-domain containing proteins, ubiquitin ligases, trafficking proteins, and many more. The interferometry assay described here can theoretically be used to investigate the conformational requirements for binding these proteins and quantify their affinity for various receptor states (bound to agonist/inverse agonist, phosphorylated or not, etc.).

5.3 - Utility of nanobodies in dissecting GPCR biology

As illustrated in chapter 2.2, nanobodies have been applied creatively in a broad range of experimental settings, and are powerful tools to study GPCR function. Based on the conformational selectivity of nanobodies, it may be possible to identify nanobodies for other conformational states of β_2AR and other GPCRs, which could then be used to more thoroughly study their activation mechanism using interferometry and/or structural biology. These types of studies would be highly complementary to biophysical techniques such as EPR, NMR, or fluorescence spectroscopy studies of receptor activation. Fluorescently-labeled nanobodies could also be used to investigate GPCR biosynthesis and trafficking to the plasma membrane. As we have demonstrated, the ability of nanobodies to raised against specific states of the G protein can also be used to dissect activation of G proteins by GPCRs. Similar nanobodies could be used to detect active conformations of other signaling proteins, such as arrestin, facilitating studies on how GPCRs generate these active states or their localization in cells.

5.4 - Allosteric communication between GPCR agonists and guanine nucleotides

The current ternary complex models were developed with a focus on allosteric interactions within the receptor itself. In these classic models, agonist binding enhances the receptor's affinity for G protein, and vice versa. Shortly after the proposal of the original TCM, it was suggested that the high-affinity agonist-receptor-G protein ternary complex may correspond to the nucleotide-free state of the G protein. Our work in chapter 3 provides further evidence for this hypothesis, and suggests an important allosteric role of guanine nucleotides - both GDP and GTP - in regulating the receptor-G protein interaction, and in turn the affinity of agonists for the receptor. Based on the modulatory role of nucleotides on the affinity of both agonist-receptor and

receptor-G protein interactions, we propose an updated model to incorporate the effects of guanine nucleotides (Fig. 5-1). This model describes the influence of nucleotides both on the kinetics of orthosteric ligand binding and on the receptor-G protein interaction.

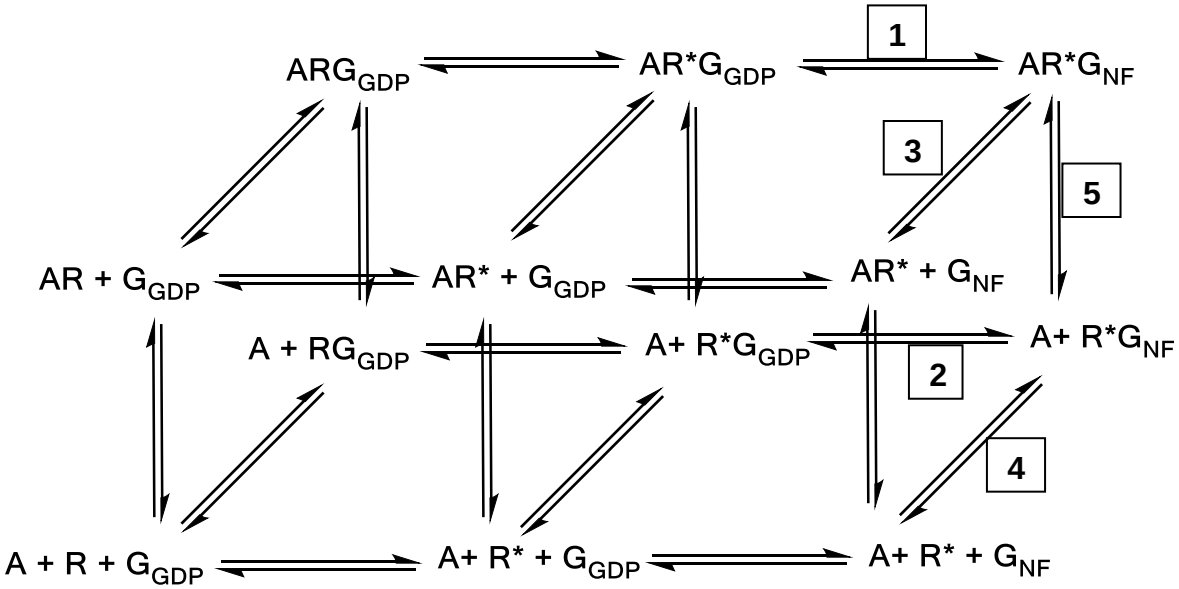

Figure 5-1. Modification of the cubic ternary complex model to include the modulatory effects of guanine nucleotides.

The cubic ternary complex model proposed by Weiss *et al.* is the left of the two cubes. We have added an additional cube describing the receptor-mediated release of GDP from the G protein, either driven by agonist or basal activation of the recptor (reactions 1 and 2), and by extension the effect of GDP on the affinity of the receptor-G protein interaction (top face of the cube). Reactions 3 and 4 describe the ability of nucleotide-free G protein to dissociate from the receptor, a process which should be unfavorable both in the presence or absence of agonist. This model also describes our observations concerning the effect of nucleotide-free G protein on agonist affinity for the activated receptor in reaction 5. For thermodynamic completeness, we have also shown the ability of the G protein to undergo spontaneous nucleotide release without binding to the receptor (front vertical plane). In this case, the rate of nucleotide loss is intrinsic to the G protein and does not depend on the state of the receptor. To avoid overcrowding the diagram we have omitted unbound free GDP in the conditions containing nucleotide-free G protein. The model illustrated here could be similarly modified to include another cube describing the binding of GTP to the nucleotide-free G protein, and the consequent effects on both receptor-G protein and agonist-receptor affinities.

5.5 - Allosteric communication between agonists and other GPCR binding partners

Similar to the phenomenon of G protein-mediated high-affinity agonist binding, the binding of arrestin has also been shown to enhance agonist affinity for multiple receptors, as discussed in chapter 3.7. Based on this observation, agonist-receptor-arrestin has been referred to as an alternative ternary complex[132]. Just as arrestin is able to stabilize conformational changes within a GPCR, evidence has also been presented for receptor-mediated stabilization of conformational changes within arrestin, including a large rotation of arrestin's two domains relative to one another[130,153–155]. Furthermore, it appears that activated receptors may be able to act catalytically in promoting arrestin signaling[156,157]. Therefore, analogous to agonist-mediated nucleotide exchange leading to activation of G proteins, agonists can promote turnover of active of arrestin molecules which dissociate from the receptor to interact with signaling partners.

Another factor that must be considered in the discussion of receptor-arrestin interactions is the action of GRKs, which are recruited to GPCRs in an agonist-dependent manner and phosphorylate residues on the receptor's intracellular to promote arrestin binding. Binding to an active receptor conformation is thought to promote kinase activity by engaging the N-terminus of the kinase, thereby allosterically stabilizing the closed, active conformation of the kinase domain. However, there have been no reports of GRK-mediated enhancement in agonist affinity for GPCRs, perhaps due to the low affinity and transient nature of the receptor-GRK interaction.

5.6 - Allosteric ligands and biased signaling at β_2AR

The actions we observed in response to the negative allosteric modulator BRAC1 and its derivatives can be explained in the context of a two-state MWC model. In this model, the receptor exists in equilibrium between R and R* states, as discussed at many points throughout

this thesis. Interaction of the R* state with either G protein or arrestin produces a response that can be measured in our assays. Under this framework, agonist efficacy is assumed to be a linear property - an agonist brings about downstream responses by stabilizing an R* state of the receptor, and an inverse agonist inhibits these responses by stabilizing the inactive R state. The behavior we observed with BRAC1 can be adequately explained using this simplified model, as BRAC1 displayed balanced antagonism for the outputs tested. BRAC1 displayed inverse agonist activity and inhibited isoproterenol-stimulated [^{35}S]GTPγS binding and arrestin recruitment equally, thus suggesting that BRAC1 shifts the R/R* equilibrium in favor of the inactive state.

Rather than a single active state, it is now appreciated that receptors may adopt a multitude of active states, and it has been proposed that each separate ligand may in fact stabilize the receptor in a unique conformational ensemble[158]. In this model, the apparent affinity of the receptor for each of its binding partners is dictated by the conformational space accessible to the receptor. Therefore, a ligand may stabilize certain receptor states that are able to bind one signaling partner (e.g. arrestin) at the expense of another (e.g. G protein), and the linear idea of efficacy must be replaced with the concept of pluridimensional efficacy[159]. As discussed in chapter 4.9, this behavior has been demonstrated previously in response to certain orthosteric ligands of β_2AR (e.g. ICI-118551 and carvedilol) which are able to inhibit G protein activation but promote arrestin-mediated signaling. Considering allosteric modulators under this framework, it is possible that the allosteric ligand may alter the conformational ensemble of agonist-bound receptor to alter the apparent bias of the orthosteric agonist. This phenomenon has been described for several GPCRs[160–162], and the effects of BRAC1 analogs on the bias of orthosteric agonists should be explored.

5.7 – Location of allosteric binding sites on β_2AR

Although we targeted a defined site in the extracellular vestibule of β_2AR, we do not yet have evidence that the modulators we discovered bind to this site, or that the different modulators bind at the same site. Work to solve the structure of β_2AR bound to these modulators is underway, in collaboration with the Kobilka laboratory. We are attempting to disrupt the proposed binding site using site-directed mutagenesis in order to experimentally test the virtual docking poses. We will also use this strategy to validate the protein-ligand interactions observed in a co-crystal structure, should one be solved. A pharmacological investigation of the BRAC1 and BRAC11 binding sites could begin with an investigation of whether BRAC11 is able to reverse the antagonism of BRAC1 (and analogs such as AS241). If so, then a Schild-style analysis of the interaction between the two ligands may be able to determine if the compounds compete for the binding to the same allosteric site on β_2AR.

Future studies will also address the issue of receptor selectivity, one of the proposed advantages of allosteric modulators over conventional orthosteric ligands. Our preliminary experiments have suggested that BRAC1-13 and AS98 are able to inhibit epinephrine binding at both β_1AR and β_2AR with similar potency. However, the possibility exists that the functional effects of modulator binding may differ between β_1AR and β_2AR, as epinephrine is less potent an agonist at β_1AR. The two receptors may also possess different free energies of activation and allosteric coupling mechanisms between the agonist binding and G protein binding sites, as evidenced by the different effects of sodium ions (see section 5.8) on the closely related receptors[163]. Therefore allosteric ligands may display different cooperativities with agonist binding or receptor activation even with closely related receptors, and the cooperativity values of the allosteric modulators with norepinephrine and epinephrine will need to be calculated at both

β_1AR and β_2AR (and perhaps even β_3AR) to definitively determine the selectivity profile. Furthermore, BRAC1 and its analogs show a similarity to known ligands for α-adrenergic receptors (Fig. 5-2). Binding of BRAC1 compounds to these receptors should also be assessed to examine their cross-reactivity outside the β-adrenergic family. Conversely, the similarity in ligands raises the possibility that some α-adrenergic receptor ligands may be able to bind weakly to an allosteric site on β_2AR.

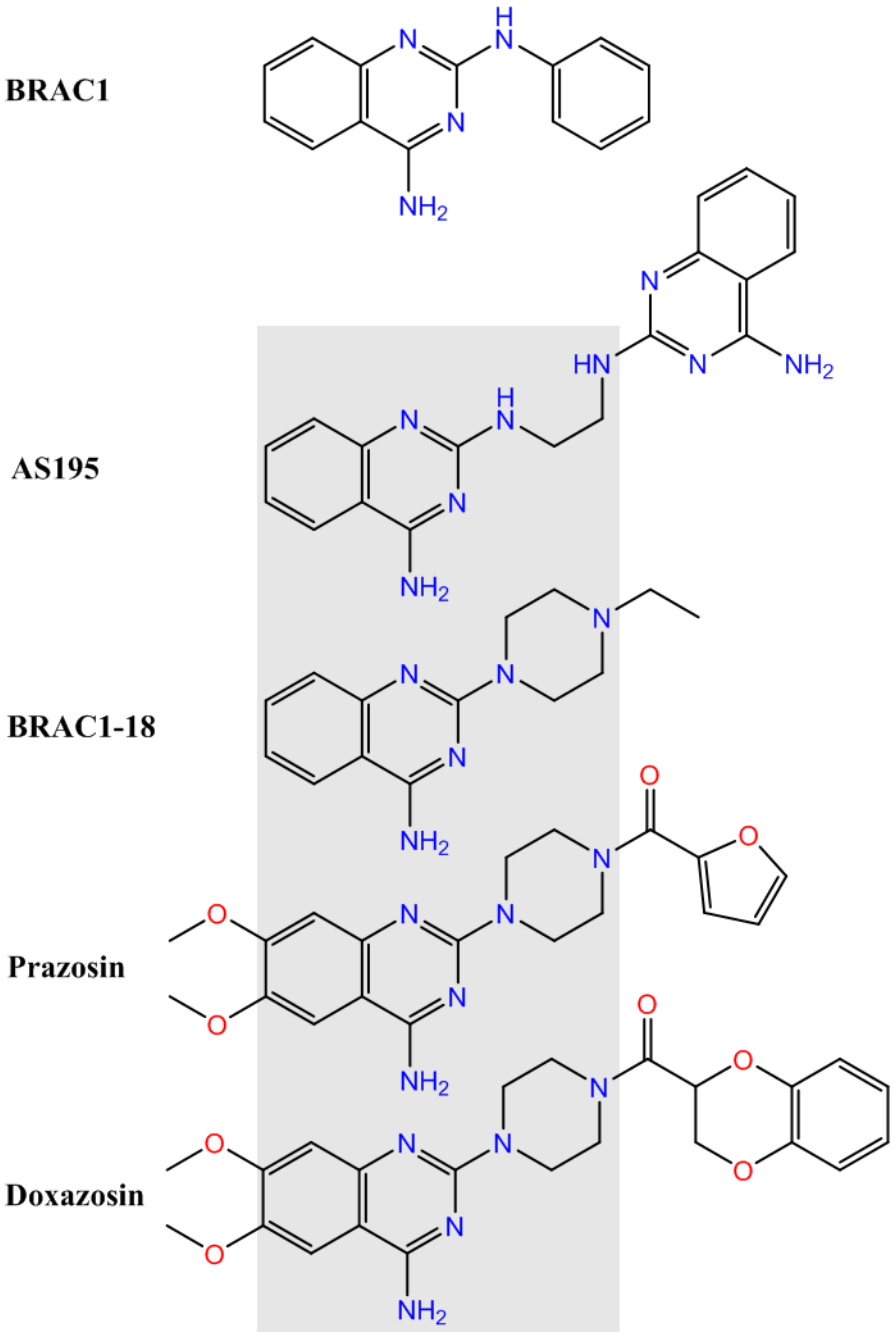

Figure 5-2. Similarity of BRAC1 and analogs to known α-adrenergic antagonists.

5.8 - Endogenous allosteric modulators of GPCRs

The ability of ligands to bind simultaneously at several sites to modulate GPCR function raises the possibility that this phenomenon may occur in a physiological context, not only when synthetic molecules are introduced to the system. Indeed, local cellular factors are able to control the conformational landscape of GPCRs and act to allosterically influence agonist affinity and G protein activation. Sodium is a well-known negative modulator of several class A GPCRs that binds to a site buried in the 7TM core to stabilize a receptor's inactive state[164]. By acting at this site, sodium is able to weaken agonist affinity as well as limit the receptor's basal interaction with G protein. However, receptors display differential sensitivities to sodium ions, illustrating the unique energy landscapes of GPCR activation[163]. Another endogenous factor that can influence the receptor's conformational dynamics is the membrane itself. Cholesterol, either through its effects on bilayer fluidity or by binding to a distinct site on GPCRs, has been shown to modulate the function of several GPCRs. Similarly, recent studies using rHDL of defined lipid composition have suggested that certain phospholipids can also influence agonist affinity for β_2AR[165]. The structural diversity of the GPCR superfamily imparts these receptors a variety of allosteric sites, and thus many endogenous substances have been proposed as allosteric modulators of various receptors[15].

5.9 – Conclusion

GPCRs are transmembrane proteins that rely on allosteric communication to transform the binding of an extracellular stimulus into an intracellular response. Ligands for GPCRs, regardless of the location of their binding site, are able to modulate the generation of cellular signals by virtue of their ability to stabilize certain receptor conformations. Together, the sum of the receptor's environment and bound ligands shapes the energetic landscape for transition between conformational states, tuning the probability of receptor activation to the needs of the physiological system.

CHAPTER 6

Materials and Methods

Large-scale Purification of β_2AR

β_2AR bearing an N-terminal FLAG tag and C-terminal 10x-His tag was expressed in *Sf*9 cells (Invitrogen) and purified as previously described[56]. YFP-tagged mu-opioid receptor (YMOPr) was purified as described by Kuszak *et al*[90]. M2 muscarinic receptor (M2R) was purified as described by Haga *et al*[110].

Expression and purification of G protein and Nanobodies.

G_s and G_o heterotrimer were expressed in HighFive™ (Invitrogen) insect cells using recombinant baculovirus and purified by chromatography on Ni-NTA (Qiagen), MonoQ, and Superdex 200 resin (both from GE Life Sciences) as previously described[166]. Nanobodies were expressed in *Escherichia coli* and purified as previously described[55,79,80].

Membrane Preparations

HEK293T cells (ATCC) were used for small-scale expression and purification of β_2AR and mutants. Cells were grown in DMEM + 10% FBS to ~70% confluency, then transfected with mYFP-β_2AR (pCMV5, 6 μg DNA per 10-cm plate) using Lipofectamine 2000. Cells were harvested 40-48 hours post-transfection in ice-cold lysis buffer buffer (50 mM HEPES, pH 8.0, 65 mM NaCl, 1 mM EDTA, 35 μg/ml phenylmethylsulfonyl fluoride, 32 μg/ml each tosyl-L-

phenylalanine-chloromethylketone and tosyl-L-lysine-chloromethylketone, 3.2 µg/ml leupeptin, 3.2 µg/ml ovomucoid trypsin inhibitor). The cell suspension was sonicated using a Branson Sonifier and centrifuged for 20 min at 25,000*g*. The pellet was resuspended in wash buffer (50 mM HEPES, pH 8.0, 100 mM NaCl with protease inhibitors listed above) using a Dounce homogenizer, then centrifuged for 20 min at 25,000*g*. The pellet was resuspended and homogenized in minimal wash buffer and the volume was adjusted to reach a final protein concentration of 5 mg/ml as measured by the Bradford protein assay. Membranes were frozen by slowly pouring into liquid nitrogen and stored at -80 °C until use.

Enrichment of β_2AR and β_2AR-Y308A from HEK293T cells

Frozen membranes were thawed on ice and NaCl, $MgCl_2$, and GTPγS were added to reach final concentrations of 300 mM, 1 mM, and 10 µM, respectively. Timolol was then added to a final concentration of 1 µM and the membranes were incubated for 10 min on ice. Receptors were solubilized for 1 hr at 4 °C in the presence of 1% dodecylmaltoside (DDM) and 0.1% cholesterol hemisuccinate (CHS). Following centrifugation for 30 minutes at 25,000g, the supernatant was applied to Ni-NTA agarose. The column was slowly washed with 20 column volumes of 20 mM HEPES, pH 8.0, 300 mM NaCl, 0.1% DDM, 0.01% CHS to remove bound timolol. Receptor was eluted in the same buffer plus 200 mM imidazole and concentrated using an Amicon 30 kDa-cutoff spin concentrator for addition to the rHDL reconstitution mixture.

Receptor Reconstitution into rHDL Particles

Reconstitutions were performed as described[88], with the amount of receptor added never exceeding 20% of the total reaction volume. For samples that contained G_s, the purified

heterotrimer was added to the pre-formed β_2AR-rHDL particles, incubated for 2 hr at 4°, and BioBeads were used to remove the added detergent. Nucleotide-free $G_s \cdot \beta_2$AR complex was prepared by incubating β_2AR·Gs-containing rHDL particles with apyrase in the presence of 1 mM $MgCl_2$ for 30 minutes at room temperature, or alternately, 2 hr at 4°. If needed, the sample was passed through a Superdex 200 gel filtration column to remove free nucleotide and apyrase.

Competition Binding Experiments using rHDL Particles

Assays were performed in Tris-buffered saline (TBS; 25 mM Tris-HCl, pH 7.4, 136 mM NaCl, 2.7 mM KCl) with a final concentration of 0.05% w/v bovine serum albumin. Receptor in HDL particles was incubated at room temperature with varying concentrations of competing ligand and a final concentration of 0.5 nM [^{3}H]DHAP. For experiments using allosteric modulators, all reactions also contained DMSO at 1% v/v final concentration. After filtration over Whatman GF/B filters pre-soaked in 0.3% w/v polyethyleneimine, filters were washed with ice-cold TBS, dried, and subjected to liquid scintillation counting on a TopCount™ NXT (Perkin-Elmer). Bound ligand never exceeded 10% of the total ligand added.

Radioligand Association Experiments using rHDL Particles

All assays were performed in Tris-buffered saline (TBS; 25 mM Tris-HCl, pH 7.4, 136 mM NaCl, 2.7 mM KCl) with a final concentration of 0.05% w/v bovine serum albumin. Reaction components were mixed and pre-incubated at room temperature (see below) before the addition of radioligand to initiate the association time course. Aliquots were withdrawn at the indicated times and filtered over Whatman GF/B filters pre-soaked in 0.3% w/v polyethyleneimine. Filters

were washed with ice-cold TBS, dried, and subjected to liquid scintillation counting on a TopCount™ NXT (Perkin-Elmer). Bound ligand never exceeded 10% of the total ligand added.

Kinetic binding experiments with [^{3}H]DHAP and Nb80, β_2AR-rHDL

For association experiments, receptor in rHDL was pre-incubated with varying concentrations of Nb80 and the reaction was started by addition of 5 nM [^{3}H]DHAP (Perkin-Elmer). For dissociation experiments, the samples were first incubated with 5 nM [^{3}H]DHAP for 30 minutes, followed by incubated with varying Nb80 concentrations for 30 minutes. The reaction was started by adding 50 μM cold alprenolol. Non-specific binding was determined in the presence of 10 μM (+/-)-propranolol.

Binding experiments with [^{3}H]DHAP and Gs-β_2AR nucleotide-free complexes

For association experiments, gel-filtered samples of apyrase-treated Gs-β_2AR-rHDL particles were incubated with 5 nM [^{3}H]DHAP to bind any receptor that was not complexed with Gs. The experiment was started by adding varying amounts of either GDP or GTPγS. For "equilibrium" binding experiments, samples were incubated with all the indicated components at room temperature for 90 minutes before filtration. Non-specific binding was determined in the presence of 10 μM (+/-)-propranolol.

[^{3}H]Formoterol Association to β_2AR

β_2AR-rHDL was incubated with the indicated concentrations of Nb80 for 30 minutes at room temperature. [^{3}H]formoterol (Moravek) was added to reach 10 nM final concentration. These

assays also contained 1 mM ascorbic acid in the reaction buffer. Non-specific binding was determined in the presence of 10 µM (+/-)-propranolol.

[^{3}H](-)-CGP-12177 Association to β_2AR

β_2AR-rHDL was incubated with the indicated concentrations of Nb80 for 30 minutes at room temperature. [^{3}H](-)-CGP-12177 (Perkin-Elmer) was added to reach 1 nM final concentration. Non-specific binding was determined in the presence of 10 µM (+/-)-propranolol.

[^{3}H]Carvedilol Association to β_2AR

Due to high amounts of non-specific [^{3}H]carvedilol binding both to bovine serum albumin (BSA) and to the glass fiber filters typically used for separation, β_2AR-rHDL was diluted into empty rHDL particles rather than into a 5x BSA solution (0.25% w/v BSA in TBS buffer) prior to addition to the assay mix. Using empty rHDL in place of BSA was critical for maintaining sample recovery from the assay plate while improving the signal-to-noise ratio of the assay. The receptor was incubated with the indicated concentrations of Nb80 for 15 minutes at room temperature, then for 30 minutes at 4 °C. [^{3}H]carvedilol (American Radiolabeled Chemicals) was added to reach 1 nM final concentration. Aliquots were withdrawn at the indicated time points and bound ligand was isolated using gel filtration on Sephadex G75 resin. Non-specific binding was determined in the presence of 10 µM (+/-)-propranolol.

[^{3}H]N-methylscopolamine Association to M2R•Go

Purified Go heterotrimer was added to M2R-rHDL in 20 mM HEPES pH 8.0, 100 mM NaCl, 1 mM EDTA, 1.1 mM $MgCl_2$ at an initial ratio of 1:100 M2R:Go and incubated for 30 minutes at

room temperature. Go was diluted at least 100-fold to minimize the amount of detergent added. The mixture was then incubated with BioBeads SM2 (BioRad) for 1 hour at 4 °C to remove any residual detergent. M2R•Go was diluted in TBS + 1 mM $MgCl_2$ and pre-incubated with 10 μM GTPγS or 5 mU/ml apyrase (New England Biolabs) for 1 hour at room temperature before addition of [^{3}H]N-methylscopolamine (Perkin-Elmer) to 1 nM final concentration. For experiments examining the effect of GDP on [^{3}H]N-methylscopolamine binding, GDP was added simultaneously with radioligand to initiate the timecourse. Non-specific binding was determined in the presence of 10 μM atropine.

[^{3}H]iperoxo Association to M2R

M2R-rHDL was incubated with the indicated concentrations of Nb9-8 for 30 minutes at room temperature. [^{3}H]iperoxo (Moravek) was added to reach 1 nM final concentration. Non-specific binding was determined in the presence of 10 μM atropine.

[^{3}H]Diprenorphine Association to MOPr•Go

MOPr•Go in rHDL was prepared as described above for M2R. MOPr•Go was diluted in TBS + 1 mM $MgCl_2$ and pre-incubated with 10 μM GTPγS or 5 mU/ml apyrase (New England Biolabs) for 1 hour at room temperature before addition of [^{3}H]diprenorphine to 1 nM final concentration. Non-specific binding was determined in the presence of 10 μM naloxone.

[^{3}H]Diprenorphine Association to MOPr•Nb39

Purified YFP-MOPr was reconstituted into rHDL as above, and pre-incubated with 100 μM active-state stabilizing nanobody Nb39 for 30 minutes at room temperature. To initiate the

timecourse, [^{3}H]diprenorphine (Perkin-Elmer) was added to reach 1 nM final concentration. Non-specific binding was determined in the presence of 10 µM naloxone.

[^{35}S]GTPγS Binding Assays

High Five insect cells were infected with baculovirus for β_2AR, $G\alpha_s$, and $G\beta_1\gamma_2$ and membranes were prepared ~40 hr post-infection. Cell membranes (5 µg/well) were incubated with various concentrations of agonist for 60 min at room temp in assay buffer (20 mM HEPES pH 7.4, 100 mM NaCl, 10 mM $MgCl_2$) containing 10 µM GDP and 0.1 nM [^{35}S]GTPγS. For experiments using allosteric modulators, DMSO was present in all wells at 1% v/v final. Reactions were filtered over Whatman GF/C and the filters were washed with ice-cold assay buffer, dried, and subjected to liquid scintillation counting on a TopCount™ NXT (Perkin-Elmer).

BIBLIOGRAPHY

1. Bjarnadottir, T. K. *et al.* Comprehensive repertoire and phylogenetic analysis of the G protein-coupled receptors in human and mouse. *Genomics* **88,** 263–273 (2006).

2. Hopkins, A. L. & Groom, C. R. The druggable genome. *Nat. Rev. Drug Discov.* **1,** 727–30 (2002).

3. McKee, E. E., Bentley, A. T., Smith Jr., R. M. & Ciaccio, C. E. Origin of guanine nucleotides in isolated heart mitochondria. *Biochem Biophys Res Commun* **257,** 466–472 (1999).

4. Shukla, A. K., Xiao, K. & Lefkowitz, R. J. Emerging paradigms of β-arrestin-dependent seven transmembrane receptor signaling. *Trends Biochem. Sci.* **36,** 457–69 (2011).

5. Dixon, R. A. F. *et al.* Cloning of the gene and cDNA for mammalian β-adrenergic receptor and homology with rhodopsin. *Nature* **321,** 75–79 (1986).

6. Horn, F. *et al.* GPCRDB: an information system for G protein-coupled receptors. *Nucleic Acids Res.* **26,** 275–9 (1998).

7. Umbarger, H. E. Evidence for a negative-feedback mechanism in the biosynthesis of isoleucine. *Science* **123,** 848 (1956).

8. Umbarger, H. E. & Brown, B. Isoleucine and valine metabolism in Escherichia coli. VII. A negative feedback mechanism controlling isoleucine biosynthesis. *J. Biol. Chem.* **233,** 415–20 (1958).

9. Pardee, A. B. & Yates, R. A. Control of pyrimidine biosynthesis in Escherichia coli by a feed-back mechanism. *J. Biol. Chem.* **221,** 757–70 (1956).

10. Monod, J., Changeux, J. P. & Jacob, F. Allosteric proteins and cellular control systems. *J.*

Mol. Biol. **6,** 306–329 (1963).

11. Monod, J., Wyman, J. & Changeux, J. P. On the nature of allosteric transitions: a plausible model. *J. Mol. Biol.* **12,** 88–118 (1965).

12. Changeux, J. P. Allostery and the Monod-Wyman-Changeux model after 50 years. *Annu. Rev. Biophys.* **41,** 103–33 (2012).

13. Ji, T. H., Grossmann, M. & Ji, I. G protein-coupled receptors. I. Diversity of receptor-ligand interactions. *J. Biol. Chem.* **273,** 17299–302 (1998).

14. Conn, P. J., Christopoulos, A. & Lindsley, C. W. Allosteric modulators of GPCRs: a novel approach for the treatment of CNS disorders. *Nat. Rev. Drug Discov.* **8,** 41–54 (2009).

15. Gentry, P. R., Sexton, P. M. & Christopoulos, A. Novel allosteric modulators of G protein-coupled receptors. *J. Biol. Chem.* **290,** 19478–88 (2015).

16. Langley, J. N. On the Physiology of the Salivary Secretion: Part II. On the Mutual Antagonism of Atropin and Pilocarpin, having especial reference to their relations in the Sub-maxillary Gland of the Cat. *J. Physiol.* **1,** 339–69 (1878).

17. Langley, J. N. On the reaction of cells and of nerve-endings to certain poisons, chiefly as regards the reaction of striated muscle to nicotine and to curari. *J. Physiol.* **33,** 374–413 (1905).

18. Maehle, A., Prüll, C. & Halliwell, R. F. Timeline: The emergence of the drug receptor theory. *Nat. Rev. Drug Discov.* **1,** 637–641 (2002).

19. Bosch, F. & Rosich, L. The contributions of Paul Ehrlich to pharmacology: A tribute on the occasion of the centenary of his nobel prize. *Pharmacology* **82,** 171–179 (2008).

20. Hill, A. V. The mode of action of nicotine and curari, determined by the form of the contraction curve and the method of temperature coefficients. *J. Physiol.* **39,** 361–73 (1909).

21. Clark, A. J. The reaction between acetyl choline and muscle cells. *J. Physiol.* **61,** 530–46 (1926).

22. Clark, A. J. The antagonism of acetyl choline by atropine. *J. Physiol.* **61,** 547–56 (1926).

23. Clark, A. J. The Mode of Action of Drugs on Cells. *Nature* **132,** 695–695 (1933).

24. Ariens, E. J. Affinity and intrinsic activity in the theory of competitive inhibition. I. Problems and theory. *Arch. Int. Pharmacodyn. thérapie* **99,** 32–49 (1954).

25. Stephenson, R. P. A modification of receptor theory. *Br. J. Pharmacol. Chemother.* **11,** 379–93 (1956).

26. Furchgott, R. F. in *Adv. Drug Res.* (Harper, N. J. & Simmonds, A. B.) 21–55 (Academic Press Inc. (London) Ltd., 1966).

27. Del Castillo, J. & Katz, B. Interaction at end-plate receptors between different choline derivatives. *Proc. R. Soc. London. Ser. B, Biol. Sci.* **146,** 369–81 (1957).

28. Karlin, A. On the application of 'a plausible model' of allosteric proteins to the receptor for acetylcholine. *J. Theor. Biol.* **16,** 306–20 (1967).

29. Rodbell, M., Birnbaumer, L., Pohl, S. L. & Krans, H. M. The glucagon-sensitive adenyl cyclase system in plasma membranes of rat liver. V. An obligatory role of guanylnucleotides in glucagon action. *J. Biol. Chem.* **246,** 1877–82 (1971).

30. Birnbaumer, L. & Rodbell, M. Adenyl cyclase in fat cells. II. Hormone receptors. *J. Biol. Chem.* **244,** 3477–82 (1969).

31. Ross, E. M. & Gilman, A. G. Reconstitution of catecholamine-sensitive adenylate cyclase activity: interactions of solubilized components with receptor-replete membranes. *Proc. Natl. Acad. Sci. United States Am.* **74,** 3715–3719 (1977).

32. Rodbell, M., Krans, H. M., Pohl, S. L. & Birnbaumer, L. The glucagon-sensitive adenyl cyclase system in plasma membranes of rat liver. IV. Effects of guanylnucleotides on binding of 125I-glucagon. *J. Biol. Chem.* **246,** 1872–6 (1971).

33. Maguire, M. E., Van Arsdale, P. M. & Gilman, A. G. An agonist-specific effect of guanine nucleotides on binding to the beta adrenergic receptor. *Mol. Pharmacol.* **12,** 335–9 (1976).

34. Zahniser, N. R. & Molinoff, P. B. Effect of guanine nucleotides on striatal dopamine receptors. *Nature* **275,** 453–5 (1978).

35. De Lean, A., Stadel, J. M. & Lefkowitz, R. J. A ternary complex model explains the agonist-specific binding properties of the adenylate cyclase-coupled beta-adrenergic receptor. *J. Biol. Chem.* **255,** 7108–17 (1980).

36. Herz, A. & Costa, T. Antagonists with negative intrinsic activity at delta opioid receptors coupled to GTP-binding proteins. *Proc. Natl. Acad. Sci. U. S. A.* **86,** 7321 – 7325 (1989).

37. Samama, P., Cotecchia, S., Costa, T. & Lefkowitz, R. J. A mutation-induced activated state of the beta 2-adrenergic receptor. Extending the ternary complex model. *J. Biol. Chem.* **268,** 4625–4636 (1993).

38. Weiss, J. M., Morgan, P. H., Lutz, M. W. & Kenakin, T. P. The cubic ternary complex receptor-occupancy model. I. model description. *J. Theor. Biol.* **178,** 151–167 (1996).

39. Weiss, J. M., Morgan, P. H., Lutz, M. W. & Kenakin, T. P. The cubic ternary complex receptor-occupancy model. II. understading apparent affinity. *J. Theor. Biol.* **178,** 169–182 (1996).

40. Weiss, J. M., Morgan, P. H., Lutz, M. W. & Kenakin, T. P. The cubic ternary complex receptor-occupancy model. III. resurrecting efficacy. *J. Theor. Biol.* **181,** 381–397 (1996).

41. Lohse, M. J. *et al.* Kinetics of G-protein-coupled receptor signals in intact cells. *Br. J. Pharmacol.* **153,** S125–S132 (2009).

42. Christopoulos, A. & Kenakin, T. G protein-coupled receptor allosterism and complexing. *Pharmacol. Rev.* **54,** 323–74 (2002).

43. Kenakin, T. Efficacy At G-Protein-Coupled Receptors. *Nat. Rev. Drug Discov.* **1,** 103–110 (2002).

44. Palczewski, K. *et al.* Crystal structure of rhodopsin: A G protein-coupled receptor. *Science* **289,** 739–45 (2000).

45. Ballesteros, J. A. & Weinstein, H. Integrated methods for the construction of three-

dimensional models and computational probing of structure-function relations in G protein-coupled receptors. *Methods Neurosci.* 366–428 (1995).

46. Gether, U. *et al.* Agonists induce conformational changes in transmembrane domains III and VI of the beta2 adrenoceptor. *EMBO J.* **16,** 6737–47 (1997).

47. Yao, X. J. *et al.* The effect of ligand efficacy on the formation and stability of a GPCR-G protein complex. *Proc. Natl. Acad. Sci. U. S. A.* **106,** 9501–6 (2009).

48. Cherezov, V. *et al.* High-resolution crystal structure of an engineered human beta2-adrenergic G protein-coupled receptor. *Science* **318,** 1258–65 (2007).

49. Rosenbaum, D. M. *et al.* Structure and function of an irreversible agonist-β(2) adrenoceptor complex. *Nature* **469,** 236–40 (2011).

50. Warne, T. *et al.* The structural basis for agonist and partial agonist action on a β(1)-adrenergic receptor. *Nature* **469,** 241–4 (2011).

51. Xu, F. *et al.* Structure of an agonist-bound human A2A adenosine receptor. *Science* **332,** 322–7 (2011).

52. White, J. F. *et al.* Structure of the agonist-bound neurotensin receptor. *Nature* **490,** 508–513 (2012).

53. Scheerer, P. *et al.* Crystal structure of opsin in its G-protein-interacting conformation. *Nature* **455,** 497–502 (2008).

54. Choe, H.-W. *et al.* Crystal structure of metarhodopsin II. *Nature* **471,** 651–5 (2011).

55. Rasmussen, S. G. F. *et al.* Structure of a nanobody-stabilized active state of the β(2) adrenoceptor. *Nature* **469,** 175–80 (2011).

56. Rasmussen, S. G. F. *et al.* Crystal structure of the β2 adrenergic receptor–Gs protein complex. *Nature* **477,** 549–555 (2011).

57. Manglik, A. & Kobilka, B. The role of protein dynamics in GPCR function: insights from the β2AR and rhodopsin. *Curr. Opin. Cell Biol.* **27,** 136–43 (2014).

58. Nygaard, R. *et al.* The dynamic process of β(2)-adrenergic receptor activation. *Cell* **152,** 532–42 (2013).

59. Dror, R. O. *et al.* Structural basis for nucleotide exchange in heterotrimeric G proteins. *Science* **348,** 1361–1365 (2015).

60. Sounier, R. *et al.* Propagation of conformational changes during μ-opioid receptor activation. *Nature* **524,** 375–8 (2015).

61. Isogai, S. *et al.* Backbone NMR reveals allosteric signal transduction networks in the β1-adrenergic receptor. *Nature* **530,** 237–41 (2016).

62. Hamers-Casterman, C. *et al.* Naturally occurring antibodies devoid of light chains. *Nature* **363,** (1993).

63. Greenberg, A. S. *et al.* A new antigen receptor gene family that undergoes rearrangement and extensive somatic diversification in sharks. *Nature* **374,** 168–73 (1995).

64. Pardon, E. *et al.* A general protocol for the generation of Nanobodies for structural biology. *Nat. Protoc.* **9,** 674–93 (2014).

65. Dmitriev, O. Y., Lutsenko, S. & Muyldermans, S. Nanobodies as Probes for Protein Dynamics in Vitro and in Cells. *J. Biol. Chem.* **291,** 3767–75 (2016).

66. Nevoltris, D. *et al.* Conformational nanobodies reveal tethered epidermal growth factor receptor involved in EGFR/ErbB2 predimers. *ACS Nano* **9,** 1388–1399 (2015).

67. Huang, Y. *et al.* Interactions between metal-binding domains modulate intracellular targeting of Cu(I)-ATPase ATP7B, as revealed by nanobody binding. *J. Biol. Chem.* **289,** 32682–32693 (2014).

68. Ward, A. B. *et al.* Structures of P-glycoprotein reveal its conformational flexibility and an epitope on the nucleotide-binding domain. *Proc. Natl. Acad. Sci.* **110,** 13386–91 (2013).

69. Chaikuad, A. *et al.* Structure of cyclin G-associated kinase (GAK) trapped in different conformations using nanobodies. *Biochem. J.* **459,** 59–69 (2014).

70. Loris, R. *et al.* Crystal structure of the intrinsically flexible addiction antidote MazE. *J. Biol. Chem.* **278,** 28252–7 (2003).

71. Möller, A., Pion, E., Narayan, V. & Ball, K. L. Intracellular activation of interferon regulatory factor-1 by nanobodies to the multifunctional (Mf1) domain. *J. Biol. Chem.* **285,** 38348–61 (2010).

72. Delanote, V. *et al.* An alpaca single-domain antibody blocks filopodia formation by obstructing L-plastin-mediated F-actin bundling. *FASEB J.* **24,** 105–18 (2010).

73. Rothbauer, U. *et al.* Targeting and tracing antigens in live cells with fluorescent nanobodies. *Nat. Methods* **3,** 887–9 (2006).

74. Kirchhofer, A. *et al.* Modulation of protein properties in living cells using nanobodies. *Nat. Struct. Mol. Biol.* **17,** 133–8 (2010).

75. Traenkle, B. *et al.* Monitoring interactions and dynamics of endogenous beta-catenin with intracellular nanobodies in living cells. *Mol. Cell. Proteomics* **14,** 707–23 (2015).

76. Maussang, D. *et al.* Llama-derived single variable domains (nanobodies) directed against chemokine receptor CXCR7 reduce head and neck cancer cell growth in vivo. *J. Biol. Chem.* **288,** 29562–29572 (2013).

77. Jähnichen, S. *et al.* CXCR4 nanobodies (VHH-based single variable domains) potently inhibit chemotaxis and HIV-1 replication and mobilize stem cells. *Proc. Natl. Acad. Sci. U. S. A.* **107,** 20565–70 (2010).

78. Staus, D. P. *et al.* Regulation of β2-adrenergic receptor function by conformationally selective single-domain intrabodies. *Mol. Pharmacol.* **85,** 472–81 (2014).

79. Kruse, A. C. *et al.* Activation and allosteric modulation of a muscarinic acetylcholine receptor. *Nature* **504,** 101–6 (2013).

80. Huang, W. *et al.* Structural insights into μ-opioid receptor activation. *Nature* **524,** 315–321 (2015).

81. Ahn, S., Shenoy, S. K., Wei, H. & Lefkowitz, R. J. Differential kinetic and spatial patterns

of beta-arrestin and G protein-mediated ERK activation by the angiotensin II receptor. *J. Biol. Chem.* **279,** 35518–25 (2004).

82. Ferrandon, S. *et al.* Sustained cyclic AMP production by parathyroid hormone receptor endocytosis. *Nat. Chem. Biol.* **5,** 734–42 (2009).

83. Feinstein, T. N. *et al.* Retromer terminates the generation of cAMP by internalized PTH receptors. *Nat. Chem. Biol.* **7,** 278–84 (2011).

84. Calebiro, D. *et al.* Persistent cAMP-signals triggered by internalized G-protein-coupled receptors. *PLoS Biol.* **7,** e1000172 (2009).

85. Kim, T. H. *et al.* The role of ligands on the equilibria between functional states of a G protein-coupled receptor. *J. Am. Chem. Soc.* **135,** 9465–9474 (2013).

86. Manglik, A. *et al.* Structural Insights into the Dynamic Process of β2-Adrenergic Receptor Signaling. *Cell* **161,** 1101–11 (2015).

87. Abdiche, Y., Malashock, D., Pinkerton, A. & Pons, J. Determining kinetics and affinities of protein interactions using a parallel real-time label-free biosensor, the Octet. *Anal. Biochem.* **377,** 209–17 (2008).

88. Whorton, M. R. *et al.* A monomeric G protein-coupled receptor isolated in a high-density lipoprotein particle efficiently activates its G protein. *Proc. Natl. Acad. Sci. U. S. A.* **104,** 7682–7 (2007).

89. Bayburt, T. H. & Sligar, S. G. Membrane protein assembly into Nanodiscs. *FEBS Lett.* **584,** 1721–7 (2010).

90. Kuszak, A. J. *et al.* Purification and functional reconstitution of monomeric mu-opioid receptors: allosteric modulation of agonist binding by Gi2. *J. Biol. Chem.* **284,** 26732–41 (2009).

91. Irannejad, R. *et al.* Conformational biosensors reveal GPCR signalling from endosomes. *Nature* **495,** 534–538 (2013).

92. Lamichhane, R. *et al.* Single-molecule view of basal activity and activation mechanisms

of the G protein-coupled receptor β2AR. *Proc. Natl. Acad. Sci. U. S. A.* **112,** 14254–9 (2015).

93. D'Antona, A. M., Xie, G., Sligar, S. G. & Oprian, D. D. Assembly of an activated rhodopsin-transducin complex in nanoscale lipid bilayers. *Biochemistry* **53,** 127–34 (2014).

94. Leitz, A. J., Bayburt, T. H., Barnakov, A. N., Springer, B. A. & Sligar, S. G. Functional reconstitution of Beta2-adrenergic receptors utilizing self-assembling nanodisc technology. *Biotechniques* **40,** 601–6 (2006).

95. Whorton, M. R. *et al.* Efficient coupling of transducin to monomeric rhodopsin in a phospholipid bilayer. *J. Biol. Chem.* **283,** 4387–94 (2008).

96. Damian, M. *et al.* High constitutive activity is an intrinsic feature of ghrelin receptor protein: a study with a functional monomeric GHS-R1a receptor reconstituted in lipid discs. *J. Biol. Chem.* **287,** 3630–41 (2012).

97. Venter, J. C. *et al.* The sequence of the human genome. *Science* **291,** 1304–51 (2001).

98. Chung, K. Y. *et al.* Conformational changes in the G protein Gs induced by the β2 adrenergic receptor. *Nature* **477,** 611–5 (2011).

99. Westfield, G. H. *et al.* Structural flexibility of the G alpha s alpha-helical domain in the beta2-adrenoceptor Gs complex. *Proc. Natl. Acad. Sci. U. S. A.* **108,** 16086–91 (2011).

100. Ross, E. M., Maguire, M. E., Sturgill, T. W., Biltonen, R. L. & Gilman, A. G. Relationship between the beta-adrenergic receptor and adenylate cyclase. *J. Biol. Chem.* **252,** 5761–75 (1977).

101. Lefkowitz, R. J. Catecholamine binding to the beta-adrenergic receptor. **74,** 515–519 (1977).

102. Ring, A. M. *et al.* Adrenaline-activated structure of β2-adrenoceptor stabilized by an engineered nanobody. *Nature* **502,** 575–579 (2013).

103. Bokoch, M. P. *et al.* Ligand-specific regulation of the extracellular surface of a G-protein-

coupled receptor. *Nature* **463,** 108–12 (2010).

104. Kikkawa, H., Isogaya, M., Nagao, T. & Kurose, H. The role of the seventh transmembrane region in high affinity binding of a beta 2-selective agonist TA-2005. *Mol. Pharmacol.* **53,** 128–34 (1998).

105. Dror, R. O. *et al.* Pathway and mechanism of drug binding to G-protein-coupled receptors. *Proc. Natl. Acad. Sci. U. S. A.* **108,** 13118–23 (2011).

106. Burgisser, E., De Lean, A. & Lefkowitz, R. J. Reciprocal modulation of agonist and antagonist binding to muscarinic cholinergic receptor by guanine nucleotide. *Proc. Natl. Acad. Sci. U. S. A.* **79,** 1732–6 (1982).

107. Bylund, D. B., Gerety, M. E., Happe, H. K. & Murrin, L. C. A robust GTP-induced shift in alpha(2)-adrenoceptor agonist affinity in tissue sections from rat brain. *J. Neurosci. Methods* **105,** 159–66 (2001).

108. Prater, M. R., Taylor, H., Munshi, R. & Linden, J. Indirect effect of guanine nucleotides on antagonist binding to A1 adenosine receptors: occupation of cryptic binding sites by endogenous vesicular adenosine. *Mol. Pharmacol.* **42,** 765–72 (1992).

109. Werling, L. L., Puttfarcken, P. S. & Cox, B. M. Multiple agonist-affinity states of opioid receptors: regulation of binding by guanyl nucleotides in guinea pig cortical, NG108-15, and 7315c cell membranes. *Mol. Pharmacol.* **33,** 423–31 (1988).

110. Haga, K. *et al.* Structure of the human M2 muscarinic acetylcholine receptor bound to an antagonist. *Nature* 3–8 (2012). doi:10.1038/nature10753

111. Manglik, A. *et al.* Crystal structure of the μ-opioid receptor bound to a morphinan antagonist. *Nature* **485,** 321–326 (2012).

112. Onaran, H. O., Rajagopal, S. & Costa, T. What is biased efficacy? Defining the relationship between intrinsic efficacy and free energy coupling. *Trends Pharmacol. Sci.* **35,** 639–647 (2014).

113. Childers, S. R. & Snyder, S. H. Differential regulation by guanine nucleotides or opiate

agonist and antagonist receptor interactions. *J. Neurochem.* **34,** 583–93 (1980).

114. Krumm, B. E., White, J. F., Shah, P. & Grisshammer, R. Structural prerequisites for G-protein activation by the neurotensin receptor. *Nat. Commun.* **6,** 7895 (2015).

115. Srivastava, A. *et al.* High-resolution structure of the human GPR40 receptor bound to allosteric agonist TAK-875. *Nature* **513,** 124–127 (2014).

116. Hanson, M. A. *et al.* Crystal Structure of a Lipid G Protein-Coupled Receptor. *Science* **335,** 851–855 (2012).

117. Bornancin, F., Pfister, C. & Chabre, M. The transitory complex between photoexcited rhodopsin and transducin. Reciprocal interaction between the retinal site in rhodopsin and the nucleotide site in transducin. *Eur. J. Biochem.* **184,** 687–98 (1989).

118. Devane, W. A., Dysarz, F. A., Johnson, M. R., Melvin, L. S. & Howlett, A. C. Determination and characterization of a cannabinoid receptor in rat brain. *Mol. Pharmacol.* **34,** 605–13 (1988).

119. Lefkowitz, R. J., Mullikin, D., Wood, C. L., Gore, T. B. & Mukherjee, C. Regulation of prostaglandin receptors by prostaglandins and guanine nucleotides in frog erythrocytes. *J. Biol. Chem.* **252,** 5295–303 (1977).

120. Grandt, R., Aktories, K. & Jakobs, K. H. Guanine nucleotides and monovalent cations increase agonist affinity of prostaglandin E2 receptors in hamster adipocytes. *Mol. Pharmacol.* **22,** 320–6 (1982).

121. Sarau, H. M., Mong, S., Foley, J. J., Wu, H. L. & Crooke, S. T. Identification and characterization of leukotriene D4 receptors and signal transduction processes in rat basophilic leukemia cells. *J. Biol. Chem.* **262,** 4034–41 (1987).

122. Dieterich, K. D., Grigoriadis, D. E. & De Souza, E. B. Corticotropin-releasing factor receptors in human small cell lung carcinoma cells: radioligand binding, second messenger, and northern blot analysis data. *Endocrinology* **135,** 1551–8 (1994).

123. Taylor, R. L. & Burt, D. R. Guanine nucleotides modulate TRH-receptor binding in sheep

anterior pituitary. *Mol. Cell. Endocrinol.* **21,** 85–91 (1981).

124. Hill, D. R., Bowery, N. G. & Hudson, A. L. Inhibition of GABAB receptor binding by guanyl nucleotides. *J. Neurochem.* **42,** 652–7 (1984).

125. Albasanz, J. L., Ros, M. & Martín, M. Characterization of metabotropic glutamate receptors in rat C6 glioma cells. *Eur. J. Pharmacol.* **326,** 85–91 (1997).

126. Doumazane, E. *et al.* Illuminating the activation mechanisms and allosteric properties of metabotropic glutamate receptors. *Proc. Natl. Acad. Sci. U. S. A.* **110,** E1416–25 (2013).

127. Farrens, D. L. *et al.* Requirement of rigid-body motion of transmembrane helices for light activation of rhodopsin. *Science* **274,** 768–70 (1996).

128. Standfuss, J. *et al.* The structural basis of agonist-induced activation in constitutively active rhodopsin. *Nature* **471,** 656–60 (2011).

129. Szczepek, M. *et al.* Crystal structure of a common GPCR-binding interface for G protein and arrestin. *Nat. Commun.* **5,** 4801 (2014).

130. Kang, Y. *et al.* Crystal structure of rhodopsin bound to arrestin by femtosecond X-ray laser. *Nature* **523,** 561–7 (2015).

131. Hofmann, K. P., Pulvermüller, A., Buczyłko, J., Van Hooser, P. & Palczewski, K. The role of arrestin and retinoids in the regeneration pathway of rhodopsin. *J. Biol. Chem.* **267,** 15701–6 (1992).

132. Gurevich, V. V., Pals-Rylaarsdam, R., Benovic, J. L., Hosey, M. M. & Onorato, J. J. Agonist-receptor-arrestin, an alternative ternary complex with high agonist affinity. *J. Biol. Chem.* **272,** 28849 (1997).

133. Christopoulos, A. *et al.* International Union of Basic and Clinical Pharmacology. XC. multisite pharmacology: recommendations for the nomenclature of receptor allosterism and allosteric ligands. *Pharmacol. Rev.* **66,** 918–47 (2014).

134. Michino, M. *et al.* What Can Crystal Structures of Aminergic Receptors Tell Us about Designing Subtype-Selective Ligands ? **023694,** 198–213 (2015).

135. Giorgioni, G., Piergentili, A., Ruggieri, S. & Quaglia, W. Dopamine D5 receptors: a challenge to medicinal chemists. *Mini Rev. Med. Chem.* **8,** 976–95 (2008).

136. Congreve, M., Langmead, C. J., Mason, J. S. & Marshall, F. H. Progress in structure based drug design for G protein-coupled receptors. *J. Med. Chem.* **54,** 4283–311 (2011).

137. Christopoulos, A. Allosteric binding sites on cell-surface receptors: novel targets for drug discovery. *Nat. Rev. Drug Discov.* **1,** 198–210 (2002).

138. Tan, Q. *et al.* Structure of the CCR5 Chemokine Receptor-HIV Entry Inhibitor Maraviroc Complex. *Science* **1387,** (2013).

139. Zhang, D. *et al.* Two disparate ligand-binding sites in the human P2Y1 receptor. *Nature* **520,** 317–21 (2015).

140. Jazayeri, A. *et al.* Extra-helical binding site of a glucagon receptor antagonist. *Nature* **533,** 274–7 (2016).

141. Burford, N. T., Traynor, J. R. & Alt, A. Positive allosteric modulators of the μ-opioid receptor: a novel approach for future pain medications. *Br. J. Pharmacol.* **172,** 277–86 (2015).

142. Irwin, J. J. & Shoichet, B. K. Docking Screens for Novel Ligands Conferring New Biology. *J. Med. Chem.* **59,** 4103–4120 (2016).

143. Carlsson, J. *et al.* Structure-based discovery of A2A adenosine receptor ligands. *J. Med. Chem.* **53,** 3748–55 (2010).

144. Carlsson, J. *et al.* Ligand discovery from a dopamine D3 receptor homology model and crystal structure. *Nat. Chem. Biol.* **7,** 769–78 (2011).

145. Kolb, P. *et al.* Structure-based discovery of beta2-adrenergic receptor ligands. *Proc. Natl. Acad. Sci. U. S. A.* **106,** 6843–6848 (2009).

146. de Graaf, C. *et al.* Crystal structure-based virtual screening for fragment-like ligands of the human histamine H(1) receptor. *J. Med. Chem.* **54,** 8195–206 (2011).

147. Lane, J. R. *et al.* Structure-based ligand discovery targeting orthosteric and allosteric pockets of dopamine receptors. *Mol. Pharmacol.* **84,** 794–807 (2013).

148. Shoichet, B. K. & Kobilka, B. K. Structure-based drug screening for G-protein-coupled receptors. *Trends Pharmacol. Sci.* **33,** 268–272 (2012).

149. Baker, J. G., Proudman, R. G. W. & Hill, S. J. Salmeterol's Extreme 2 Selectivity Is Due to Residues in Both Extracellular Loops and Transmembrane Domains. *Mol. Pharmacol.* **87,** 103–120 (2014).

150. Auffinger, P., Hays, F. A., Westhof, E. & Ho, P. S. Halogen bonds in biological molecules. *Proc. Natl. Acad. Sci. U. S. A.* **101,** 16789–94 (2004).

151. Iñiguez-Lluhi, J. A., Simon, M. I., Robishaw, J. D. & Gilman, A. G. G protein beta gamma subunits synthesized in Sf9 cells. Functional characterization and the significance of prenylation of gamma. *J. Biol. Chem.* **267,** 23409–17 (1992).

152. Li, B., Wang, C., Zhou, Z., Zhao, J. & Pei, G. β-Arrestin-1 directly interacts with Gαs and regulates its function. *FEBS Lett.* **587,** 410–6 (2013).

153. Xiao, K., Shenoy, S. K., Nobles, K. & Lefkowitz, R. J. Activation-dependent conformational changes in {beta}-arrestin 2. *J. Biol. Chem.* **279,** 55744–53 (2004).

154. Nobles, K. N. *et al.* Distinct phosphorylation sites on the β(2)-adrenergic receptor establish a barcode that encodes differential functions of β-arrestin. *Sci. Signal.* **4,** ra51 (2011).

155. Lee, M.-H. *et al.* The conformational signature of β-arrestin2 predicts its trafficking and signalling functions. *Nature* **531,** 665–668 (2016).

156. Eichel, K., Jullié, D. & von Zastrow, M. β-Arrestin drives MAP kinase signalling from clathrin-coated structures after GPCR dissociation. *Nat. Cell Biol.* **18,** (2016).

157. Nuber, S. *et al.* B-Arrestin biosensors reveal a rapid, receptor-dependent activation/deactivation cycle. *Nature* **531,** 661–664 (2016).

158. Reiter, E., Ahn, S., Shukla, A. K. & Lefkowitz, R. J. Molecular mechanism of β-arrestin-

biased agonism at seven-transmembrane receptors. *Annu. Rev. Pharmacol. Toxicol.* **52,** 179–97 (2012).

159. Luttrell, L. M. & Kenakin, T. P. Refining efficacy: allosterism and bias in G protein-coupled receptor signaling. *Methods Mol. Biol.* **756,** 3–35 (2011).

160. Fay, J. F. & Farrens, D. L. A key agonist-induced conformational change in the cannabinoid receptor CB1 is blocked by the allosteric ligand Org 27569. *J. Biol. Chem.* **287,** 33873–33882 (2012).

161. Davey, A. E. *et al.* Positive and negative allosteric modulators promote biased signaling at the calcium-sensing receptor. *Endocrinology* **153,** 1232–41 (2012).

162. Noetzel, M. J. *et al.* A Novel Metabotropic Glutamate Receptor 5 Positive Allosteric Modulator Acts at a Unique Site and Confers Stimulus Bias to mGlu5 Signaling. *Mol. Pharmacol.* **83,** 835–847 (2013).

163. Miller-Gallacher, J. L. *et al.* The 2.1 Å resolution structure of cyanopindolol-bound β1-adrenoceptor identifies an intramembrane Na+ ion that stabilises the ligand-free receptor. *PLoS One* **9,** e92727 (2014).

164. Katritch, V. *et al.* Allosteric sodium: a key co-factor in class A GPCR signaling. *Trends Biochem. Sci.* **39,** 233–244 (2014).

165. Dawaliby, R. *et al.* Allosteric regulation of G protein-coupled receptor activity by phospholipids. *Nat. Chem. Biol.* **12,** 35–9 (2016).

166. Kozasa, T. & Gilman, A. G. Purification of recombinant G proteins from Sf9 cells by hexahistidine tagging of associated subunits. *J. Biol. Chem.* **270,** 1734–41 (1995).